

POLITECNICO DI TORINO

Master of Science in Automotive Engineering

Master Thesis

# Electric motor test bench for efficiency maps generation



Director  
Prof. Silvio Vaschetto

Author  
Gianluca LANZARA

Co-directors:  
Prof. Miguel Delgado Prieto  
Eng. Carles Colls Castro

March 2021



“Stutat sunt  
lampiuncell”

(Nonno Bruno)

## Acknowledgements

Ringrazio il mio relatore, il professor Silvio Vaschetto, per il tempo che mi ha dedicato e le indicazioni che mi ha offerto. I suoi consigli sono stati fondamentali per la realizzazione del lavoro e per la stesura di questo documento.

Ringrazio l'ingegner Carles Colls Castro che mi ha guidato nella realizzazione del progetto. La sua disponibilità e il suo metodo sono le fondamenta di questa tesi.

Ringrazio il professor Miguel Delgado Prieto che mi ha consigliato e supportato per la realizzazione di questo documento.

Ringrazio i miei genitori e le mie sorelle, Francesca e Alessandra. Loro mi hanno sostenuto e hanno creduto in me fino alla fine. Questo traguardo lo devo a loro.

Ringrazio i miei nonni che mi hanno sempre regalato un sorriso anche a tantissimi chilometri di distanza.

Ringrazio i miei zii e i miei cugini e tutti coloro che mi hanno sostenuto anche solo con un messaggio.

Ringrazio tutti i miei amici. Mi sono stati vicini e mi hanno accompagnato fin qui, fino a questo importantissimo traguardo. Grazie a loro ho imparato ad affrontare le difficoltà con coraggio e a brindare ai fallimenti dimenticandoli sul fondo di un boccale di birra.

Uno speciale ringraziamento a Silvia che, nonostante i grandi ostacoli incontrati per portare avanti questo lavoro di tesi, non mi ha mai permesso di mollare.

Un particolare ringraziamento ad Andrea che mi ha affiancato nella traduzione del documento.

Ringrazio tutti coloro che mi hanno dato sostegno in questo percorso accademico e non solo.

Per i sacrifici che ho fatto, per la lontananza da casa, per le nottate di studio, per gli esami superati e per quelli andati male, per la tenacia che mi ha guidato fin qui e per altre mille ragioni, dedico questo lavoro a me e a tutti quelli che hanno creduto che ce l'avrei fatta.



# Index

Acknowledgements .....	IV
Index of figures .....	VII
Index of tables .....	IX
I. Abstract .....	1
1. Introduction.....	3
2. State of Art .....	5
2.1 Electrical vehicles architecture.....	5
2.2 Electric motor design.....	6
2.3 E-Motor validation for automotive applications .....	7
2.4 Efficiency maps development .....	9
3. Equipment for the test .....	14
3.1 Test Bench architecture.....	14
3.2 Electronics .....	16
3.3 Sensors.....	18
3.3.1 Position/Velocity Sensor.....	18
3.3.2 Temperature Sensor .....	19
3.3.3 Torque Sensor.....	19
3.3.4 Current transducers.....	20
3.3.5 Voltage transducers.....	20
3.3 Load Motor .....	21
3.4 Inverter .....	22
3.5 Security devices .....	23
3.5.1 Anti-opening device.....	23
3.5.2 Clutch limiter detection system.....	23
3.5.3 Emergency buttons.....	23
3.6 Acquisition program .....	25
3.7 Limits .....	28
4 Motor under test .....	29
4.1 MUT control.....	30
4.2 Software strategy .....	34
4.3 LabVIEW state-machine development .....	36
5. Automatized generation of efficiency maps .....	39
5.1 Map development strategy .....	40
5.2 Speed and Torque control .....	43
5.2.1 Set speed .....	43

5.2.2	Set torque .....	43
5.2.3	Increment model .....	44
5.3	Speed acquisition.....	45
5.3.1	Constant speed verification.....	45
5.3.2	Speed in range verification.....	45
5.4	Torque Acquisition.....	47
5.4.1	Torque verification .....	47
5.5	Current acquisition .....	48
5.6	Voltage acquisition .....	51
5.7	Mechanical Power .....	53
5.8	Electrical Power .....	53
5.8.1	Period.....	54
5.9	Efficiency and Post processing .....	55
5.10	Algorithm .....	55
5.11	User Interface .....	61
5.12	Specifications and limits .....	65
6.	Test .....	66
6.1	Preparation for the test.....	66
6.2	Test settings.....	67
6.3	Post-processing.....	68
6.4	Validation of measurements .....	69
7.	Results .....	72
7.1	Expected results .....	72
7.2	Achieved results .....	75
8.	Conclusions.....	80
8.1	Future works.....	81
	Bibliography.....	82

## Index of figures

Figure 1 – Vehicle sales trends over the last decade (ANFIA 2020) .....	3
Figure 2 – Average vehicles CO <sub>2</sub> emissions over the last decade (ANFIA 2020).....	4
Figure 3 – Constituent parts of a plug-in hybrid electric vehicle (Oghomwen Igbinovia 2016) .....	5
Figure 4 – Electric motor design process.....	6
Figure 5 – “Imc Test & Measurement GmbH” test rig .....	8
Figure 6 – “Application System” test rig.....	9
Figure 7 – “Kistler” test rig.....	9
Figure 8 – Power losses in an electric motor.....	10
Figure 9 – Efficiency mapping strategy (HBM 2016) .....	11
Figure 10 – Efficiency map of AC electric motor (HBM 2016) .....	11
Figure 11 – Total losses map of AC electric motor (HBM 2016).....	12
Figure 12 – Copper losses map of AC electric motor (HBM 2016) .....	12
Figure 13 – Iron and mechanical losses map of AC electric motor (HBM 2016) .....	13
Figure 14 – MAPRO test bench.....	14
Figure 15 – MAPRO test bench MUT and shaft details .....	15
Figure 16 – MAPRO test bench transmission parts.....	16
Figure 17 – MAPRO test bench electric cabin .....	16
Figure 18 – SINAMICS inverter and compact RIO devices.....	17
Figure 19 – MAPRO test bench connection diagram .....	18
Figure 20 – MAPRO test bench anti-opening device.....	23
Figure 21 – MAPRO test bench torque limiter device.....	23
Figure 22 – MAPRO test bench emergency button devices .....	24
Figure 23 – MAPRO test bench acquisition tool.....	25
Figure 24 – Acquisition tool: Control and Capture tab.....	26
Figure 25 – Acquisition tool: Calibration tab .....	27
Figure 26 – Acquisition tool: Setup tab .....	27
Figure 27 – Acquisition tool: state indicators.....	28
Figure 28 – Test region .....	30
Figure 29 – INFRANOR Inverter for MUT control .....	30
Figure 30 – Power Supply .....	32
Figure 31 – Diagram for connecting Arduino to the Inverter logical ports .....	32
Figure 32 – Experiment-based correlation between PWM and RPM .....	33
Figure 33 – Errors over the obtained function respect to the experimental values .....	33
Figure 34 – Finite state machine diagram .....	35
Figure 35 – LabVIEW programming code for the "Initialize" state .....	36
Figure 36 – LabVIEW programming code for “Connecting” state.....	36
Figure 37 – LabVIEW programming code for “Stand-by” state.....	37
Figure 38 – LabVIEW programming code for "Drive Reset" action .....	37
Figure 39 – LabVIEW programming code for "Control" state .....	38
Figure 40 – LabVIEW programming code for "Error" state .....	38
Figure 41 – Efficiency map filling strategy.....	39
Figure 42 – Efficiency map partial regions filling strategy.....	40
Figure 43 – Torque-speed point .....	40
Figure 44 – Efficiency map: Vertical filling strategy .....	41
Figure 45 – Torque-speed map temperature behavior for vertical filling strategy.....	41
Figure 46 – Efficiency map: Horizontal filling strategy .....	42
Figure 47 – Efficiency map: separate areas filling strategy .....	42

Figure 48 – Program motor settings.....	44
Figure 49 – Acquisition of the encoder position signal .....	45
Figure 50 – Speed signal in rpm derived from position input data and verification of required range.....	46
Figure 51 – Torque signal and verification of required range .....	47
Figure 52 – Torque signal after installing a 100nF capacitor and verification of the required range .....	48
Figure 53 – Current sensor operating system scheme .....	48
Figure 54 – Current sensors connection diagram .....	49
Figure 55 – Current sensor connection on the bench.....	49
Figure 56 – Current sensors connection to the electric cabin.....	50
Figure 57 – Acquisition of a current signal [A] from one phase .....	50
Figure 58 – Acquisition and filtering of a current signal [A] from one phase .....	51
Figure 59 – Voltage transducers connection diagram.....	51
Figure 60 – Voltage transducers connection to the motor (on the left) and to the cabin (right side) .....	52
Figure 61 - Three phase voltage acquired signal .....	52
Figure 62 – Difference between filtered (below) and unfiltered (above) voltage signal .....	53
Figure 63 – Program workflow .....	55
Figure 64 – LabVIEW programming code for “Set Speed” action .....	56
Figure 65 – LabVIEW programming code for “Set Torque” action.....	56
Figure 66 – LabVIEW programming code for “Range torque check” action: constant torque test .....	57
Figure 67 – LabVIEW programming code for “Range torque check” action: torque range test .....	57
Figure 68 – LabVIEW programming code for “Range speed check” action: constant speed test.....	58
Figure 69 – LabVIEW programming code for “Range speed check” action: speed range test.....	58
Figure 70 – LabVIEW programming code for “Period” action: determine the period .....	59
Figure 71 – LabVIEW programming code for “Period” action: save the period.....	59
Figure 72 – LabVIEW programming code for “Save results” action .....	60
Figure 73 – LabVIEW programming code for “Save results” action .....	60
Figure 74 – LabVIEW programming code for “Set new point” action.....	61
Figure 75 – LabVIEW interface for “Control” sub-tab .....	62
Figure 76 – LabVIEW interface for “Measurement settings” sub-tab .....	63
Figure 77 – LabVIEW interface for “Acquisitions” sub-tab.....	64
Figure 78 – LabVIEW interface for “Results” sub-tab.....	64
Figure 79 – Heatsink connection .....	67
Figure 80 – Auto-phasing procedure.....	67
Figure 81 – Visualization of TDMS results with DIAdem software .....	69
Figure 82 – Power analyzer connection diagram .....	69
Figure 83 – Power Analyzer in operation mode .....	70
Figure 84 – Speed Acquisition for $\omega=2000$ rpm .....	72
Figure 85 – Torque Acquisition for $T = 2.0$ Nm .....	72
Figure 86 – Encoder Acquisition .....	73
Figure 87 – Phase B voltage acquisition .....	73
Figure 88 – Phase B current acquisition .....	74
Figure 89 – Three phase voltage acquisition .....	74
Figure 90 – Three phase current acquisition .....	74
Figure 91 – Efficiency map for a SMPM motor - (Efficiency maps of electrical machines” 2015) .....	75
Figure 92 – Resistant torque of the bench as function of speed .....	75
Figure 93 – Resistant torque of the bench as function of speed: division among areas .....	76
Figure 94 – Efficiency map results of the MUT.....	77
Figure 95 – Efficiency map of assessed and non-assessed region .....	77

Figure 96 – Efficiency maps comparison .....	78
Figure 97 – Losses map.....	79

## Index of tables

Table 1 – Position sensor specifications .....	19
Table 2 – Temperature sensor specifications.....	19
Table 3 – Torque sensor specifications .....	20
Table 4 – Current transducer specifications.....	20
Table 5 – Voltage transducer specifications.....	21
Table 6 – Load motor specifications .....	21
Table 7 – Inverter specifications.....	22
Table 8 – Inverter drive settings .....	22
Table 9 – Motor under test specifications.....	29
Table 10 – Finite state machine: States description.....	34
Table 11 – Finite state machine: Input description .....	34
Table 12 – Finite state machine: Control description .....	34
Table 13 – Arduino output error description .....	35
Table 14 – Calibration settings .....	66
Table 15 – Experimental correlation between acquisition frequency and detected efficiency .....	68
Table 16 – Electric power comparison and error statement.....	70
Table 17 – Efficiency comparison and error statement .....	71
Table 18 – Power factor results .....	78

# I. Abstract

The document proposes an algorithm for autonomous efficiency map generation which is intended to be of particular interest for the study of electric motors characteristics. A program has been developed in LabVIEW platform to test motors in all their operating points to autonomously generate efficiency maps.

The development of this project is motivated by the rising expansion of electric motors in automotive applications for electric and hybrid powertrains. New electric motors, before being released by the manufacturer, are tested and evaluated according to an iterative process whose final stage is the validation of the prototype on a test rig. Therefore, the attention has been focused on the validation phase proposing a tool to automatize the validation tests.

The project presented in this report aims to optimize the motor validation process by automating the study of its performance in stationary working conditions. The program independently tests the electric motor and provides the user with collected data for each operating point and, at the end of the acquisitions, automatically generates the efficiency map of the tested machine.

The development of the tool takes place in five phases starting from the implementation of the theoretical algorithm strategy up to the validation of the results in a real simulation of an Electric Motor on the test rig.

The first step of the project focuses on the study of a strategy for the acquisition of different working points of a motor and on the definition of parameters required to perform that analysis. In this stage, a primitive algorithm, capable of applying the acquisition strategy under ideal conditions, has been developed.

The second step is the Software-in-the-Loop (SIL) side where a function capable of simulating temperature, speed, torque, voltage, current and noise signals has been programmed. In this phase the algorithm developed in the previous step is simulated in a virtual environment and the functionalities of the program were tested by also taking into consideration cases outside the ideal one, for instance a case of high torque ripple.

The third phase has a mixed software-hardware approach; the program is configured to send signals to an external electronic platform to rotate the motor under test. While the input signals are still simulated, the output ones are sent to the hardware and actual actions are performed. In this way it is possible to evaluate the reactions of the electric motor by simulating different working conditions of the program.

The fourth step consists in the transition of the program to work in a real environment. In this stage the software can both read the signals acquired by the sensors and send output signals to hardware devices. In this phase, some acquisitions are performed to carry out the proper adaptations to make the algorithm more robust.

In the final phase the program is tested in a real environment by analyzing the performance of an electric motor installed on the test bench and developing the efficiency map. The acquisitions made by the program are compared with those of a professional Power Analyzer in order to validate the functionality of the project.

The document is structured as follows:

Chapter 1 “Introduction” provides an overview of current mobility with a focus on the application of electric powertrain as a solution to increase vehicles efficiencies and decrease carbon dioxide emissions.

Chapter 2 “State of Art” illustrates the current trend of automotive architectures with reference to the evolution of the powertrain in hybrid and electric vehicles. Particular attention is put to electric thrusters by

presenting their design phases and validation tactics. In the final part of the chapter, the aim is to illustrate the latest generation of test benches and the strategies used in the industrial field to test electric motors and develop their efficiency maps.

Chapter 3 “Equipment for the test” presents features, advantages, limitations and technical specifications of the hardware and software equipment used for the development of the program.

Chapter 4 “Motor under test” explains the choice of the motor used to perform the tests and the state machine control strategy adopted.

Chapter 5 “Automatized generation of efficiency map” describes the map development strategy and the model used to control speed and torque. Moreover, the acquisition strategies and their processing are presented.

Chapter 6 “Tests” explains the settings of parameters to perform the tests, the sensor calibration method and the model used for data acquisition.

In Chapter 7 “Results”, the acquired signals are collected and analyzed, the efficiency map is computed and the results are compared with the expected one justifying divergences between expectation and actual results.

In Chapter 8 “Conclusions”, the goals of the document are compared with the results obtained in order to validate the project and underline its limits. The developed tool results to be a valid choice for optimizing the user's work in generating efficiency maps and the quality of the results will be closely related to that of the test bench.

# 1. Introduction

The transport sector is responsible for 30% of Europe's total CO2 emissions, 72% of which is produced by road transport itself. In an effort to limit CO2 emissions, the EU has set a target to reduce transport emissions levels by 60% from 1990 to 2030. (European Parliament, 2019)

In the last decade, vehicle sales went from almost 75 million in 2010 to 96 million in 2017, with a growth of 28%, equal to 21 million new vehicles; later on, the market has dropped to 95.8 million in 2018 and 91.5 million in 2020.

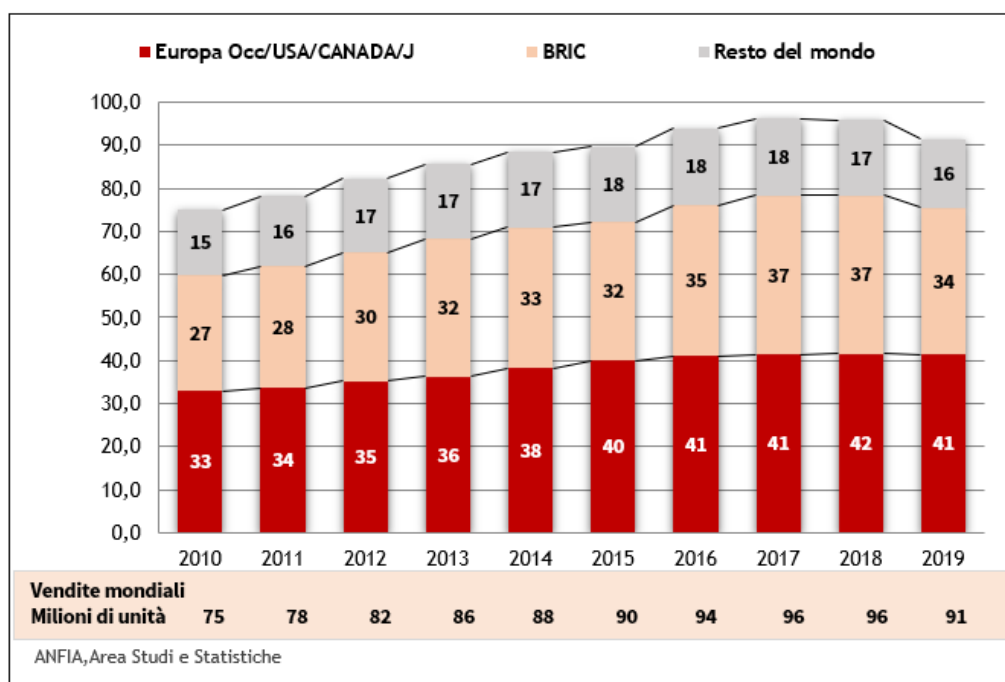


Figure 1 – Vehicle sales trends over the last decade (ANFIA 2020)

In 2019 the market mix for engines changed. There was a 13.9% decline in diesel car sales, a 5% increase in gasoline cars and a 41% increase in alternative fuel cars. The EU recorded a growth of 43% in alternative fuel cars.

Nevertheless, the increase in sales of alternative fuel cars was not enough to contain the increase in carbon dioxide emissions

The manufacturers had to change strategic plans, the production mix of powertrains and prepare massive investments for the electrification of vehicles. Achieving the CO2 emission reduction targets for 2020-2021, but especially for 2025-2030, is such a hard task without a massive release of electric vehicles on the market.

In addition to the widespread diffusion of the charging infrastructure throughout the territory, two more types of issues need to be considered: one linked to the production of batteries, the other linked to the production of energy from renewable sources to bring the level of pollution produced by vehicles closer to zero.



In the figure 2 is represented the average CO2 emissions of new registered cars.

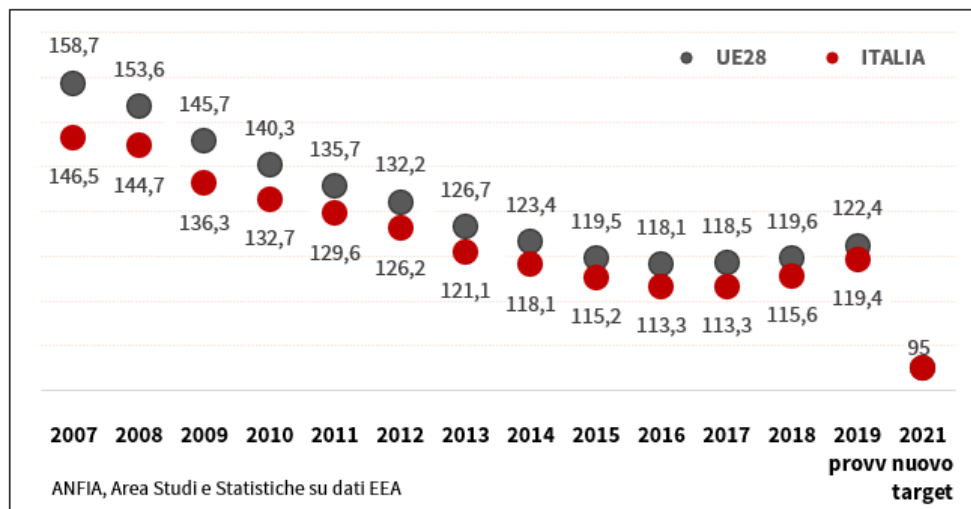


Figure 2 – Average vehicles CO<sub>2</sub> emissions over the last decade (ANFIA 2020)

Worldwide sales of electric vehicles (ECVs) totaled over 2 million units in 2018 and in 2019 the ECV market is estimated at 2.39 million units. Despite the global slowdown in light vehicle sales, which have been slowing since 2018, the electric vehicle market has grown significantly and is worth 2.7% of the total light vehicle market (ANFIA 2020).

In Europe, the massive car market will have to adapt its fleet of cars to a limit of 95g / km of CO<sub>2</sub> for a reference mass of the car equal to 1,379.88 kg on a WLTP cycle.

The introduction of electric thrusters, to replace thermal ones or in addition to the latter, is dictated by the high efficiency of the electric motors which can therefore increase the overall efficiency of the vehicle. Furthermore, the electric motor also aims to recover mechanical energy during the braking phases that later can be used as propulsive energy.

The installation of electric motors alongside thermal engines allows to reduce fuel consumption and implement some strategies such as "start and stop" or "engine off-coast".

The lack of charging stations spread throughout the territory, the high charging times and the high costs of full electric cars seem to push consumers towards hybrid solutions.

The hybrid and full electric trend are expanding not only in the sector of compact and sedan cars but also in the area of hyper-cars and heavy duty vehicles. A clear proof of that is Ferrari SF90, a super-sport plug-in hybrid electric vehicle in which the 22 % of the total power is supplied by electric powertrains.

## 2. State of Art

### 2.1 Electrical vehicles architecture

The electric system of a vehicle is made up of three main elements: a power source, a power converter and an electric motor.

Each of these components has its own efficiency to be considered in the design phase in order to compute the mechanical power delivered and to calculate the amount of losses produced.

In Figure 3 is shown simplified diagram of a generic hybrid thermal-electric traction system for a vehicle.

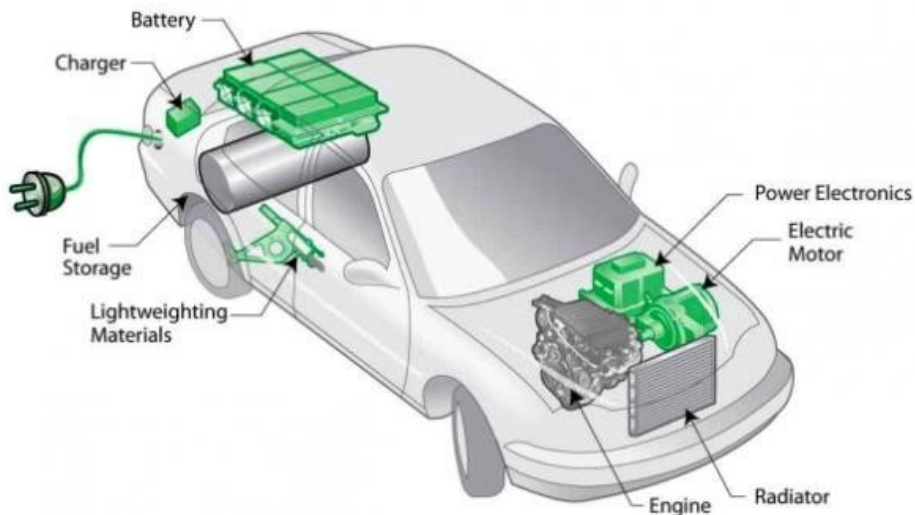


*Figure 3 – Constituent parts of a plug-in hybrid electric vehicle (Oghomwen Igbinovia 2016)*

Considering the performances of these components, the Li-ion battery efficiency is around 85%, typical inverter efficiencies exceed 95% under most operating conditions, while the three-phase motor has efficiencies that vary with respect to its working point and they can generally be considered, for a permanent magnet motor, in a range between 70% and 95%.

Optimizing the efficiencies is necessary to achieve greater performances and lower consumptions.

Permanent magnet motors are the primary type of electric traction machine used for commercial electric and hybrid passenger vehicles. This takes place because they offer a combination of high torque density and high efficiency which is difficult to surpass with other motor types (Lei, Zhu, & Guo, 2016).

Additionally, the high torque density is a decisive factor in the choice of P.M. motors because the smaller volume of the machine allows the motor to be installed even in hybrid vehicles applications where the available space is reduced due to the overall dimensions of the internal combustion engine and gearbox.

## 2.2 Electric motor design

The design of an Electric Motor follows two different approaches: empirical approach or F.E.A. modelling one.

The **empirical approach** involves building the motor with theoretical parameters: the strategy is to evaluate how the motor works and its performances can be optimized through an iterative procedure, which is hugely time-consuming and high costs.

**Finite Element Analysis** (F.E.A.) modelling is the new generation approach in which the design is made by CAD simulation of the geometry and a model is built to simulate magnetism and electromagnetism domain. This procedure is much cheaper than the previous one and allows to predict the behavior of the e-motor for defined working conditions (Meier 2002).

FEA follows four main steps, as shown in Figure 4.

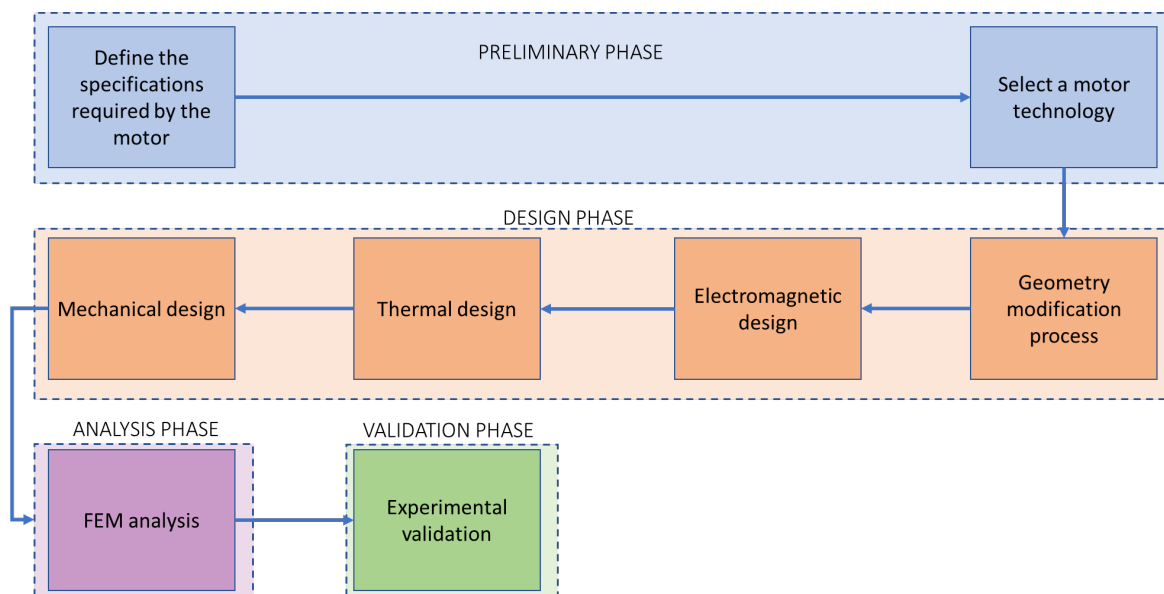


Figure 4 – Electric motor design process

1. **Preliminary phase:** it defines the specification of the electrical machine required by a given application which includes rated power, speed range, voltage, current, efficiency, volume and cost in steady state and dynamic performances.
2. **Design phase:** it selects the motor technology and the related power electronic between different technologies as PM motor, induction machines, synchronous machines, DC machines, reluctance machines etc. Then it includes geometry development process, electromagnetic, thermal and mechanical design.
3. **Analysis phase:** it considers the FEA to validate the choices made in the design phase and to correct some parameters in an iterative way.
4. **Validation phase:** the validation of the design occurs when the first motor prototype has already been produced and it is ready to be tested. In the validation phase the motor behavior is evaluated for different working conditions and the results of the finite elements analysis can be confirmed or refuted.

In the validation phase, the motor is tested on a test rig allowing to verify the results achieved by the FEM analysis, evaluate the motor performances and draw up efficiency maps.

## 2.3 E-Motor validation for automotive applications

The test bench essentially consists of a device capable of applying a modulating resistant torque to the axis of the motor under test and a series of sensors able to detect various parameter such as speed, torque, current and voltage. The test rig is used in automotive industry both for electric motor and for internal combustion engines tests.

A distinction is made between the following types of electric-motor test benches:

- Development test bench
- Endurance test bench
- Test bench for auditing electric drives
- EOL test bench (End-of-Line test bench)
- HiL test bench (Hardware-in-the-Loop)

Different motor test rigs are designed to perform different type of tests as

- Service life testing under maximum mechanical loading (full load);
- Function and performance tests for monitoring and predictive maintenance;
- Testing with customer-specific load profile with specification of rotational speed and torque;
- Determination of the efficiency of the engine or drive system;
- Determination of characteristic curves of the engine or drive system;
- Type testing of electric motors;
- Routine testing of electric motors;
- Qualification of electric motors;
- Testing in accordance with standards EN 60034-2-1 and 60034-2-3.

The development of drive systems for electromobility and highly efficient motors in the industrial sector increased demands on electric-motor test benches with respect to flexibility and operability. It is necessary to cover various power, speed and torque ranges, even high speeds of up to, e.g., 50,000 rpm or torques in the range of several kilonewton meter (kNm).<sup>1</sup>

In addition, testing the power of electric motors and their efficiency is becoming increasingly important. Because the drive technology consumes over two thirds of industrial power, a great deal of carbon dioxide can be avoided.

Test benches must determine the energy efficiency of electric motors in accordance with the "Minimum Energy Performance Standards" (MEPS) introduced worldwide and comply with the legal regulations regarding measurement accuracy. Standards IEC 60034-30-1, NEMA MG1 and others define the efficiency classes and minimum requirements on electric motors in power class 0.75 to 375 kW.

The major improvements regarding the test benches during the years result in simplification of sensor integration and channel synchronization, higher samples rate up to 2MS/s, more precise sensors and higher capacity in terms of supported power up to hundreds of kW. The automation of the processes greatly simplifies the work of users who are only interested in the final measurements provided by the test bench; consequently, new generation test benches can automatically synchronize the sample rates of the different channels and input cards.

---

<sup>1</sup> Kistler Group – Testing Electric Motors

Thanks to software improvements, the acquisition process has been extremely optimized. The use of LabVIEW allows a smart communication between sensors on the bench and acquisition devices, and to save data in TDMS format to rapidly storage large amounts of data. This also facilitates the subsequent data analysis using a wide range of postprocessing software.

Many test rigs have been developed to satisfy the numerous requests of the current automotive manufacturers. Three typologies, considered most significant to understand the state of the art, are described in the following.

*Imc Test & Measurement GmbH* proposes a test bench equipped with an extremely wide working range from 100mW to 100kW suitable to support the load machine for the active and passive operation of the test object in the range from 0.5 to over 20,000 RPM, sampling frequency up to 100 kHz and analog bandwidth up to 48 kHz for fast measurement channels. The main advantage of this bench is the possibility to align the motor with the bench shaft in a fast and precise way. Moreover it is possible to exchange the torque measuring shaft without the need to realign.



Figure 5 – “Imc Test & Measurement GmbH” test rig

*Application Systems* produces a test bench designed for Automotive and Industrial applications. The peculiarity of this bench is the possibility to test powers from 20W to 750W with very high torques, up to 5000 Nm while maintaining optimal working conditions as the load motor is liquid cooled. The maximum speed allowed is 30'000 rpm with a resolution of 1rpm and a torque accuracy of 0.1Nm. The very high supported torque also allows to test geared motors used mainly for industrial applications.

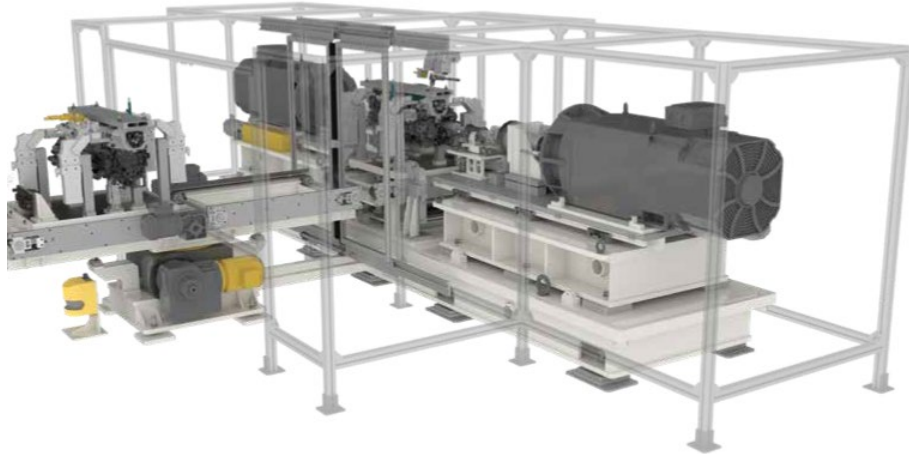


Figure 6 – “Application System” test rig

The third bench, shown in Figure 7, is produced by the Kistler company. With this machine it is possible to test motors in various temperature conditions. The bench is equipped with a climatic chamber, which can lead the engine to work at temperatures between 0 and 250 ° C. This bench supports motors up to 81kW with a maximum torque of 700 Nm. Electrical data acquisitions are carried out by the highly precise power analyzer in conjunction with precision current converters.



Figure 7 – “Kistler” test rig

## 2.4 Efficiency maps development

Even though the efficiency of the whole system is affected by the components of the electric machines, there is generally greater focus on the efficiency of the electric machine; this happens because the efficiency of electric motors is normally lower than inverters and shows a greater variability with operating point and type of machine.

An efficiency map for an electric machine is a contour plot of the machine efficiency on axes of torque and speed. It describes the maximum efficiency for any speed/torque combination and is a convenient way to represent the motor drive behavior over a wide range of operating.

The efficiency is defined as

$$\eta = \frac{P_{out}}{P_{in}}$$

the input power is defined as

$$P_{in} = P_{out} + P_{loss}$$

The input power is the electric power when the electric machine work as a motor and the mechanical power when the machine is used as a generator.

The losses in the motor can be divided into mechanical losses, electric losses, and magnetic losses:

- The mechanical losses are due to windage and friction in bearings; the friction increases with the square of the speed while the windage increases at cube of speed.
- The electric losses occur in the stator and in the rotor for non-permanent magnet motors; they depend on the current and on the winding's material resistance. As the Joule effect states, the losses increase proportionally with the square of the current. Moreover, considering the relation between R and temperature, the electric losses can increase also when temperature raises. For a three-phase machine the electric losses are:

$$P_{e\_losses} = 3R \cdot I^2$$

- The magnetic losses are due to hysteresis and to eddy current losses and they depend on the flux density, on the material characteristics and on the speed.

All the losses are transformed into thermal energy, which must be dissipated.

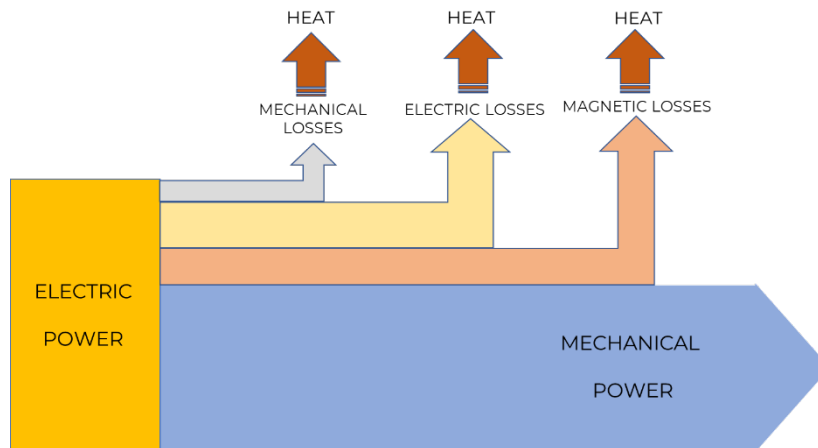


Figure 8 – Power losses in an electric motor

In order to build an efficiency map, the area of torque-speed chart is analyzed by creating a network of operational reference points. The speed changes from a minimum value  $\omega_{min}$  to a maximum value  $\omega_{max}$ : the speed range  $\omega_{max} - \omega_{min}$  is divided into parts of equal length  $\Delta\omega$  and is properly chosen to get a number reasonable of  $N$  points. For each speed, the torque changes between a minimum value  $T_{min}$  and a maximum value  $T_{max}$  with steps of  $\Delta T$  properly chosen to obtain a number of reasonable points  $M$ .

Consequently, the network in the torque-speed plane contains  $P = N \times M$  points.



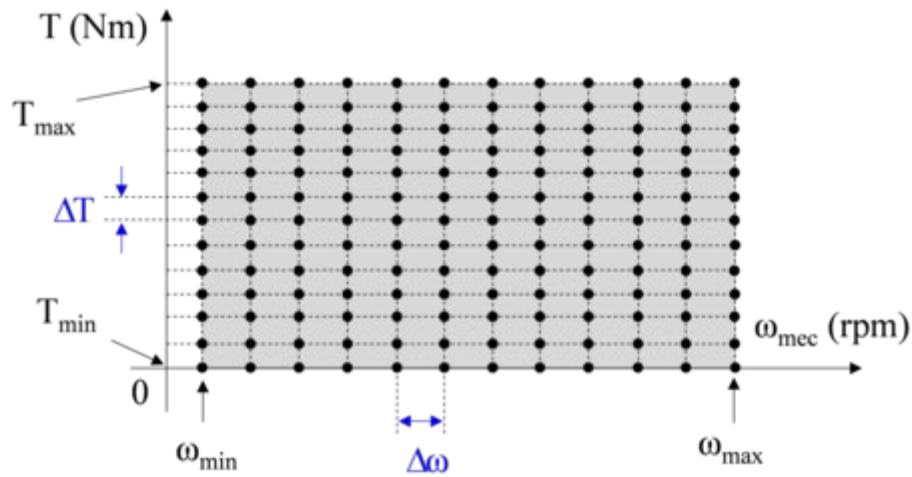


Figure 9 – Efficiency mapping strategy (HBM 2016)

Only when all the points have been processed the electrical input power and the mechanical output power are known for each evaluated point, the efficiency map can be generated.

In Figure 10 is shown the efficiency map of a synchronous electric motor.

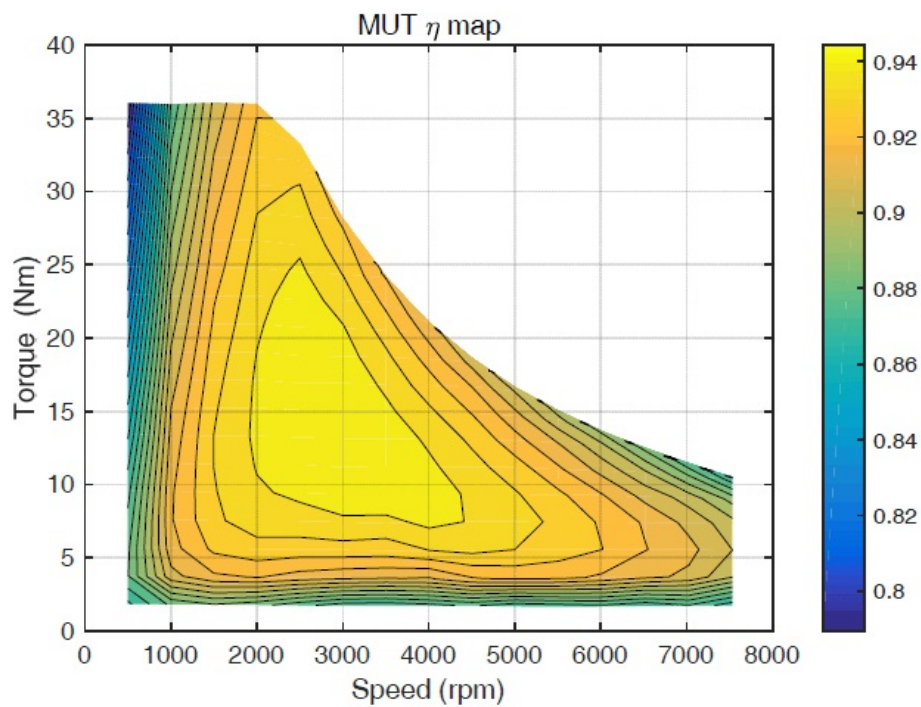


Figure 10 – Efficiency map of AC electric motor (HBM 2016)

From the efficiency values it is possible to obtain the losses of the motor and to evaluate the magnitude of the individual type of loss through analytical relations.

In this way it has a clear report of the engine performance.



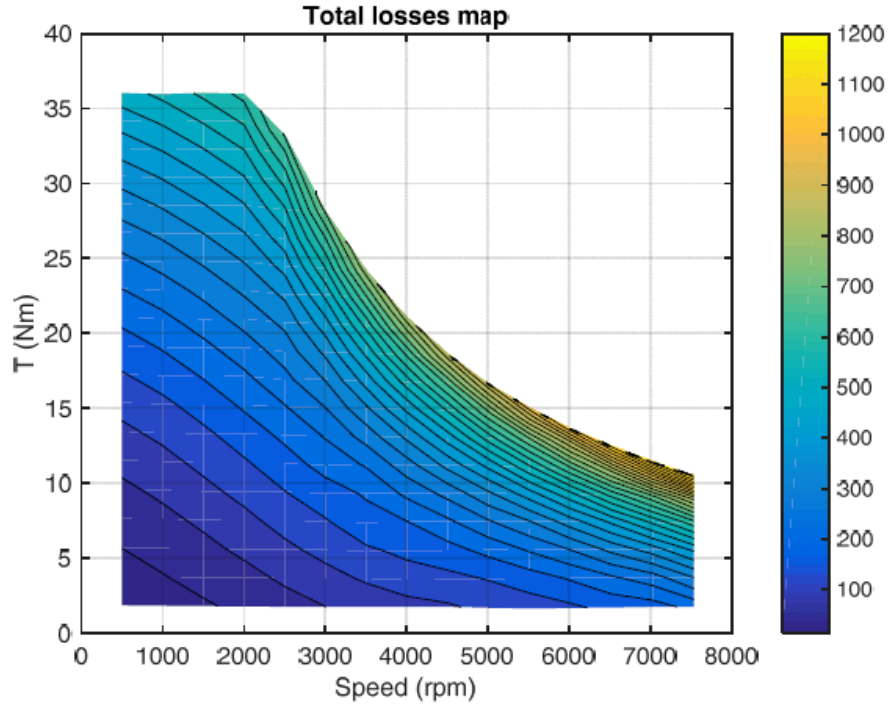


Figure 11 – Total losses map of AC electric motor (HBM 2016)

The copper losses are evaluated as

$$P_j = R_{s,avg} \frac{1}{T} \int_0^T (i_a^2 + i_b^2 + i_c^2) dt (W)$$

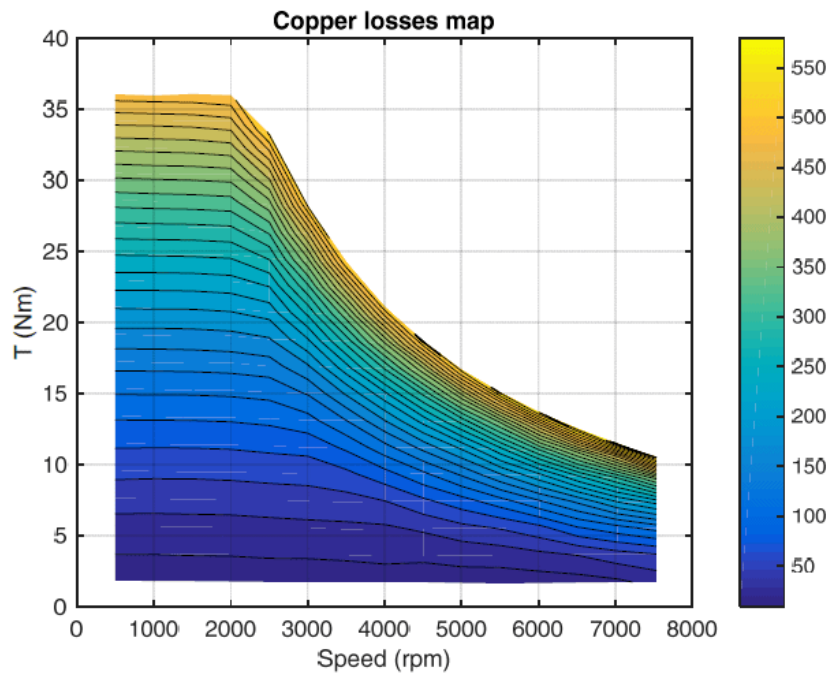


Figure 12 – Copper losses map of AC electric motor (HBM 2016)

The iron and mechanical losses are evaluated as

$$P_{FeMec} = P_e - P_m - P_j$$

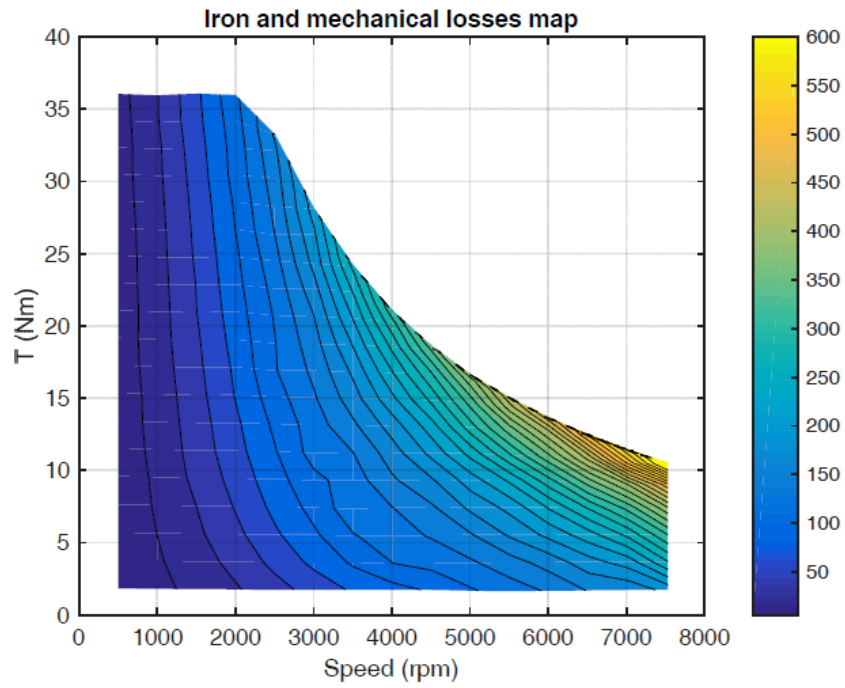


Figure 13 – Iron and mechanical losses map of AC electric motor (HBM 2016)

### 3. Equipment for the test

The laboratory where the test is carried out houses a test bench designed for testing electric motors essentially made up of a mechanical section, an electronic and a software one.

The mechanical section includes a device capable of applying a modulating resistant torque to the axis of the motor under test, two mechanical joints for the alignment of the motor under test (MUT) shaft and a structure that supports the bench itself.

The electronic part includes the sensors installed on the bench, the electronics for data acquisition and a SINAMICS inverter to impose a braking torque to the MUT.

The software to control the operations is a LabVIEW program able to perform the capturing of data and to control the load motor. In addition, the software allows to save data in TDMS format for later post-processing.

The motor under test is a permanent magnet motor with surface mounted magnets powered by an inverter connected directly to the main power source.

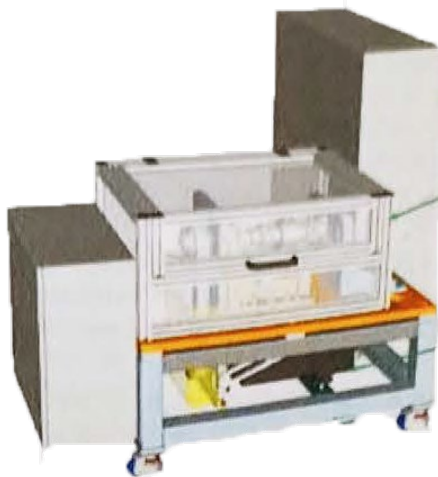


*Figure 14 – MAPRO test bench*

#### 3.1 Test Bench architecture

The test bench has been developed by the M.C.I.A. Research Center for testing medium power electric motors.

The mechanical part of the test bench is shown as a steel and transparent plastic structure in which it is possible to house the electric motor to be tested. The shaft of the electric motor is splice to the central shaft of the bench so that the rotation of the two is integral.

A system of elastic couplings is installed for the mechanical transmission to absorb small misalignments that may appear between the drive shaft and the motor shaft.

To make the measurements robust it is necessary to align the motor shaft with that of the test bench as much as possible so that vibrations and noise during tests will be reduced. The correction of misalignments takes place by changing the height and inclination of the MUT and acting on the bolts that support it.

The torque sensor is installed on the shaft of the bench, located in the center between two elastic joints; the position sensor is then placed on the left, after the second joint.

The following figure, Figure 15, illustrates the architecture of the test bench.

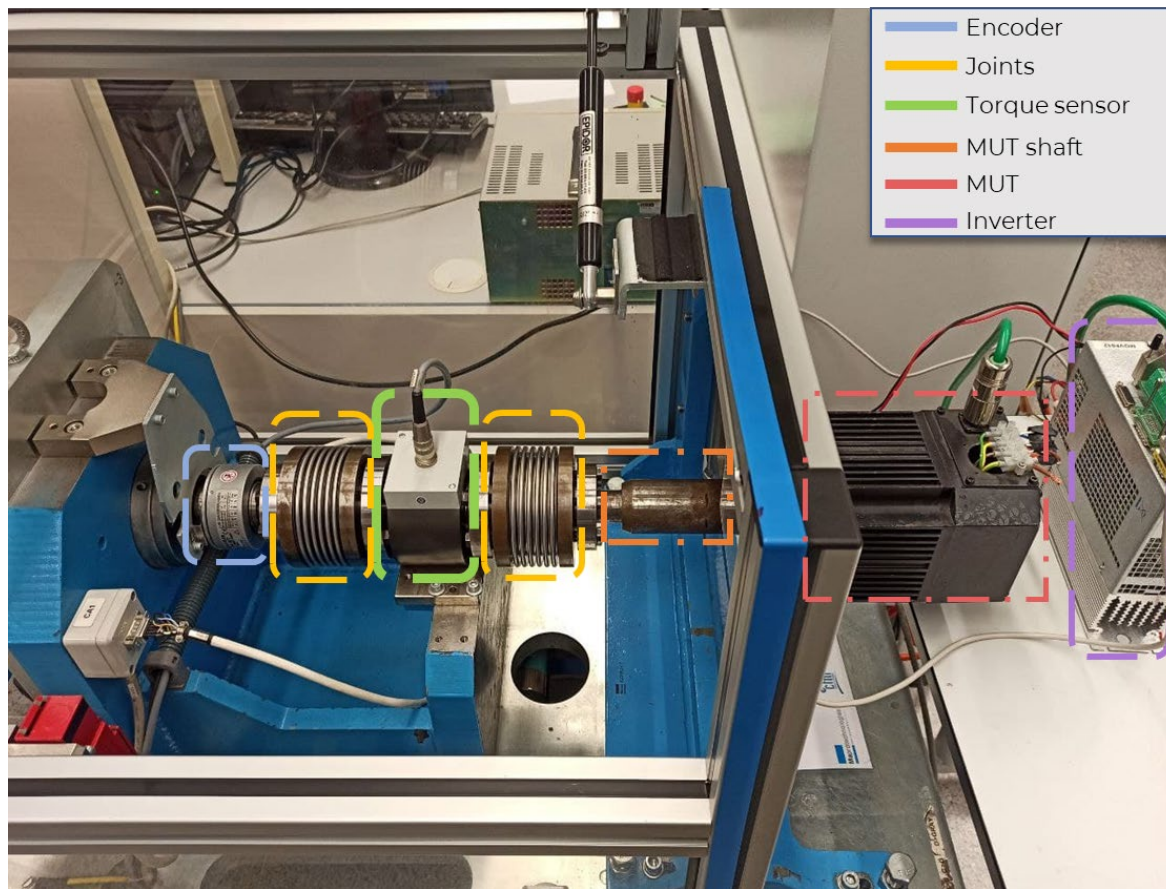


*Figure 15 – MAPRO test bench MUT and shaft details*

The central drive shaft of the test bench is connected, via a belt-pulley system, to an electric motor installed on the lower level of the test bench which allows, during the test phase, to impose a load on the tested motor.



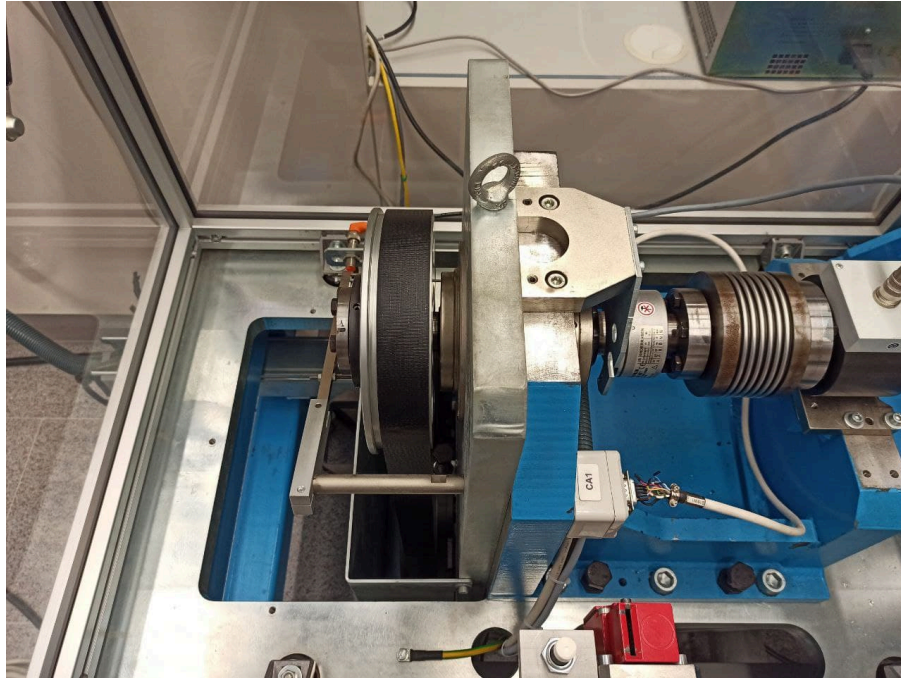


*Figure 16 – MAPRO test bench transmission parts*

The transmission ratio between the MUT and the load motor is 1: 1, for the measurements it is noted how the rotation directions of the two motors is the same and the counterclockwise rotation direction is assumed to be positive.

### 3.2 Electronics

The electrical part is enclosed in a cabin positioned next to the mechanic branch of the bench.



*Figure 17 – MAPRO test bench electric cabin*

The electrical cabin is composed of a CompactRIO for reading data from the sensors, a "SINAMICS" inverter to operate the load motor, voltage transducers, temperature sensors for reference and some safety devices to stop operation in the event of malfunction or if the emergency button is pressed.

The Compact RIO is an industrial controller made by National Instruments for control systems that holds a combination of real-time controllers.

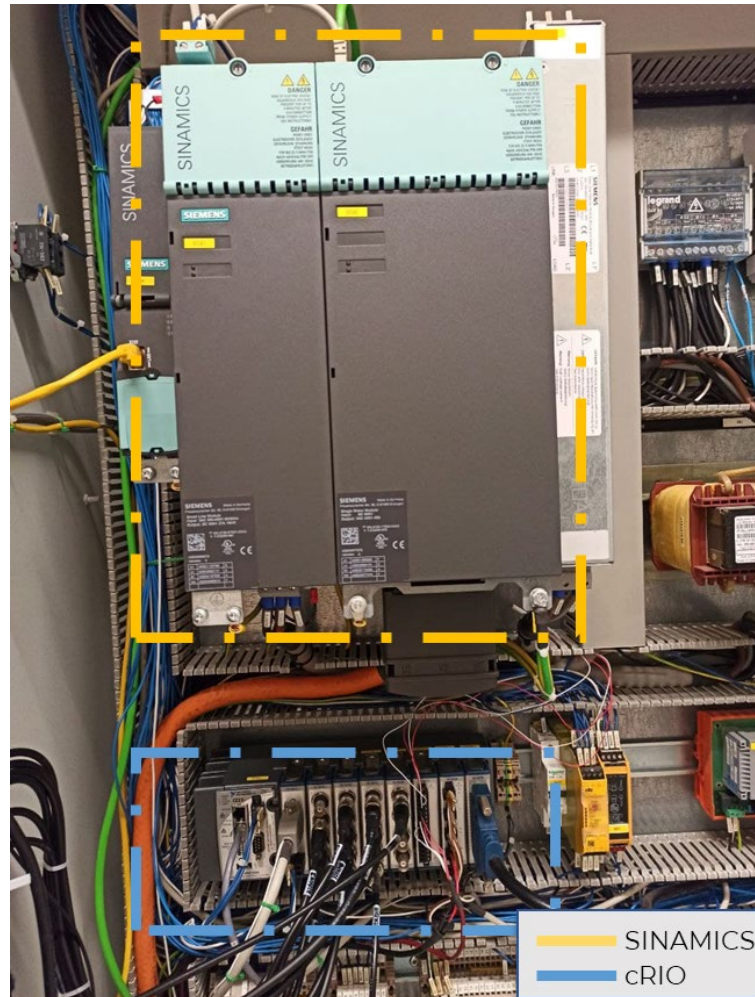


*Figure 18 – SINAMICS inverter and compact RIO devices*

The figure below is a simplified diagram of the electrical and mechanical connections in the bench: the left band indicates the power sources of the system; the central band highlights the electrical connections inside the cabin; the last band shows the mechanical arrangement of the components.

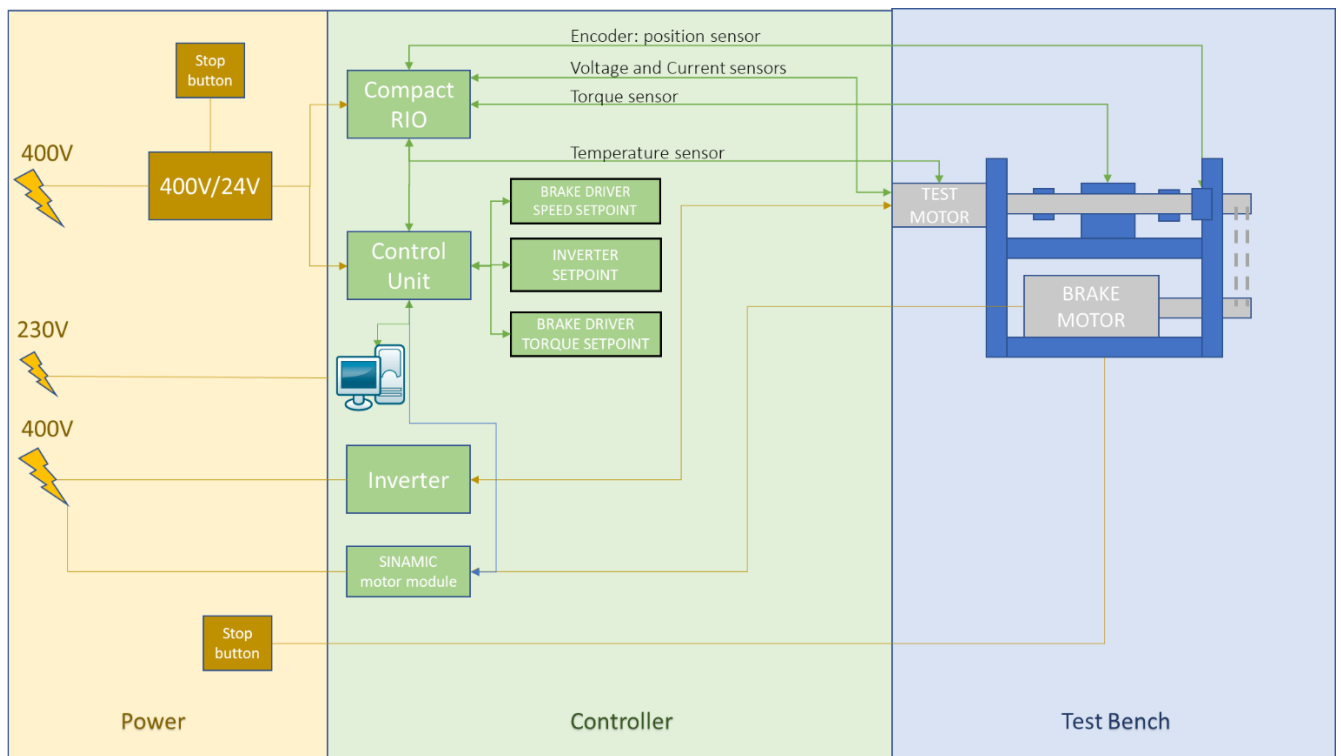


Figure 19 – MAPRO test bench connection diagram

### 3.3 Sensors

#### 3.3.1 Position/Velocity Sensor

An angular position transducer is an electromechanical device capable of converting angular position or motion into a digital code. It is placed in the test bench between the elastic joint and the pulley and it is useful to measure speed and acceleration of the motor.

The characteristics of this sensor are:

ENCODER	HENGLSTER
Housing diameter	76 mm
Shaft diameter	15 to 40 mm
Protection class shaft input	IP40
Protection class housing	IP50
Max speed	6000 rpm
Torque	Up to 10 Ncm
Moment of inertia	200 gcm <sup>2</sup>
Vibration resistance	10g = 100 m/s <sup>2</sup>
Shock resistance	100g = 1000m/s <sup>2</sup>
Operating temperature	-25°C to +100°C
Material housing	Aluminum
Weight	400g
Connection	Cable, radial

<b>General design</b>	DIN EN 61010 protection class III, contamination level 2, overvoltage class II
<b>Supply voltage</b>	DC 5V $\pm$ 10% or DC 10-30V
<b>Max current w/o load</b>	60mA (DC 5V or 10V), 35mA (DC 24V)
<b>Max pulse frequency</b>	300z

Table 1 – Position sensor specifications

### 3.3.2 Temperature Sensor

There are two temperature sensors: one is in the cabin to detect the external environment temperature used as reference, while the other is on the motor to evaluate the motor temperature.

Sensor characteristics are reported in the Table 2.

TEMPERATURE SENSOR	LABFACILITY PT100
<b>Min. Temperature</b>	-50 °C
<b>Max. Temperature</b>	+250 °C
<b>Resistance</b>	100 $\Omega$
<b>External diameter</b>	5 mm
<b>Height</b>	35 mm
<b>Material</b>	Ceramic

Table 2 – Temperature sensor specifications

### 3.3.3 Torque Sensor

To record torque variations throughout the tests there is a torque transducer which acquires torque using combined gauge technology, strain gauges and non-contact power. It provides a  $\pm 5$  V output signal while the nominal rotating speed is 9000 rpm

The max torque that the sensor can measure is 500 Nm: it is oversized because the test bench is already limited at 180Nm due to transmission system.

Torque sensor model	T22	
<b>Accuracy class</b>	0.5	
<b>Nominal torque M</b>	500	Nm
<b>Nominal sensitivity Voltage output</b>	5	V
<b>Nominal sensitivity Current output</b>	8	mA
<b>Sensitivity tolerance Voltage output</b>	$\pm 0.2$	%
<b>Sensitivity tolerance Current output</b>	$\pm 0.2$	%
<b>Output signal for zero torque V</b>	0 $\pm 0.2$	V
<b>Output signal for zero torque A</b>	10 $\pm 0.2$	mA
<b>Nominal Voltage output signal for positive nominal torque</b>	+5	V
<b>Nominal Voltage output signal for negative nominal torque</b>	-5	V
<b>Nominal Current output signal for negative nominal torque</b>	+18	mA
<b>Nominal Current output signal for negative nominal torque</b>	+2	mA
<b>Load resistance</b>	>1	M $\Omega$
<b>Group delay</b>	450	$\mu$ s
<b>Nominal voltage supply</b>	11.5 $\div$ 30	V



<b>Current consumption in measuring mode</b>	<0.2	A
<b>Nominal power consumption</b>	2.4	W
<b>Nominal temperature range</b>	+5 ÷ +45	°C
<b>Operating temperature range</b>	-5 ÷ +70	°C
<b>Storage temperature range</b>	+0 ÷ +60	°C
<b>Nominal rotation speed</b>	9000	rpm
<b>Limit torque related to nominal</b>	200	%
<b>Longitudinal limit force</b>	4	kN
<b>Lateral limit force</b>	1.4	kN
<b>Bending limit moment</b>	54	Nm
<b>Weight</b>	2000	g

Table 3 – Torque sensor specifications

### 3.3.4 Current transducers

The current sensor is a Hall effect current transducer installed between the inverter output and the motor input to detect the electric current delivered.

The advantages of the model of installed are:

- Very high accuracy;
- Low noise on output signal;
- Wide frequency bandwidth;
- High immunity to external field.

Technical data are reported in Table 4.

<b>Current Transducer</b>	<b>LEM IT 65-S ULTRASTAB</b>
<b>Supply Voltage</b>	DC 5V ± 10% or DC 10 - 30V
<b>Current w/o load</b>	60 mA (DC 5V), 60mA (DC 10V), 35 mA (DC 24V)
<b>Operating temperature range</b>	-40 ÷ +85 °C
<b>Max pulse frequency</b>	300 kHz
<b>Pulse shape</b>	Square wave
<b>Pulse duty factor</b>	1:1
<b>Accuracy</b>	0.002 %

Table 4 – Current transducer specifications

### 3.3.5 Voltage transducers

These voltage sensors have been chosen for their characteristics as low power consumption, excellent accuracy, very good linearity, low response time, high immunity to external interference.

Technical data are reported in Table 5.

<b>Voltage Transducer</b>	<b>AV100 Series - model AV750</b>
<b>Nominal RMS or DC voltage</b>	750 V
<b>Primary Voltage measuring range</b>	±1125 V
<b>RMS voltage for AC isolation test</b>	4.3 kV
<b>Measuring resistance at V = 11.4 V</b>	47 Ω
<b>Measuring resistance at V = 22.8 V</b>	184 Ω

<b>Secondary nominal RMS current</b>	50 mA
<b>Supply voltage</b>	12÷24 V ±5%
<b>Current consumption</b>	50 mA + I <sub>s</sub>
<b>Accuracy at T<sub>A</sub> = +25°C</b>	± 0.7 %
<b>Accuracy at T<sub>A</sub> = -25 ÷ 70°C</b>	± 1.5 %
<b>Accuracy at T<sub>A</sub> = -40 ÷ 85°C</b>	± 1.7 %
<b>Linearity at T<sub>A</sub> = +25°C</b>	<0.1 %
<b>Response time at 10% of V<sub>pmax</sub></b>	10 ± 13 μs
<b>Frequency bandwidth</b>	13 kHz
<b>Ambient operating T</b>	-40 ÷ +85
<b>Mass</b>	375 g

Table 5 – Voltage transducer specifications

### 3.3 Load Motor

The charging motor is a synchronous motor with nominal power of 13 kW, nominal speed of 1500 rpm, nominal torque of 83 Nm and maximum torque of 220 Nm. The complete characteristics of this motor are shown in the following table.

<b>Motor name</b>	<b>SIEMENS 1FT6108-8SB7</b>	
<b>Rated speed</b>	1500	rpm
<b>Number of poles</b>	8	-
<b>Rated torque</b>	83	Nm
<b>Rated current</b>	31	A
<b>Stall torque</b>	90	Nm
<b>Stall current</b>	31	A
<b>Optimum operating speed</b>	1500	rpm
<b>Optimum power</b>	13	kW
<b>Max speed</b>	5600	rpm
<b>Max torque</b>	220	Nm
<b>Max current</b>	116	A
<b>Torque constant</b>	2.91	Nm/A
<b>Voltage constant</b>	195	V/1000rpm
<b>Winding resistance at 20°C</b>	0.19	Ohm
<b>Rotating field inductance</b>	4.4	mH
<b>Electrical time constant</b>	23	ms
<b>Shaft torsional stiffness</b>	92000	Nm/rad
<b>Mechanical time constant</b>	1.8	ms
<b>Thermal time constant</b>	20	min
<b>Weight with brake</b>	66	kg
<b>Weight without brake</b>	61.5	kg

Table 6 – Load motor specifications

### 3.4 Inverter

The inverter directly controls the motor torque and speed from the information provided by a high-resolution position sensor.

Technical data are reported in Table 7.

Model	PAC 400
Design	Stand-alone
Cooling	Forced air
Operating power supply voltage	110 to 230 VAC single phase 50-60Hz
Under voltage threshold	100 VDC
Braking threshold	390 VDC
Overvoltage threshold	430 VDC
Integrated braking resistor	100R / 35W
External braking resistor	Minimum 50Ω
Minimum phase-to-phase inductance	1mH
Galvanic isolated auxiliary supply voltage	24VDC +/- 15% 400mA
Control loops of digital drive	
Current loop	62.5 μs
Speed and position loop	500 μs
Max speed	25'000 rpm
Continuous motor current	Losses
4 A	56 W
10 A	140 W
22 A	314 W
35 A	489 W
Temperature limits	
Max heatsink temperature	70°C
Max surrounding air Temp	50°C From 40°C the current is reduced by 3% per °C

Table 7 – Inverter specifications

The heat transfer is ensured by an external heatsink, which works with forced air-cooling system. For a proper running of the drive, the following specifications shall be fulfilled:

- The contact surface between the drive and the heatsink shall be at least as large as the drive plate.
- The planarity of the heatsink shall be better than 0.05 mm all over the rear of the drive.
- The temperature of the heatsink should never exceed 70°C.
- Maximum surrounding air temperature is 50°C and from 40°C, the rated current must be reduced by 3% per Celsius degree.

Drive configuration

Parameter	Value	Measuring unit
Max speed	3000	rpm
Phase order	120	degree
Position offset	90	degree
Max current	18	A
Rated current	9	A

Table 8 – Inverter drive settings

### 3.5 Security devices

#### 3.5.1 Anti-opening device.

To prevent the user from accessing the rotating motor shaft while the tests are being carried out, a security device with anti-opening door is installed.



*Figure 20 – MAPRO test bench anti-opening device*

#### 3.5.2 Clutch limiter detection system

To guarantee the integrity of the mechanical elements of the bench, and especially of the transmission shaft, designed to withstand torques of up to 200Nm, a clutch system with a mechanical limiter set at 180Nm has been incorporated. If the clutch trips, the latter guarantees a safety stop of the system to prevent it from continuing with the tests.

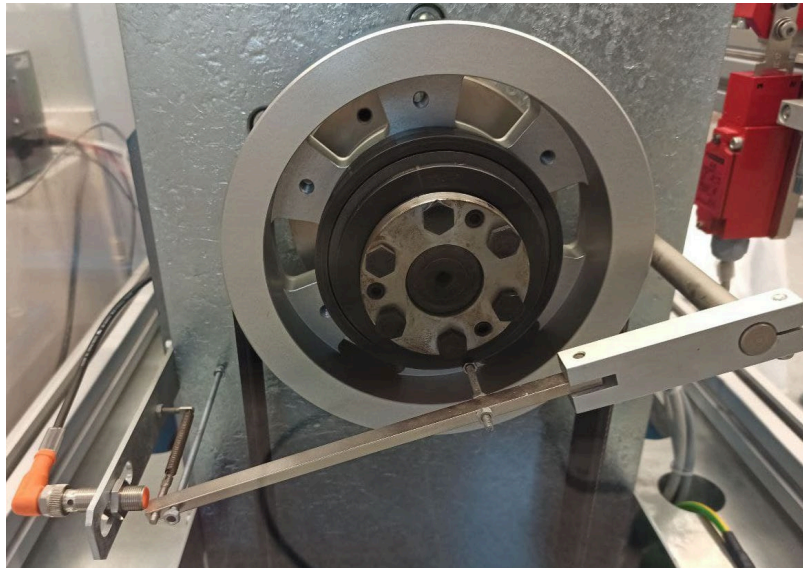


*Figure 21 – MAPRO test bench torque limiter device*

#### 3.5.3 Emergency buttons

The user can manually stop the operation by pushing the emergency button. In this condition a message of error is released and the state-machine reaches an Error state condition.

There are three main emergency buttons: two are installed on the sides cabin itself and one is positioned next to the user's workstation.

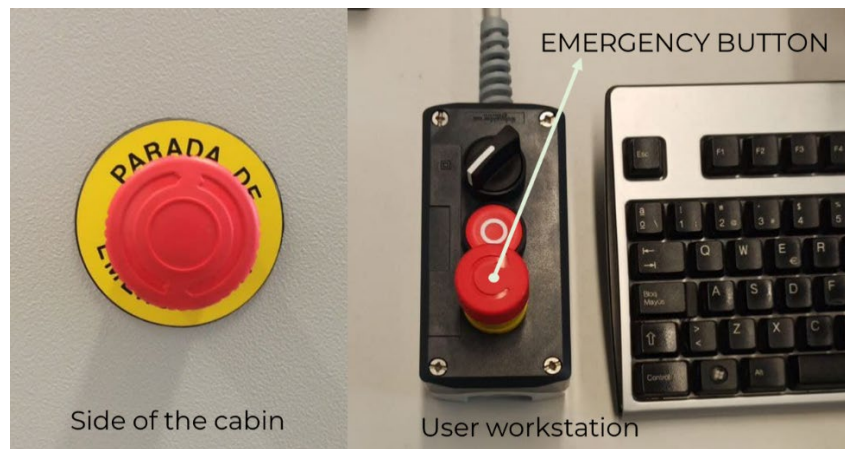


*Figure 22 – MAPRO test bench emergency button devices*

### 3.6 Acquisition program

The software for controlling the load motor and to perform data acquisition is programmed in LabVIEW platform.

The program has two main objectives: the first is to acquire sensor data from the compact RIO, convert them into user-readable values and save them in TDMS format, while the second is to communicate with the inverter to control the speed and torque of the load motor.

The program is implemented according to a *Producer / Consumer* strategy: The *Producer / Consumer* pattern gives the system the ability to easily handle multiple processes at the same time while iterating at individual rates. What makes this pattern unique is its added benefit of buffered communication between application processes. When there are multiple processes running at different speeds, buffered communication between processes is extremely effective.

The project consists of two main programs: *HOST* and *RTMain* which are executed simultaneously: the first one in the user control panel, while the second indicates the status of the components.

The interface of the "Host" sub-program is shown in *Figure 23*.

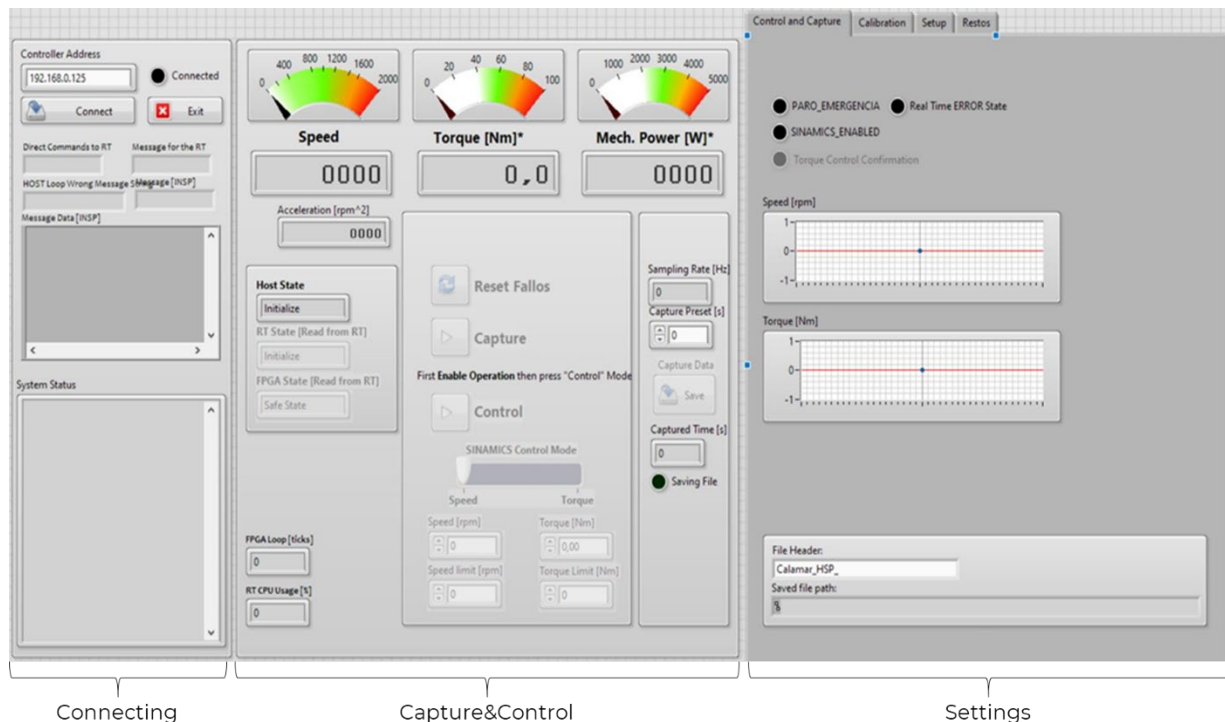


Figure 23 – MAPRO test bench acquisition tool

"Host" can be divided into three main regions: "Connecting", "Capture & Control" and "Settings". The first manages the connection with the FPGA; the second monitors the sensors and allows the acquisition of data and the control of the SINAMICS inverter; finally, *Settings* allows to set the acquisition frequency, calibrate the sensors and change the other minor parameters.

- "Connecting" is the section of the program in which the connection between the software and the acquisition electronics is established and in which messages for the user are reported. Therefore, the first step to start capturing data is to establish a connection pressing on the connect button. The green light on the right indicates the connection status.

- Capture & Control is the main section of the software: the user can acquire data pressing on Capture button and control load or speed of the load motor pressing on *Control* button. The user will immediately see the Speed, Torque and mechanical power delivered by the motor and, on the right, the actual sampling rate at which the acquisition is performed.

- Settings splits up in three tabs:

- **Control and Capture**

The three lights on the top are respectively the *Emergency Button Indicator*, which switches on when the stop button is pressed, Real Time Error State that reports to the attention of the user that an error occurs, and *Sinamics Enabled* that is the status of the load motor inverter. The LED must be ON to control the load.

The charts below, as the label indicates, represents speed and torque waveform.

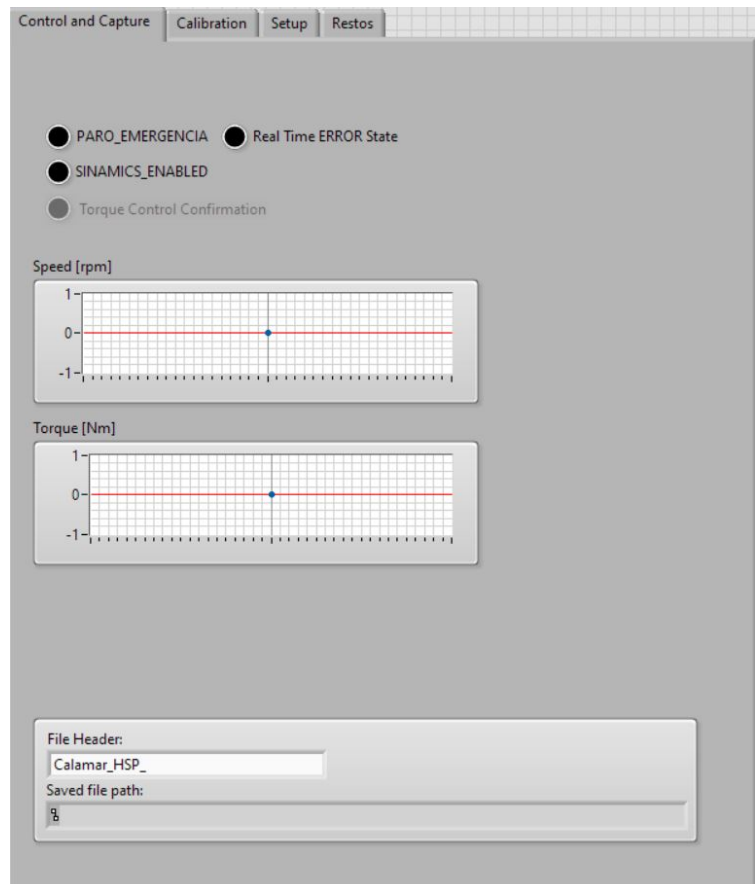


Figure 24 – Acquisition tool: Control and Capture tab



### ○ Calibration

At the top there is the possibility to change, save or import the Setpoints for the calibration; below the acquisitions of electrical and digital signals are shown in the chart with some control to adjust the horizontal and vertical range.

Additionally, there is the possibility to calibrate the signals acquired by modifying offset, conversion factor or calibration value.

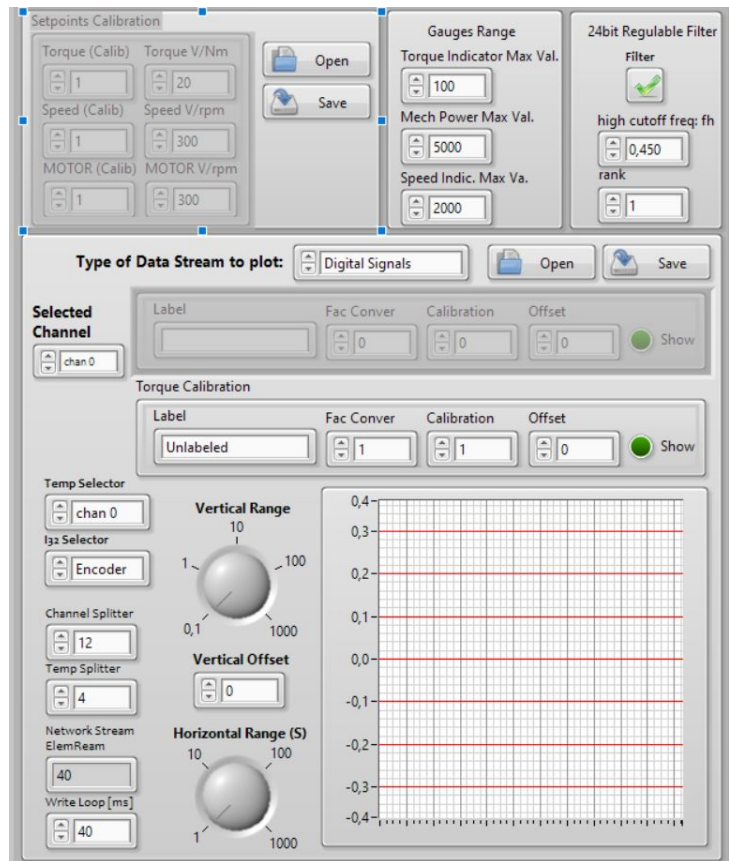


Figure 25 – Acquisition tool: Calibration tab

### ○ Setup

The FPGA settings can be modified in this tab or imported from a file that had been previously saved.

In this section it is possible to define the electrical period ticks and consequently the acquisition frequency. The maximum acquisition frequency allowed by the system is of 82kHz.

In the tab on the bottom, it is possible to change the path of the acquisition file.

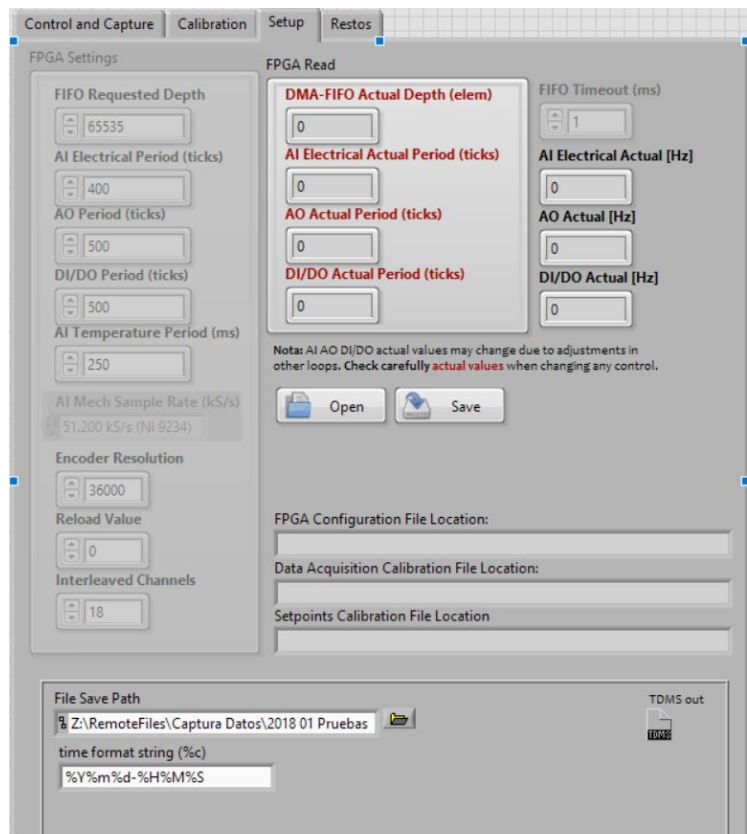


Figure 26 – Acquisition tool: Setup tab



The interface of the "Real Time" program is shown in *Figure 27*.

It is possible to check the status of the components by means of the LEDs,

- *PARA\_EMERGENCIA*: if Emergency button is pressed, the LED is ON;
- *SINAMICS\_ENABLED*: if SINAMICS is in ON state then the led will be ON;
- *ENABLE\_OPERATION*: when the state-machine enters the "Operation" state it will be possible to control the load motor. This status is indicated both by the appropriate LED and by the status in the textbox above called "*RealTime State*";
- *ERROR\_RESET*: the LED is ON if the user presses the button to reset errors;
- *HOST\_COM\_ENABLED*: if the HOST program is started and correctly connected to the cRIO the led status is ON;
- *FPGA\_COM\_ENABLED*: indicates the status of communication with FPGA has been established;
- *SETPOINT\_RESET*.

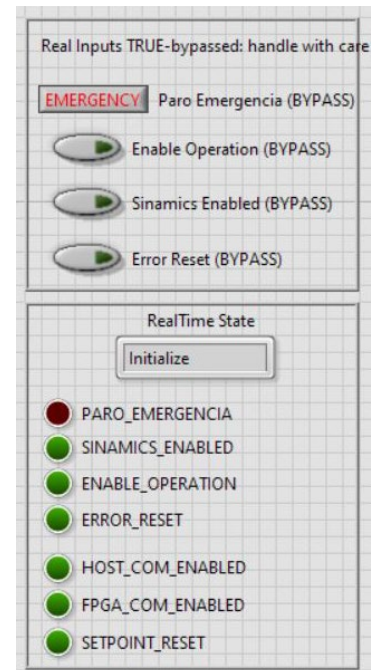


*Figure 27 – Acquisition tool: state indicators*

### 3.7 Limits

The limits of the test bench are dictated, from the mechanical point of view, by the transmission with pulley and by the maximum power of the braking motor; from the electrical point of view the limit is related to the sensors and acquisition constraints. The software results to be stable for acquisitions up to 82kHz.

The maximum power that the bench can support is 13kW as this is the limit of the braking motor with a maximum speed of 2000rpm. The maximum supported torque is 180Nm because of the belt-pulley transmission.

Moreover, the tests can be performed in a temperature range between 5 and 40 ° C.

## 4 Motor under test

The motor used for testing and validation of the developed program is a Surface Mounted Permanent Magnet (SMPM) electric motor.

SMPM electric motors have the magnets affixed to the exterior of the rotor surface. Due to this mechanical mounting, their mechanical strength is weaker than that of IPM motors. This feature limits the motor's maximum safe mechanical speed. In addition, these motors exhibit very limited magnetic saliency ( $L_d \approx L_q$ ). Inductance values measured at the rotor terminals are consistent regardless of the rotor position. Because of the near unity saliency ratio, SMPM motor designs rely significantly, if not completely, on the magnetic torque component to produce torque. (Christopher Jaszczolt 2017)

The characteristics of the e-motor are shown in *Table 9*.

Motor	MOVINOR SB6008	
Phases	Three phase motor	
Type	SMPM	
Rated speed	3000	Rpm
Maximum speed	6000	Rpm
Peak current	16	A
Stall current	8.5	A
Torque constant	0.85	Nm/A
Inertia	1.19	$\text{g} \cdot \text{m}^2$
Inductance	6.4	mH
Pole pairs	2	-
Nominal power	1500	W

*Table 9 – Motor under test specifications*

The choice of the motor under test is made considering two fundamental parameters: performance of the motor adequate to the test bench limits and low maximum torque to be in a safety zone in the event of a fault of the program under development.

It works in a safety zone since the aim is to test the program on a motor in safe conditions for the other components. The maximum speed of the motor is 6000 rpm, but the one supported by the bench is 2000 rpm. Therefore the motor test region will be limited by the bench as regards the maximum speed and by the motor itself regarding the torque.

Figure 28 – Test region shows the test region identified by the intersection between characteristics of the bench and of the MUT.

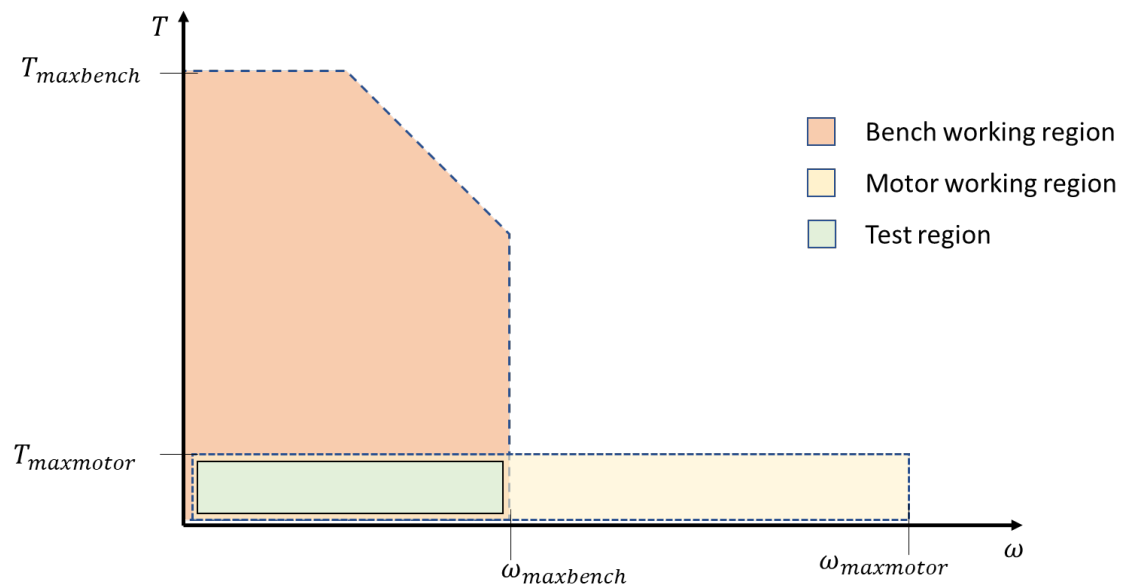


Figure 28 – Test region

#### 4.1 MUT control

The motor under test is controlled by the inverter INFRANOR whose specifications are in the chapter “Equipment for the test”. The inverter is connected to the main AC source. Inside it includes an AC-DC converter and a DC-AC converter to power the motor. In addition, the logic unit of the inverter is powered separately with a 24V DC power source.

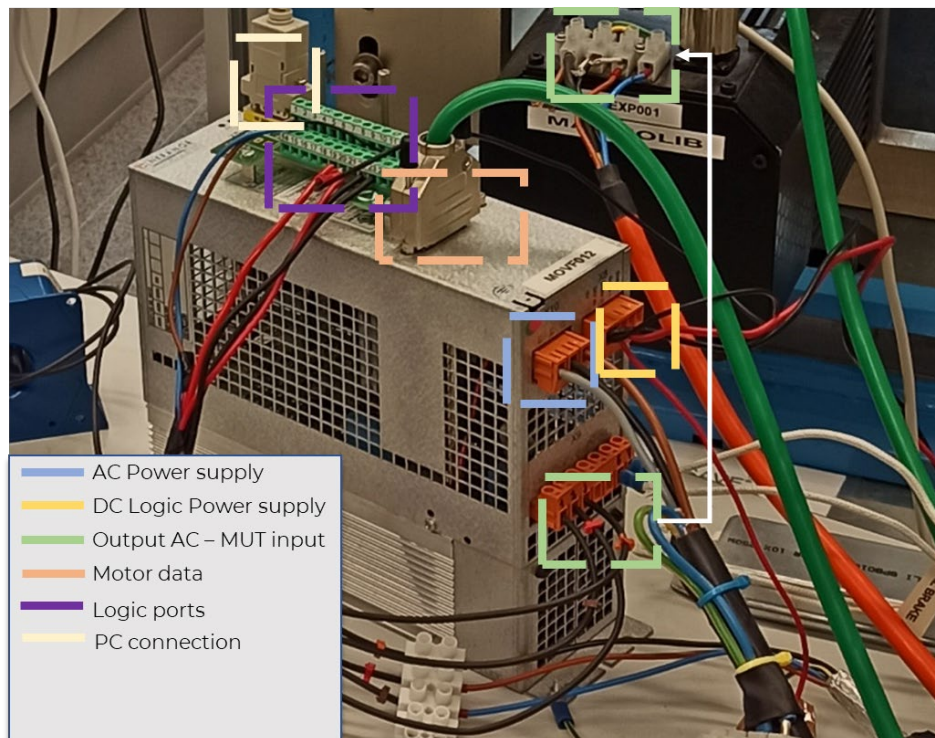


Figure 29 – INFRANOR Inverter for MUT control

The inverter commands the MUT through a vector control and the rotation speed can be managed either by connecting the device to the PC, using the inverter's proprietary software called Gem Drive Studio, or through external hardware by sending analog and digital signals to the logic ports of the inverter.

Since the purpose of the project is to control the motor automatically using LabVIEW software, it is not possible to use the proprietary software, reason why it was agreed to install an Arduino board capable of generating signals.

Three logic gates of the inverter were used: two digitals to reset errors and operate the drive and one analog to set the motor speed value.

The errors are reset by sending a 24V digital signal to a predefined input port. To do that a relay controlled by Arduino is installed. The relay is necessary as Arduino provides 5V output, so the DC power source is used to supply 24V. The errors are reset by sending a digital signal 1 and then returning the signal to 0, thus opening and then closing the circuit.

Similarly, to move the drive in operating condition a relay is installed. It can send a digital signal to the designated logic gate. The drive is ON if the digital signal is 0, and it is OFF if the signal is 1. In case of errors, however, the drive will be set to off regardless of the digital input.

The relays are connected in normally open condition (NOC), which means that their default position in the absence of control by the electronic board is open.

The speed adjustment is carried out by sending an analog signal between 0 and 5v to the inverter which will consequently adjust the motor speed to a value between 0 and 2000 rpm; this last speed corresponds to the maximum motor speed that can be tested on this bench.

Note that under maximum conditions the motor can reach 6000 rpm but, in such case, they are not considered as the limit of the test bench is lower than this value.

Since Arduino is not designed to send an analog output signal, the digital ports of the electronic board are exploited, generating Power with Modulation (PWM) signals.

Therefore, the PWM signal varies in a range between 0 and 255 where the first corresponds to zero speed while the second corresponds to the maximum rated speed of 2000 rpm.

In the inverter settings, a low pass filter function has been set at 10Hz to eliminate any discontinuity in the input signal. It is noted in a series of detections that for a value  $PWM = 0$  the analog output of the board is 20mV and not 0 mV. The speed of the motor is not zero for  $PWM=0$  and this condition is unacceptable, reason why a deadband equal to 20mV has been set to ensure that  $PWM = 0$  corresponds to zero speed.

To sum up, the motor rotation speed set by the user is converted into a value between 0 and 255. This value is interpreted by Arduino in an analog output value between 0 and 5V which in turn the inverter interprets as an angular speed value between 0 and 2000 rpm.

In Figure 30 is shown the 24V power generator.

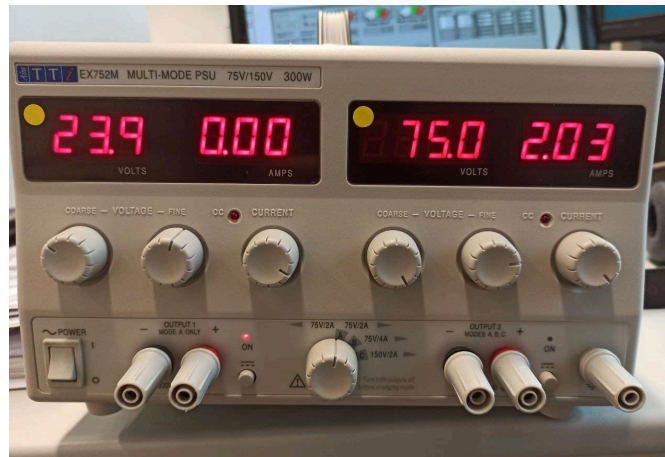


Figure 30 – Power Supply

The picture in Figure 31 illustrates the connection between Arduino and the Inverter.

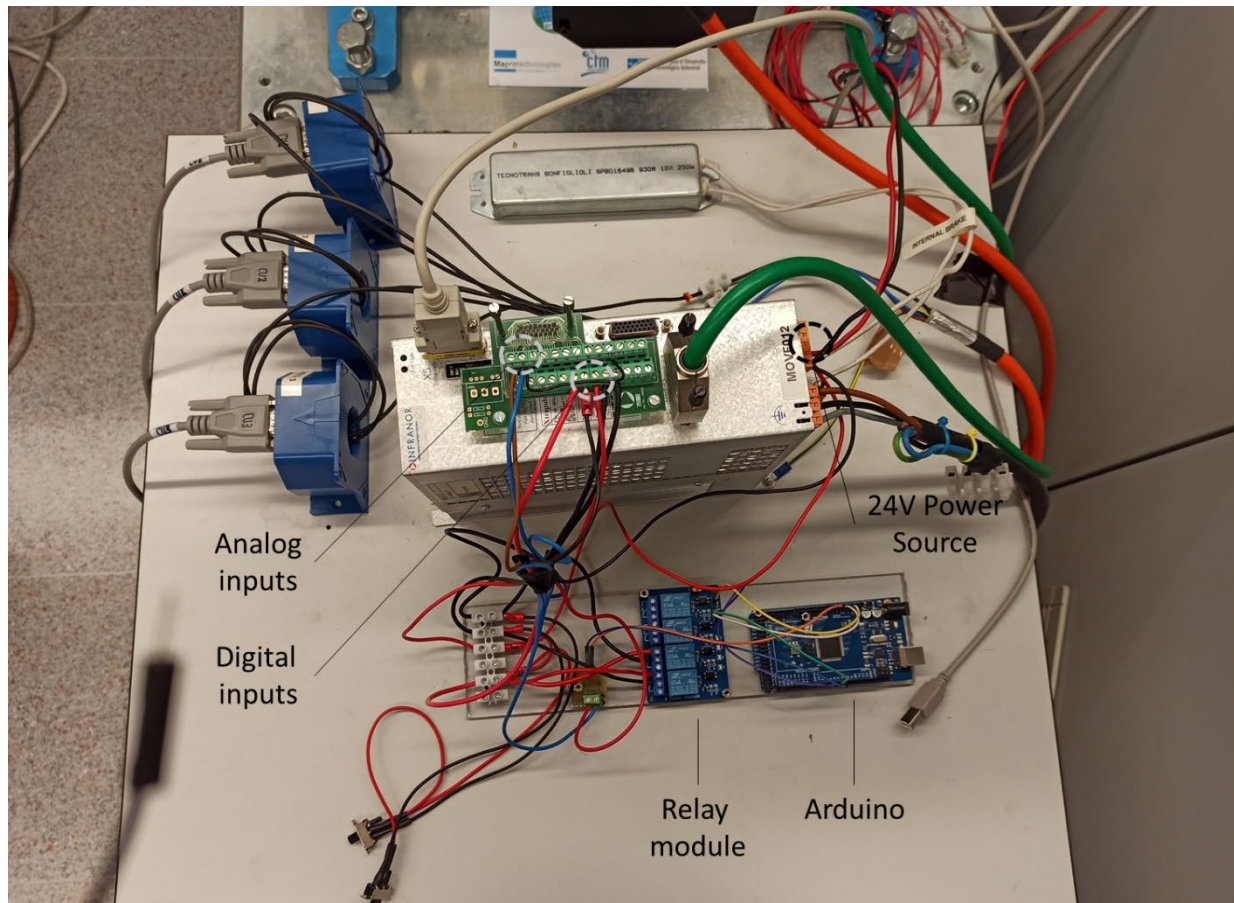


Figure 31 – Diagram for connecting Arduino to the Inverter logical ports

To relate the PWM value with the angular speed of the motor, a function  $f(PWM, rpm)$  is build acquiring fifty values of speed and reporting their respective PWM value.



The function  $f(PWM, rpm)$  is plotted in the flowing chart.

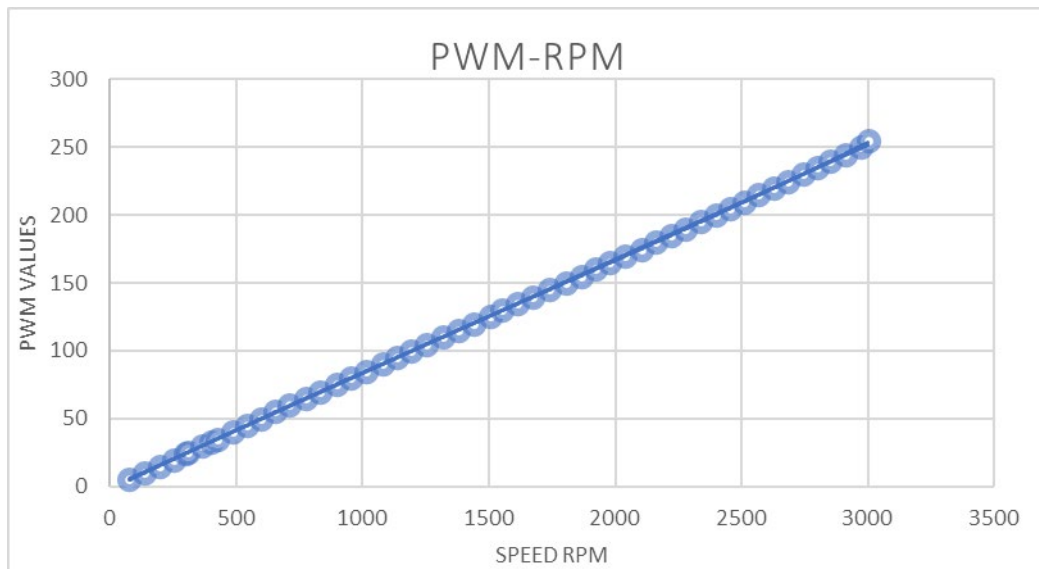


Figure 32 – Experiment-based correlation between PWM and RPM

The trend is almost linear. Precisely, it was found that the relationship between  $y \equiv PWM$  and  $x \equiv rpm$  is expressed by the following polynomial trend line.

$$y = 2E - 13x^4 + 5E - 11x^3 - 3E - 06x^2 + 0,0887x - 1,9495$$

Applying the function there is an error between speed and PWM value shown in the following graph

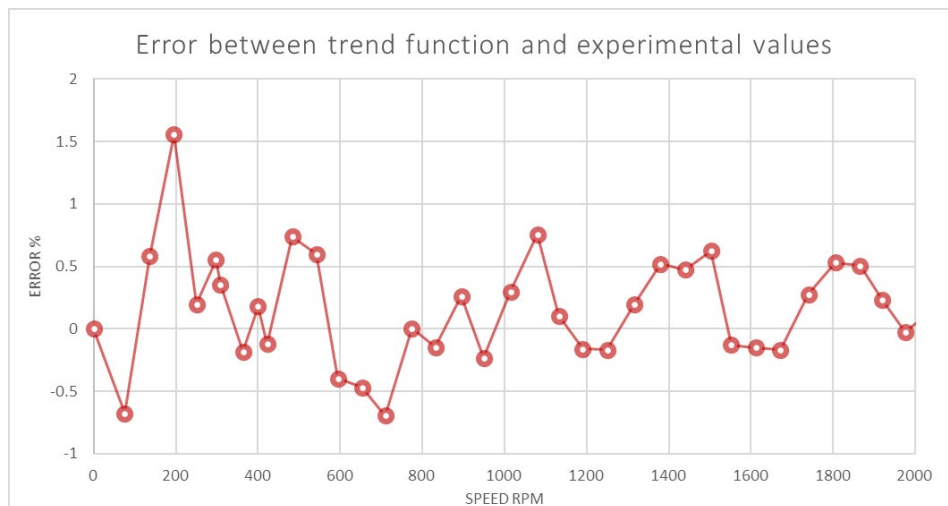


Figure 33 – Errors over the obtained function respect to the experimental values

## 4.2 Software strategy

The Finite State Machine (FSM) mathematical model was applied to manage the communication between LabVIEW program and Arduino.

The finite state automation is described by the set of states  $Q$ , variables  $\Sigma$ , the initial state  $q_0$ , a set of states of acceptance indicated in  $F$  and a transition function  $\delta: Q \times \Sigma \rightarrow Q$ .

$$\begin{aligned} Q &= \{C_{CONNECTING}, S_{TAND-BY}, C_{ONTROL}, E_{RROR}\}; \\ \Sigma &= \{1,0\} \rightarrow \Sigma^3\{C, E_C, E_R\} \\ q_0 &= C_{CONNECTING} \\ F &= \{C_{ONTROL}\} \end{aligned}$$

Each state performs an action and generates an output that, together with any user inputs, defines the transition function from one state to another (John E. Hopcroft et al. 1981).

The states are described in the following table, Table 10.

STATE	ACTION	OUTPUT
<b>CONNECTING</b>	Initialize connection with Arduino	$E_C$
<b>STAND-BY</b>	<ul style="list-style-type: none"> <li>- Send digital signal to switch on the Drive</li> <li>- PWM value = 0</li> <li>- Wait</li> </ul>	$E_C$
<b>CONTROL</b>	Vary PWM value as user requires	$E_C$
<b>ERROR</b>	Stop, put Drive OFF	

Table 10 – Finite state machine: States description

The variables are described in Table 11.

INPUT	NAME	INPUT TYPE
$C$	Enable Control (button)	User input
$E_C$	Connection Error	Arduino input
$E_R$	Error Reset (button)	User input

Table 11 – Finite state machine: Input description

The next table, Table 12, depicts the transition functions and considers the variables of the system to define the next state. The value 'X' means that the variable considered does not affect the state.

The initial state of the state machine is *CONNECTING*

STATE \ INPUT	$E_C$		$C$		$E_R$	
	1	0	1	0	1	0
$C_{CONNECTING}$	Error	Stand-by	X	X	X	X
$S_{TAND-BY}$	Error	Stand-by	Control	Stand-by	X	X
$C_{ONTROL}$	Error	Control	Control	Stand-by	X	X
$E_{RROR}$	X	X	X	X	Connecting	Error

Table 12 – Finite state machine: Control description

*CONNECTING* state tries to initialize a connection with Arduino and the  $E_C$  variable allows as output value 1 or 0. If the status is 1 it means that the Connection Error variable has a value of "TRUE". Therefore, the connection failed and the transition function brings the new status to *ERROR*. Otherwise  $E_C$  will have value 0 the next status is *STAND-BY*. *Control* button and *Error Reset* button do not affect the transition function when the state is *CONNECTING*.

Once in STAND-BY, the system remains in this state if the connection error has the value "FALSE" and the user does not define any input. If the user presses the Control button, this takes the value 1 and the status varies from STAND-BY to CONTROL. In the CONTROL state it is possible to send the PWM signal to modify the motor speed.

The system stays in control state, which is defined as the case of acceptance or final state, until an error occurs or the control variable assumes the value 0. In the first case it goes to the ERROR state, while in the second it returns to STAND-BY.

From the ERROR state, the machine can be initialized again by pressing "Error Reset" button  $E_R$ . By doing so the errors are eliminated, the previous connection is closed and the connection is retried by moving to the CONNECTING state.

Below is shown the diagram of the state machine for controlling the Arduino platform by LabVIEW platform.

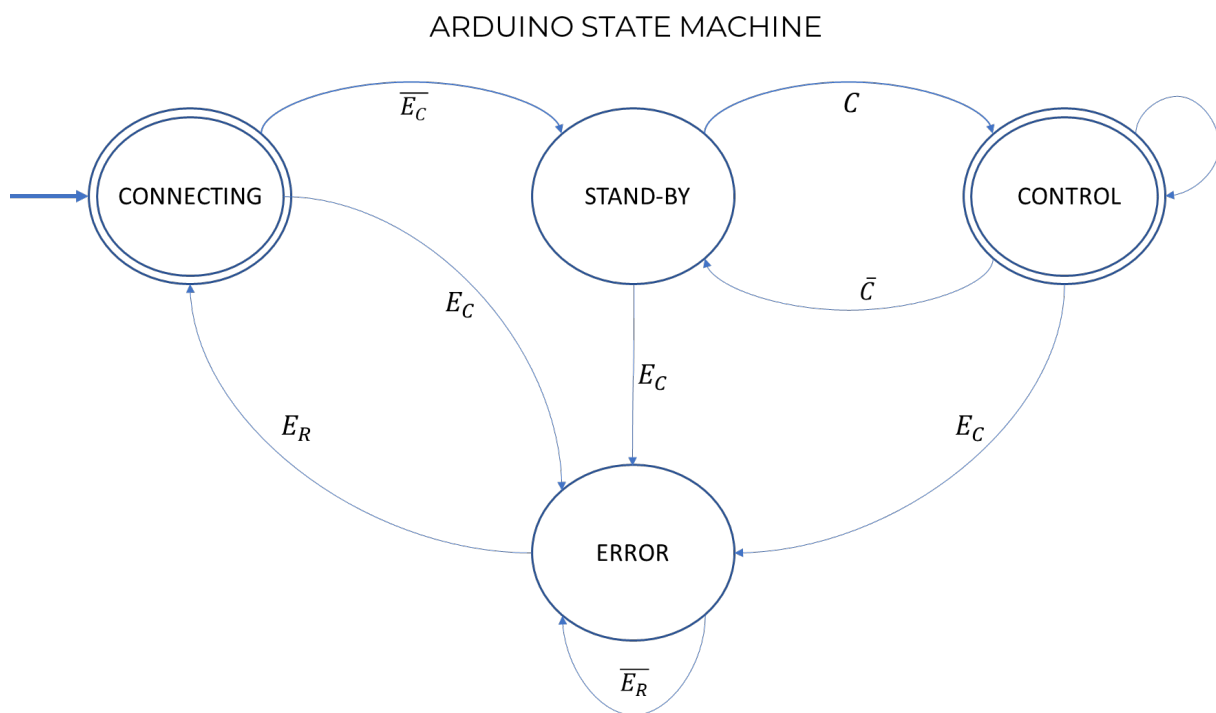


Figure 34 – Finite state machine diagram

In the user interface, it is shown the status of the machine and the error code of any failure. Noting the error code, it refers to the following table to establish the nature of the error.

Error code	Description
<b>5001</b>	You are trying to send a digital signal to a PIN not present on the board
<b>5002</b>	A connection with Arduino could not be established
<b>5003</b>	A timeout occurred while reading / writing a signal to a port
<b>5005</b>	Arduino not found in the specified COM port
<b>1073676418</b>	Generic error

Table 13 – Arduino output error description



To develop the control of the Arduino electronic board on the LabVIEW platform, it is adopted the State-Machine template provided by National Instruments.

The algorithm uses the shift register to pass from one state to the next,

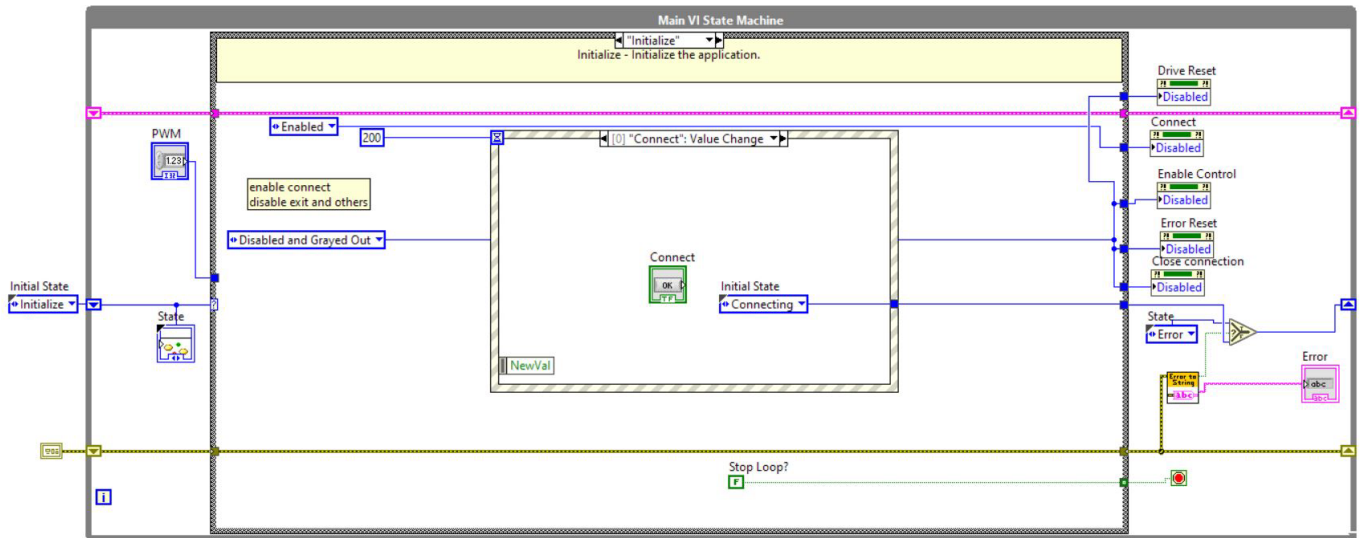


Figure 35 – LabVIEW programming code for the "Initialize" state

The initial state is called *Initialize*. In this condition, the finite state machine (FSM) waits for user's commands intercepted with an event structure. If the button called *Connect* is pressed, the next state is *CONNECTING* and the state machine enters its loop.

The *CONNECTING* status displayed in *Figure 36* shows the initialization of a connection between the PC and Arduino connected via USB protocol.

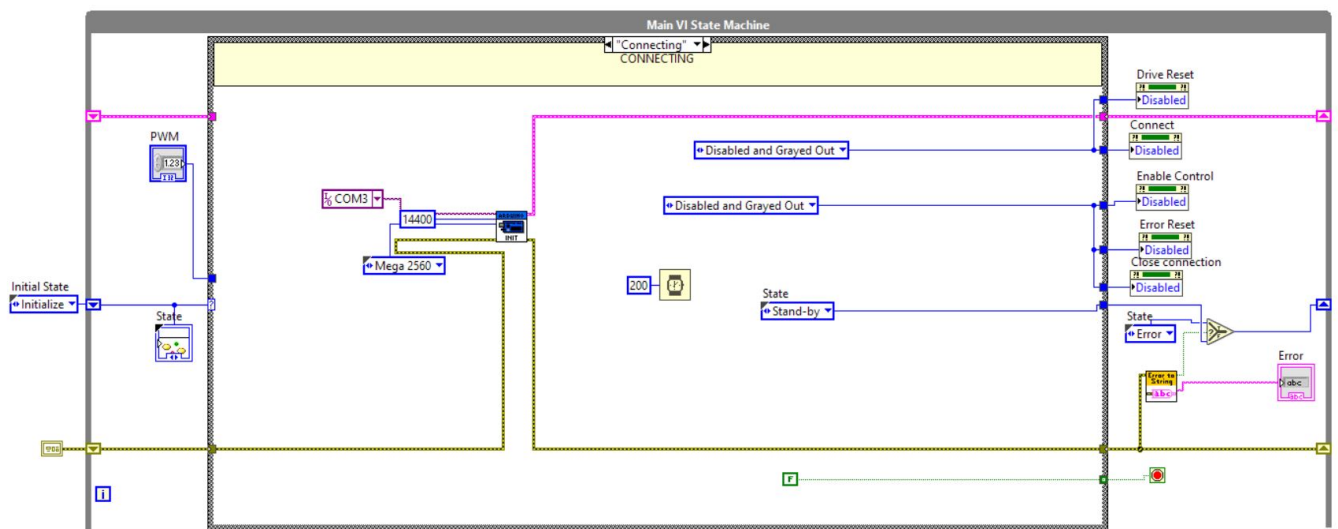
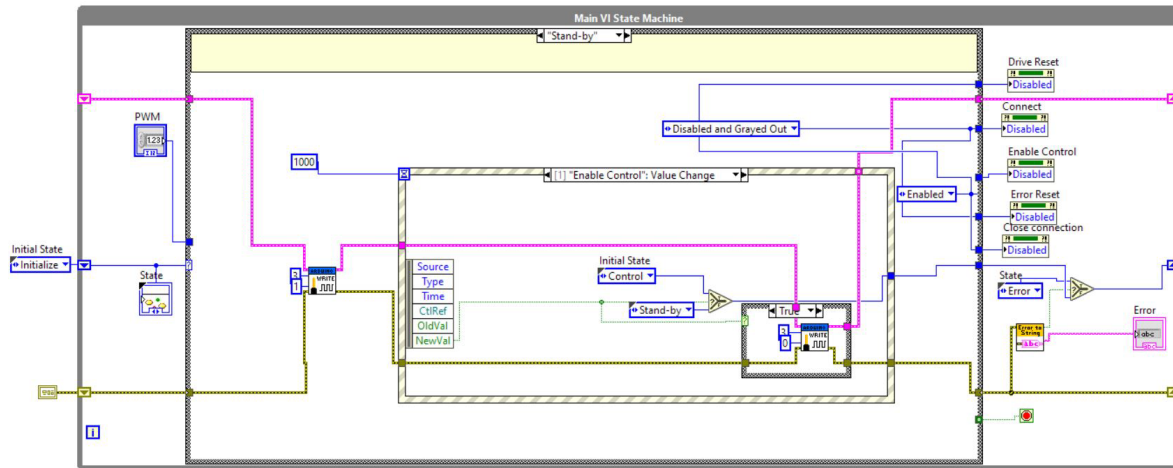
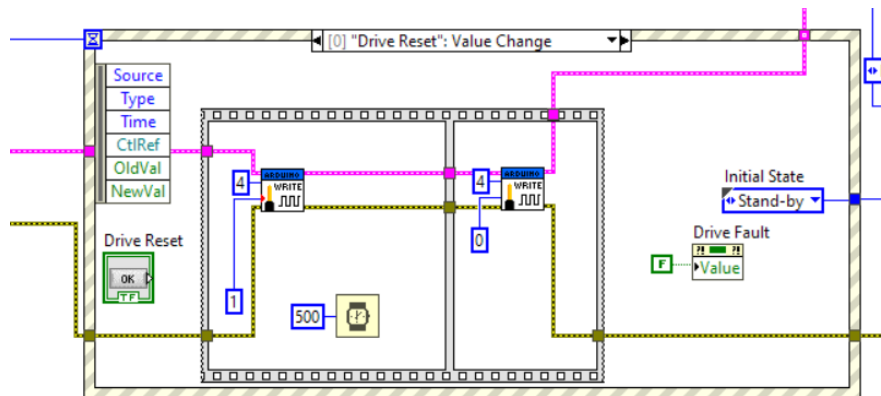


Figure 36 – LabVIEW programming code for “Connecting” state

Once the connection has been established, the next state is STAND-BY, whose diagram is shown in the following image, *Figure 37*.



In this state, a writing action is performed on digital port 3 to keep the drive in the OFF state and the *Drive Error Reset* button is enabled: pressing it the user can reset the drive errors by sending a second digital signal to port 4.



If the user enables the *Enable Control* button, the drive is switched on by sending a digital signal to port 3. The FSM now is in *CONTROL* state, in that condition the PWM value is converted into an analog signal between 0 and 5V: the user can control the motor rotation.

Figure 39 shows the algorithm for the Control state.

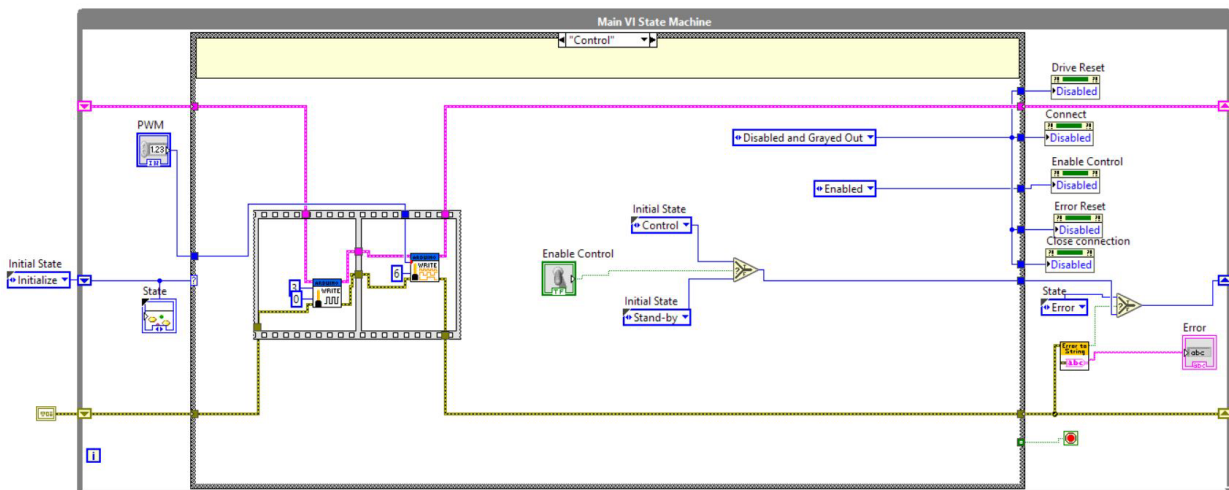


Figure 39 – LabVIEW programming code for "Control" state

Figure 40 illustrates the algorithm for the Error state where the connection is interrupted and the error status is shown to the user. Pressing the button *Error reset* the user can close the previous connection, restart a new one and reset errors.

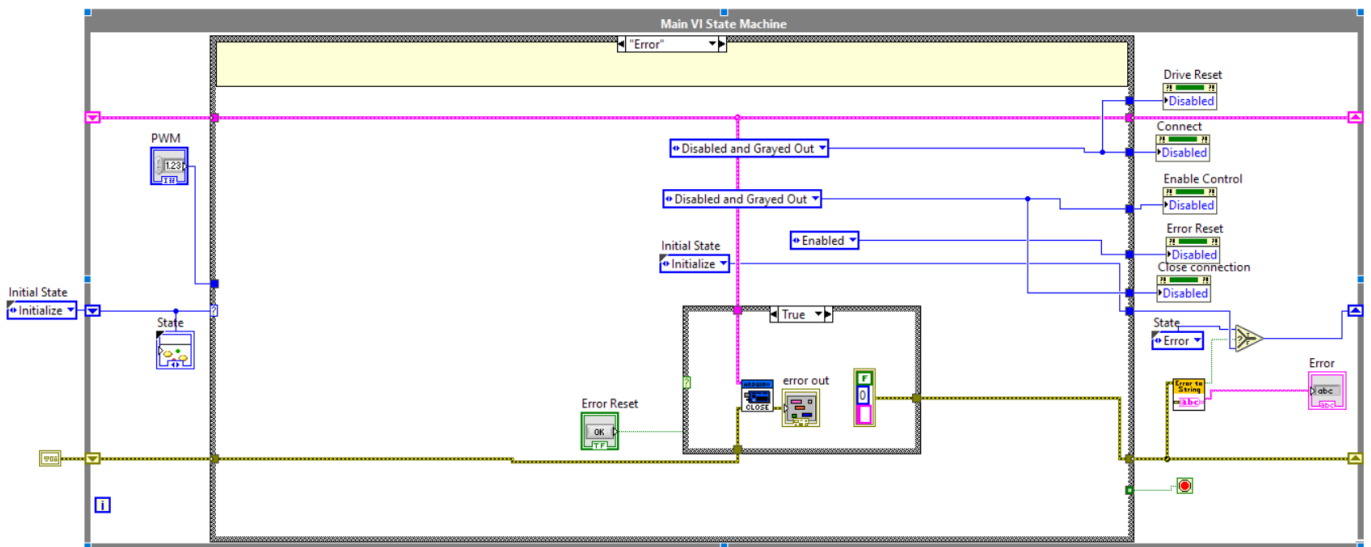


Figure 40 – LabVIEW programming code for "Error" state

Exiting from the *Error* state involves the FSM to start again from the *Initialize* state.

## 5. Automatized generation of efficiency maps

The program has the goal to develop efficiency maps from electric motor test bench in an automatic way with autonomous translation between working points.

For each work point, the program imposes the motor to rotate at the required speed and set the torque. Once the conditions are stationary, i.e. both speed and torque have reached the desired value and are constant, acquisitions of speed, torque, current and voltage are saved in an array.

The mechanical power is calculated from speed and torque values, while the electrical power is calculated from voltage and current; the ratio between the two powers is the efficiency of the motor at the point considered.

The measurements are made in steady state in terms of speed, torque and temperature. The temperature is a parameter considered in the measurements since it indirectly affects losses as the resistance of the windings varies according to the temperature (Dilshad et al. 2016).

Each point of the map is evaluated in order to complete all possible motor working points.

A theoretical completely evaluated map is represented in *Figure 41*.



*Figure 41 – Efficiency map filling strategy*

The program is also able to perform a partial study of the map modifying the initial settings and therefore deciding to evaluate a specific region or just a specific working point. The next figure, for instance, shows the approach for a partial study of the map in two specific areas.

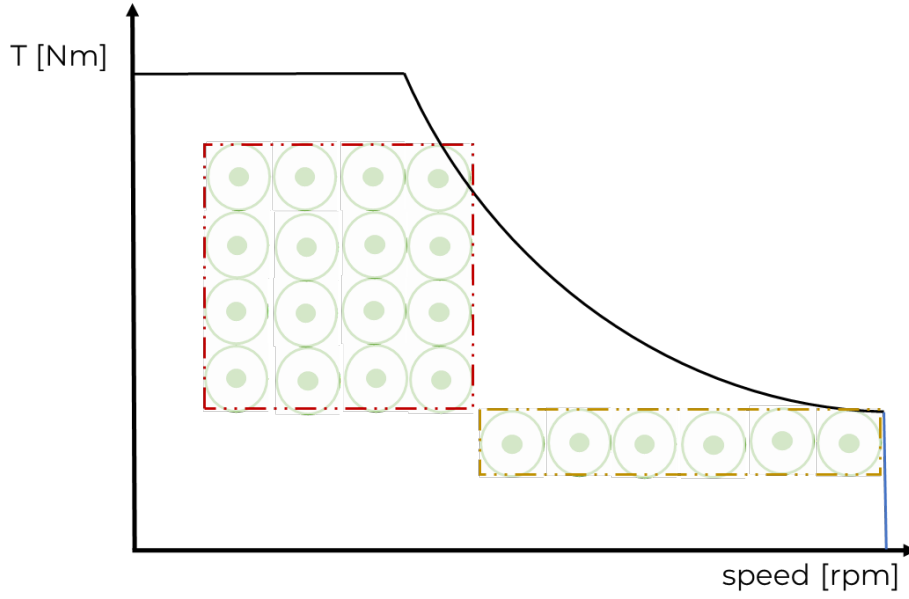


Figure 42 – Efficiency map partial regions filling strategy

The order in which you move from one work point to the next can be performed by adopting different strategies, three of them are analyzed in this report.

### 5.1 Map development strategy

The development of an efficiency map for an electric motor consists in the evaluation of all points in a speed-torque diagram, which can be reached by the motor in stationary working conditions.

A working point is defined by the coordinates of velocity and torque plus a neighborhood of the point itself, that is an error region

$$\begin{aligned} speed &= speed_{imposed} \pm error_{speed} \\ torque &= torque_{imposed} \pm error_{torque} \end{aligned}$$

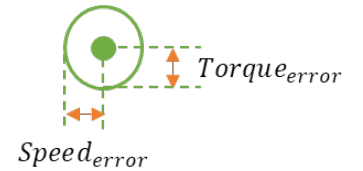


Figure 43 – Torque-speed point

Where the error factor defines the extremes of a range of values in which the speed or torque can oscillate while remaining acceptable. The error is justified by the fact that the measuring signals have noise in the signal, a finite measurement sensitivity and by the fact that the inverter has a PID control to monitor the speed which will therefore cause fluctuations in the values.

The error value is entered by the user: minimum error values will give both more accurate measurements and the ability to evaluate a greater number of points. However, if the error is less than the sensibility of the measuring instruments no measurement can be performed.

The first approach proposed for determining the efficiency map is the verticalization of the acquisition which, given a torque-speed graph, it proceeds from bottom to top to analyze all the torque points for a given constant speed.

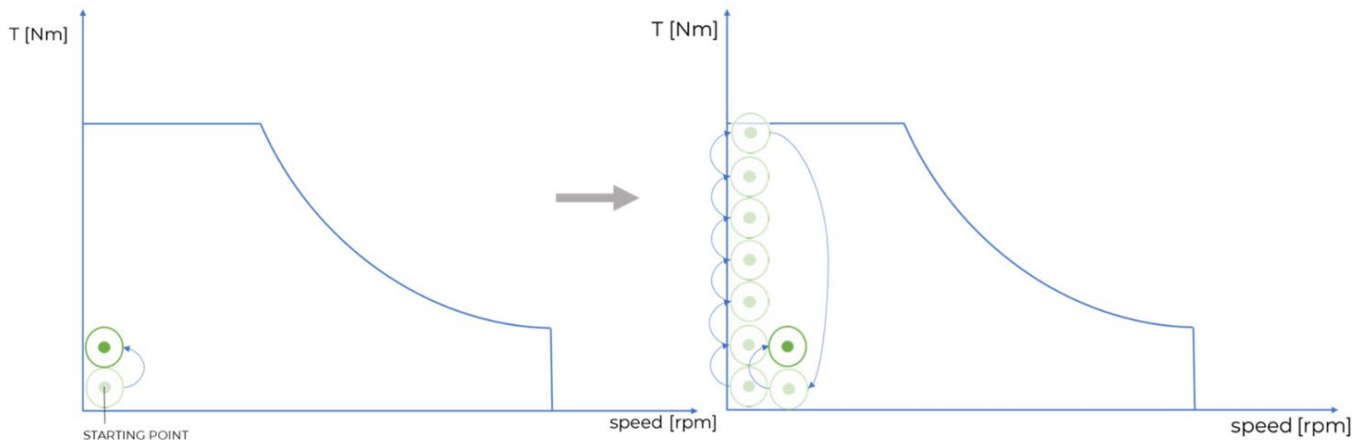


Figure 44 – Efficiency map: Vertical filling strategy

However, such method is not very effective because by increasing the torque at each point, the temperature, that is a function of the current, will increase accordingly due to the Joule effect.

The increase in temperature leads to a non-stationary condition and the software will not acquire any value until the temperature itself is constant. Therefore, since the temperature increases as the torque increases, it is necessary to wait for the temperature to stabilize for each working point, enormously increasing the acquisition times between one point to the next.

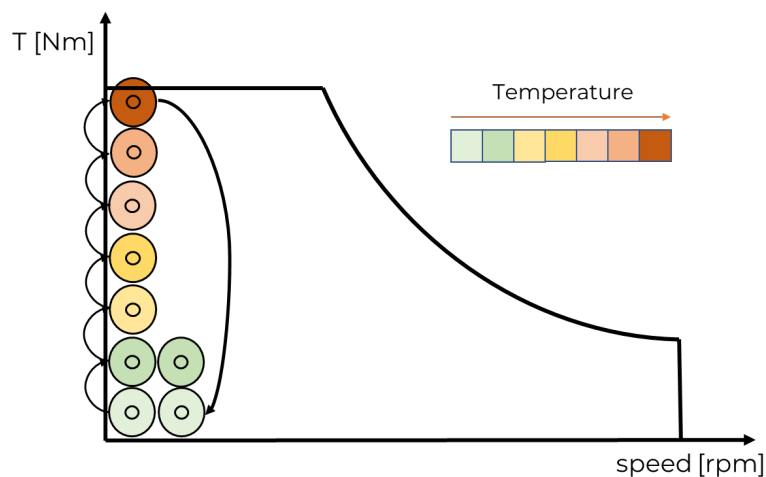


Figure 45 – Torque-speed map temperature behavior for vertical filling strategy

The vertical strategy, therefore, is inefficient in terms of time. Hence, the next strategy focuses on the horizontal filling of the map.

In this condition, the temperature gap between one working condition and the other will be smaller; therefore, the temperature will tend to be stationary "faster".

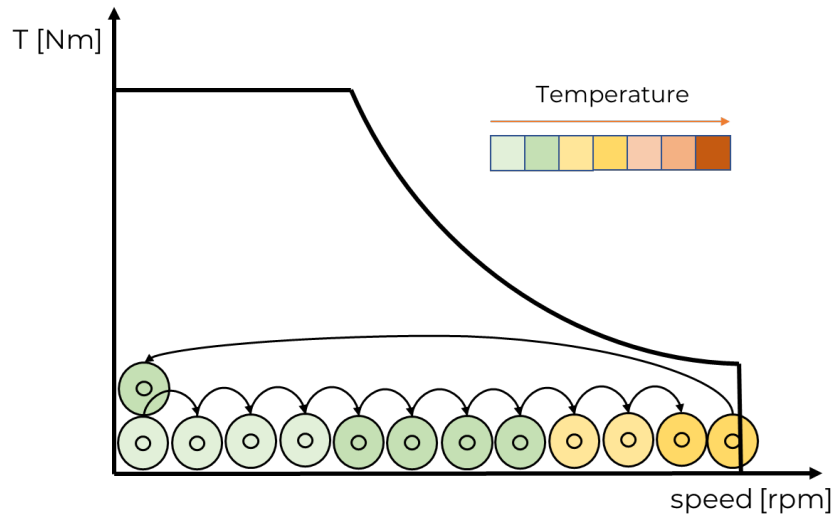


Figure 46 – Efficiency map: Horizontal filling strategy

This strategy is optimal when normal working conditions are considered. In case of flux weakening, as the speed varies, there is a more consistent rise in temperature because the current vector, generating a magnetic flux opposite to that of the permanent magnets, is directly correlated to the increase of angular speed and therefore determines an increase of internal temperature.

The third approach involves analyzing areas with almost constant temperature by dividing the nominal region by the flux weakening region.

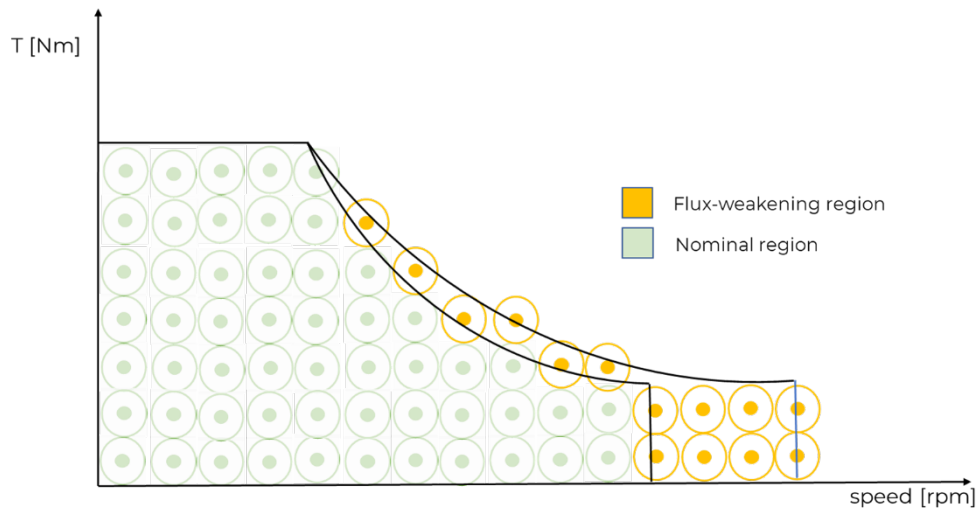


Figure 47 – Efficiency map: separate areas filling strategy

The third strategy, in fact, considers the presence of the two regions and works horizontally within a region but vertically in the transition from one region to another.

The nominal region is for  $V < bemf$  and the flux weakening region for  $V = Vmax$  where the speed is increased by varying the magnetic flux.

The work strategy adopted is identified with the horizontal advancement strategy without considering the flux-weakening as the latter occurs at higher speeds than those that can be tested with the current test bench.

Therefore, it enters in the heart of the strategy by illustrating the method by which the working points are reached, how the signals are acquired and by which method the data are processed.

## 5.2 Speed and Torque control

A point is characterized by the same speed and the same torque over time so, in test-phase both speed and torque must reach constant and stationary values.

### 5.2.1 Set speed

The motor speed, as illustrated in the “Motor Under Test control” chapter, is controlled by a PWM signal calculated by a function  $f(PWM, rpm)$  which relates the Arduino analog output value between 0 and 5V to an angular velocity value.

Therefore, for each working point the program determines the new PWM value and sends the command to the board Arduino.

The initial working point is defined by default by a speed equal to 100 rpm and a null torque. Starting from this point, proceeding horizontally and therefore increasing the speed while keeping the torque constant, the efficiency map is completed.

The motor is tested for positive speed values; therefore, the direction of the speed is counterclockwise.

The initial speed value can in any case be modified by the user as long as values allowed by the program are inserted: if the user sets the initial speed as zero the speed value will be automatically set equal to the increment value; on the contrary there are not accepted negative speeds since the Arduino analog signal is in a range between 0 and +5V.

### 5.2.2 Set torque

The torque is imposed by the load motor and it is transferred to the MUT via a belt-pulley transmission that connect the two motors.

The load motor is controlled via the SINAMICS inverter, and the torque value is imposed via a LabVIEW program already present in the system.

To define the torque, it is necessary to set both the desired torque value and the limit value: the former defines the target value of torque, while the latter defines the intensity with which the torque is varied knowing that limit. The greater the torque limit with respect to the desired torque, the more abrupt the variation to reach it.

Note how, to reach a work point, it first proceeds by setting a speed and only when the speed is reached it sets the torque. In the opposite case, if the torque is set without having defined a speed yet, the MUT will rotate in the opposite direction without control. Such condition must be avoided absolutely.

The increment of speed and torque between one point and the next is set by the user following two main models: step increment model or fixed increment model.



### 5.2.3 Increment model

#### 5.2.3.1 "Step" increment model

The step model is a strategy in which, once the user has defined a maximum motor speed and a number of steps, the increment is automatically set according to the following equation.

$$\Delta\omega = \frac{\omega_{max}}{N_{steps}}$$

Similarly, the torque increment is defined as

$$\Delta T = \frac{T_{max}}{N_{steps}}$$

The program will stop to increase the speed if the motor reaches its actual max speed or the max speed defined by the user. As for the Torque, the program will impose increasing torques until a value is reached so that the MUT will no longer be able to rotate and the drive will go into a fault condition. This condition will be discussed later.

Note that higher the number of steps, higher will the number of evaluated points be. On the other hand the acceptable error range decreases; to perform the test the user must define a tradeoff between error and the number of points to study.

#### 5.2.3.2 "Fixed" increment model

The fixed model is a way in which the user imposes manually the increment value in rpm.

Obviously, the value set by the user must be greater than zero and not greater than the maximum speed value of the motor. If one of these parameters is not respected, the speed is set by default to 100 rpm.

The *fixed model* and the step one can be used both for speed and torque increment, the final increment value is shown in the appropriate section.

Figure 48 shows a configuration of the fixed increment model

The screenshot displays a software interface for motor settings. It is divided into three main sections: MOTOR SETTINGS, INCREMENT MODEL, and INCREMENT CONDITIONS. In the MOTOR SETTINGS section, Max speed is set to 1000, Max Torque to 6, and Pole pairs number to 2. The INCREMENT MODEL section has two columns: SPEED and TORQUE. Under SPEED, the Model is set to FIXED (indicated by a blue square), and the Number of S steps is 10. Under TORQUE, the Number of T steps is 10. Below these, the Fixed Speed increment [rpm] is set to 100 and the Fixed Torque increment [Nm] is set to 0,5. The INCREMENT CONDITIONS section at the bottom shows the Speed increment [rpm] as 100 and the Torque increment [Nm] as 0,5.

MOTOR SETTINGS		
Max speed	Max Torque	Pole pairs number
1000	6	2

INCREMENT MODEL	
SPEED	TORQUE
Model: <input checked="" type="radio"/> STEP <input checked="" type="radio"/> FIXED	
Number of S steps: 10	Number of T steps: 10
Fixed Speed increment [rpm]: 100	Fixed Torque increment [Nm]: 0,5

INCREMENT CONDITIONS	
Speed increment [rpm]: 100	Torque increment [Nm]: 0,5

Figure 48 – Program motor settings

### 5.3 Speed acquisition

The speed is acquired by calculating the variation over time of the encoder signal. The encoder is a sensor that sends a 16bit signal, which indicates the rotation of the motor shaft in a range of values between 0 and 36000, the last value indicates a complete rotation.

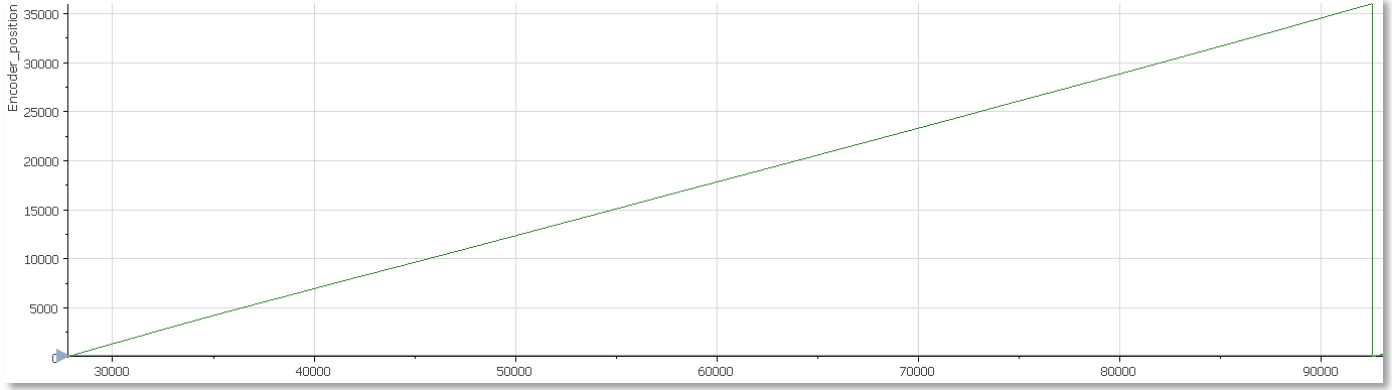


Figure 49 – Acquisition of the encoder position signal

Defined a full rotation  $\Delta_{encoder}$ , known the number of ticks in which this rotation took place  $N_{ticks}$  and known the acquisition frequency  $f$  measured in *ticks/s* the speed  $\omega$  can be determined.

$$\omega = \frac{\Delta_{encoder}}{N_{ticks}} \cdot f$$

The calculated speed values are inserted into a defined array called "Speed array".

The next step of the program involves two inspections: "CONSTANT CHECK" and "RANGE CHECK": the first monitors that the speed is in a stationary condition, while the second verifies that the speed is consistent with that set by the user.

#### 5.3.1 Constant speed verification

To check the stationarity of the system, two sub-arrays are extracted from the main speed array and compared with each other. It evaluates that the moving average of the values of the two sub-arrays is similar, i.e. within a small range.

CONSTANT CHECK is a continuous operation. To exit from this status, the speed has to be constant or if the number of iterations is higher than 200, the speed is defined not constant and the acquisition stops. A message of error appears on the user interface. In the case the speed is constant, the next step is the RANGE CHECK.

#### 5.3.2 Speed in range verification

The aim of this step is to inspect the speed array to check if the speed is included in the range set by the user. The range of acceptable values  $I$  is equal to

$$I = \omega \pm \varepsilon$$

Where  $\omega$  is the imposed speed and  $\varepsilon$  is the maximum error acceptable for that speed, the error is defined by the user.

If, for example, it is willing to test a point at a speed equal to 100 rpm and an error equal to 10 rpm, the range of values is

$$I = 100 \pm 10 \text{ rpm}$$

The following image, *Figure 50*, shows the velocity vector chart and the extremes of the range, note how in this case the "RANGE CHECK" will provide a positive result.

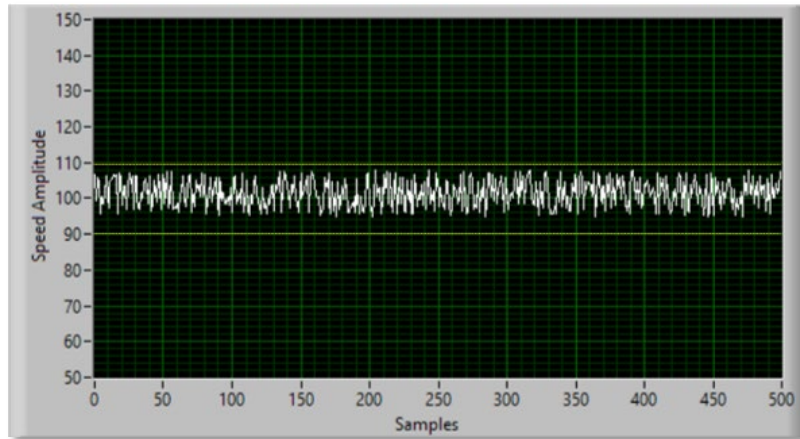


*Figure 50 – Speed signal in rpm derived from position input data and verification of required range*

The RANGE CHECK verifies that every point is within the range by calculating the maximum and minimum of the array and verifying whether these are included in the specified range.

In the event that the "RANGE CHECK" gives a negative result, it means that the current speed is different than the imposed one. Therefore the program can automatically correct the PWM value through the "AUTO-ADJUSTING FUNCTION" in order to reach the speed indicated by the user.

#### *5.3.2.1 Auto-adjusting function*

The auto adjusting function is activated if, although the speed is stationary, it does not fall within the desired range.

By analyzing the array, in the event that the maximum value is less than the minimum of the range, the PWM value is increased by one unit.

$$\text{if } \omega_{actual\_max} < \omega - \varepsilon$$

$$PWM = PWM + 1$$

Otherwise

$$\text{if } \omega_{actual\_min} > \omega + \varepsilon$$

$$PWM = PWM - 1$$

the PWM value is decreased by one unit.

If the speed fails to obtain a positive result at the "RANGE CHECK" after the function is performed the program will advise the user to vary the error range as the control by analog signal of the MUT is unable to be accurate as required.

If the speed is not in the chosen range and the PWM value has reached the maximum value, the acquisition of the speed cannot continue because the maximum motor speed has been reached.

In the case of the motor under study, the function  $f(PWM, rpm)$  it is very accurate and therefore does not require ADJUSTING FUNCTION which, however, has been implemented anyway since the program is designed to perform tests for a generic electric motor. In addition, this function allows the user to perform the tests even without knowing the function  $f(PWM, rpm)$ .

## 5.4 Torque Acquisition

Torque is acquired through a torque sensor which outputs a 24bit electrical signal between 0 and 10V. The signal is acquired by the program, converted into Nm according to the function

$$T[Nm] = \frac{T[V]}{k[V/Nm]}$$

where  $k = 0.02 V/Nm$

and saved in an array.

### 5.4.1 Torque verification

Similarly to speed verification, the torque values saved in the "Torque array" are inspected to perform the two functions "CONSTANT CHECK" and "RANGE CHECK".

In the initial experimentation phase, it was found that the noise of the received signal was very high, this condition makes the RANGE CHECK function always FALSE as maximum and minimum peaks are easily reached far outside the chosen acquisition range.

Defined a maximum error equal to 20% of the set torque, an acceptable range is obtained for

$$I = 1 \pm 0.2 Nm$$

While in the real acquisition the detected error exceeds 100% as shown in the next figure, *Figure 51*.

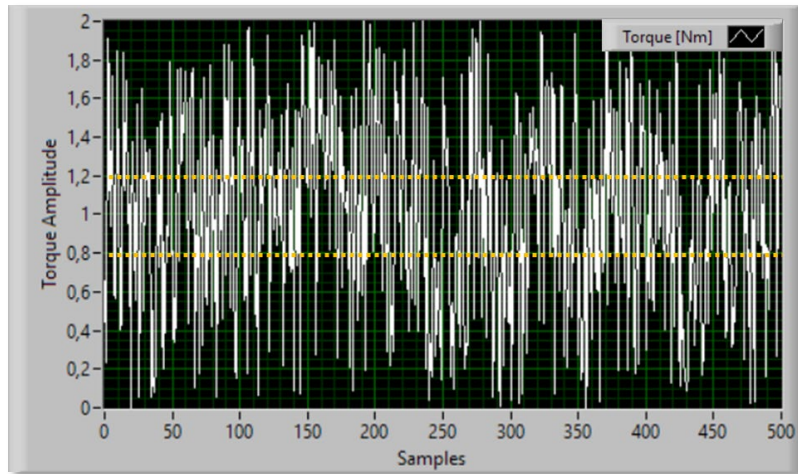


*Figure 51 – Torque signal and verification of required range*

The only way to overcome this constraint is to impose an error greater than 100% of the torque value: this condition is unacceptable.

In order to solve this, a 100nF capacitor was installed to filter out unwanted frequencies and obtain a smoother signal. The result is shown in the next picture, *Figure 52*.

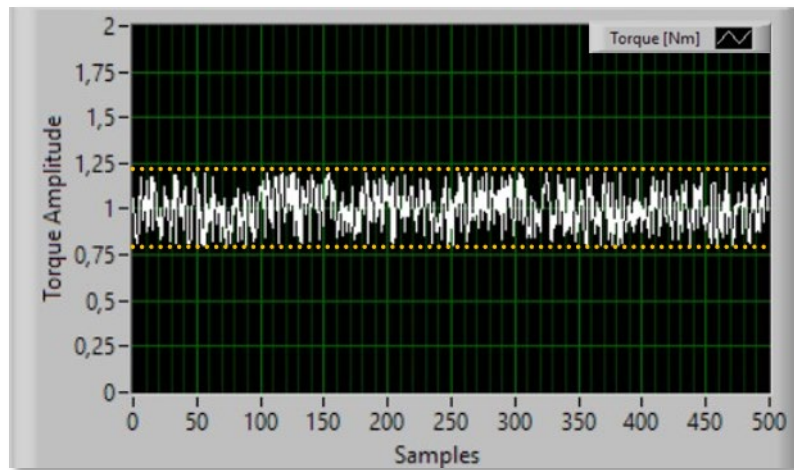


Figure 52 – Torque signal after installing a 100nF capacitor and verification of the required range

Note that the CONSTANT CHECK function, on the other hand, is not affected by the noise as it only analyzes the average of the acquired values.

## 5.5 Current acquisition

The acquisition of the current is performed using LEM current sensors described in the Equipment chapter.

The sensors exploit the Hall effect, that is the physical phenomenon for which it observes a potential difference in a transverse direction in a conductor crossed by an electric current in the longitudinal direction when this is subjected to a perpendicular magnetic field. It provides an electrical signal between 0 and 5V translated by the program into a current value.

The operating system of a current sensor is shown schematically below in Figure 53.

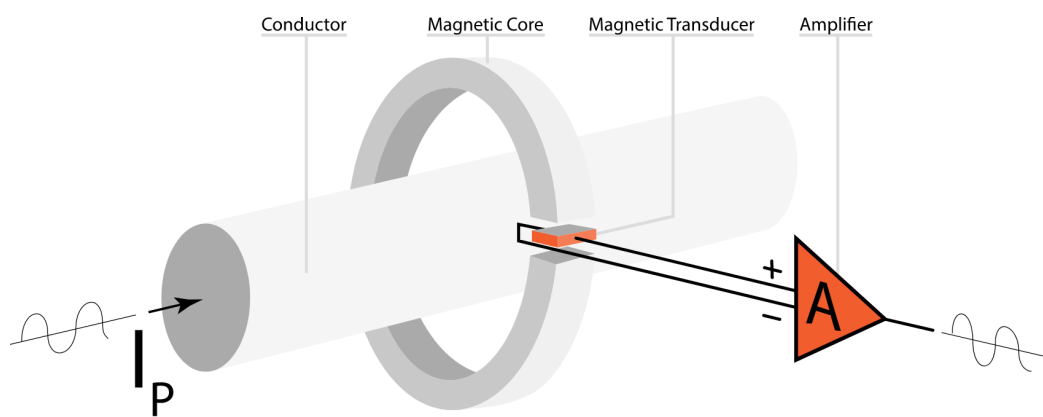


Figure 53 – Current sensor operating system scheme

These sensors are positioned between the inverter and the motor and are connected as shown in the following diagram in Figure 54.

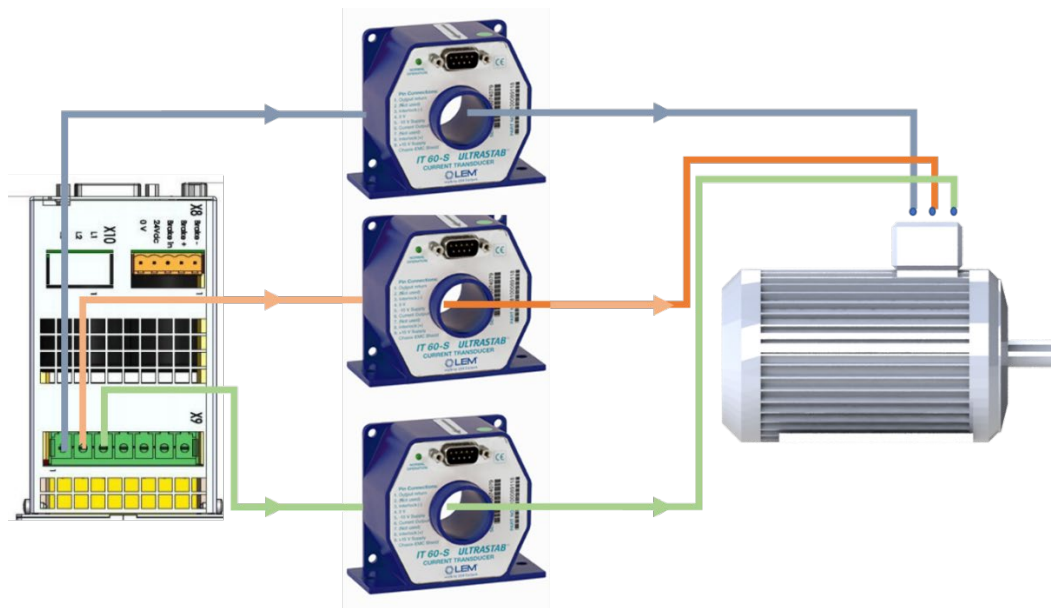


Figure 54 – Current sensors connection diagram

The sensors are connected to the cabin for power supply and data exchange.

Figure 55 shows the positioning of the sensors.

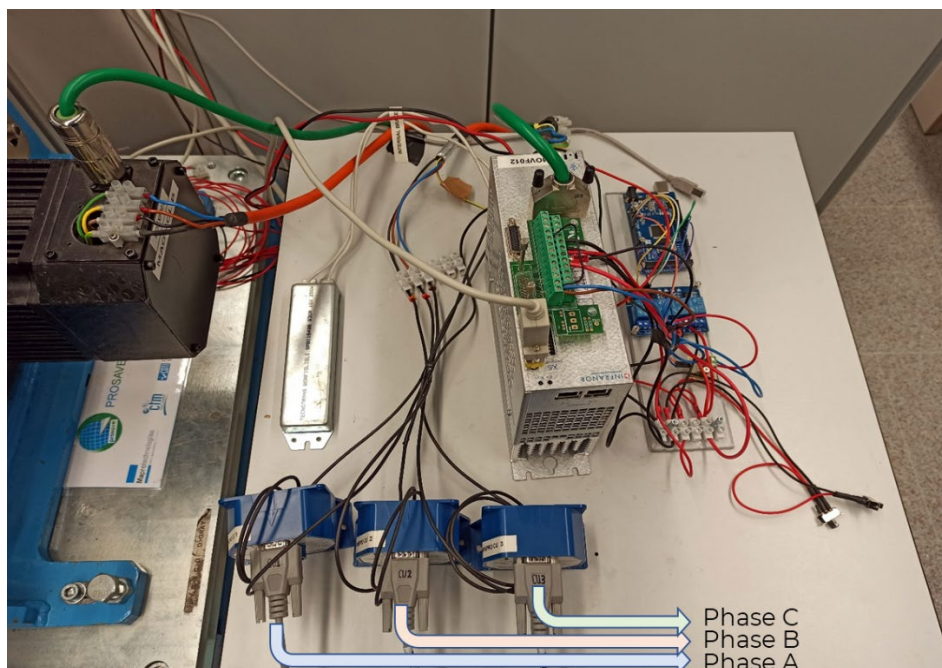


Figure 55 – Current sensor connection on the bench



In Figure 56 is shown the connection of the sensors to the electrical cabinet.



Figure 56 – Current sensors connection to the electric cabin

Note how the electronic allows to connect up to six current sensors at the same time, in the case of study only the CU01, CU02 and CU03 ports will be used for the three sensors, the other ports are left disconnected.

The acquired data of the three sensors are saved in three arrays, one for each phase, called respectively “Current A”, “Current B” and “Current C”.

The data contained in the arrays, before being processed, are filtered to eliminate noise and acquisition defects. In this regard, LabVIEW provides various functions to filter the signal: a Lowpass Butterworth Filter has been chosen.

In Figure 57 is represented a current acquisition. Moreover, it is proposed a comparison between filtered and not filtered current signal.

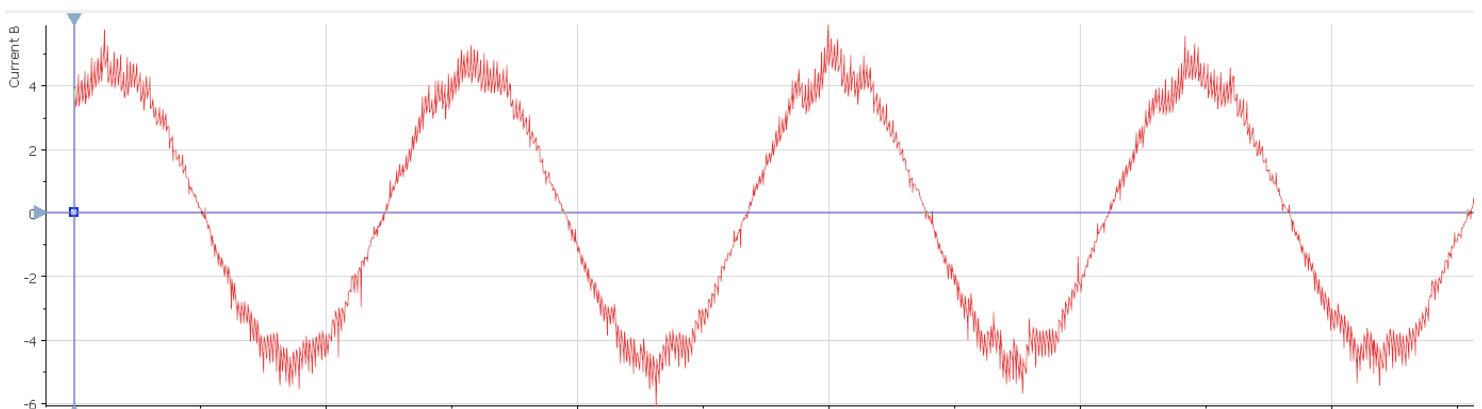


Figure 57 – Acquisition of a current signal [A] from one phase

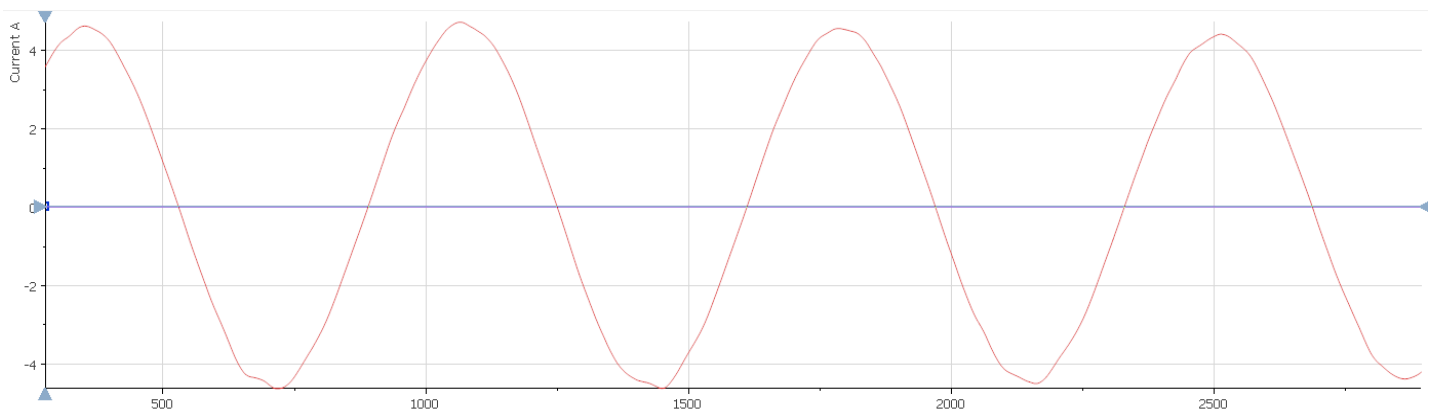


Figure 58 – Acquisition and filtering of a current signal [A] from one phase

## 5.6 Voltage acquisition

The windings of the three phases of the motor are connected with star geometry to each other. The voltage sensors are positioned between the inverter and the motor and they are connected at the ends of each winding to measure the voltage waveform of each phase. It uses a common ground connection for the sensor that is a typical feature of the star connection.

Figure 59 shows the wiring diagram of the connection to the voltage sensors.

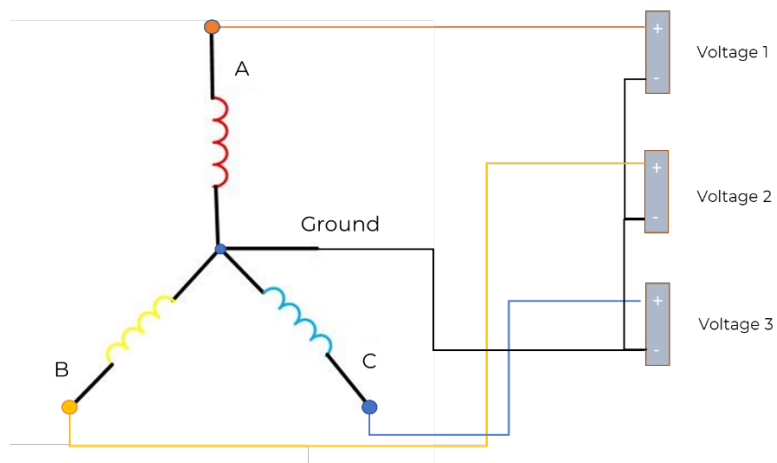


Figure 59 – Voltage transducers connection diagram



Figure 60 shows the connection of the voltage sensors on the motor side (on the right) and on the cabinet side (on the left).

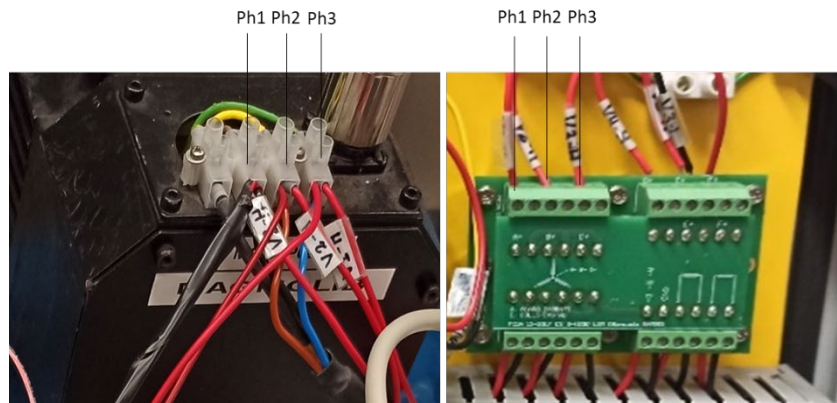


Figure 60 – Voltage transducers connection to the motor (on the left) and to the cabin (right side)

A printed electronic circuit (on the right) connects the phases in star configuration joining the negative poles of each phase to the ground.

The three voltage values of the three phases are saved in the respective three arrays named as “Voltage A”, “Voltage B” and “Voltage C”.

The results obtained for three phase acquisition at 50Hz are shown in the image below

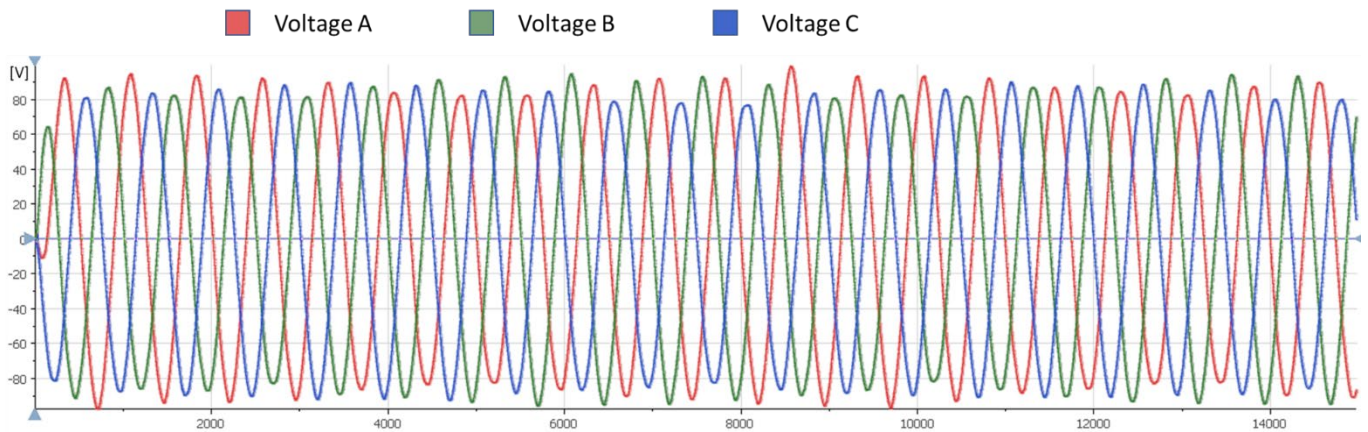


Figure 61 - Three phase voltage acquired signal

Similarly to the case of current acquisition, the voltage values are filtered with a Lowpass type Butterworth Filter.

Figure 62 shows a comparison between the acquired Voltage B signal (above) and the case in which it is filtered post-acquisition (below).

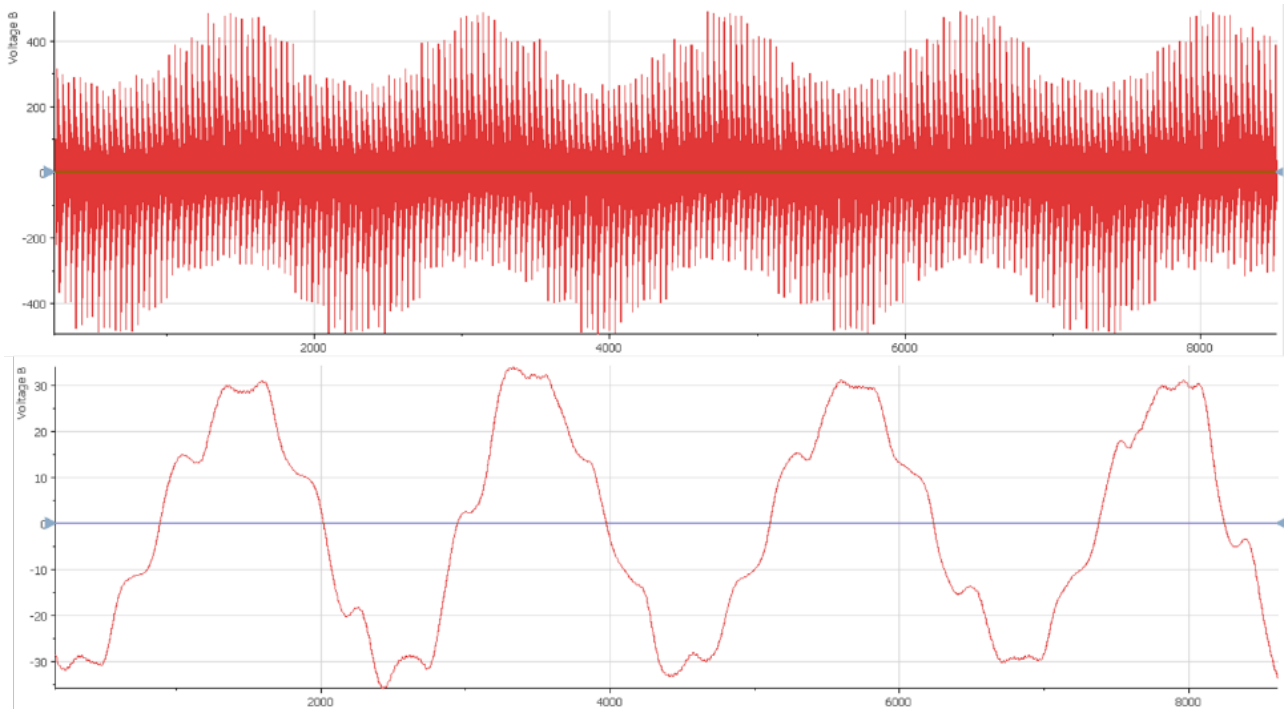


Figure 62 – Difference between filtered (below) and unfiltered (above) voltage signal

## 5.7 Mechanical Power

Mechanical power for an electric motor is defined as

$$P_m = \omega \cdot T$$

According to measurement units of SI, angular velocity is converted from *rpm* to *rad/s* while torque is measured in *Nm*.

Calculating the instantaneous mechanical power for each acquired torque and speed value has little significance with respect to the purpose of the project, furthermore the acquisition frequency of the torque sensor is different from that of the speed sensor and therefore there would be two arrays of different sizes.

In order to calculate the mechanical power delivered by the motor at a given point, the arithmetic mean of the speed and torque is determined, the result obtained is the following

$$\overline{P_m} = \overline{\omega} \cdot \overline{T}$$

The obtained value is saved in an array called “Mechanical Power”

## 5.8 Electrical Power

The electric power is established by its definition since the current and voltage values are known

$$P_e(t) = V(t) \cdot i(t)$$

The arithmetic mean, that is useful in determining the mechanical power average, is meaningless in computing electrical power because the motor is supplied by AC current, then voltage and current have a sinusoidal behavior whose average is null.

Therefore, the average electric power is calculated from the definition

$$\bar{P}_e = \frac{1}{T} \int_0^T V(t) \cdot i(t) dt$$

That for a three-phase motor is

$$\bar{P}_e = \frac{1}{T} \int_0^T (V_a(t) \cdot i_a(t) + V_b(t) \cdot i_b(t) + V_c(t) \cdot i_c(t)) dt$$

The integral is a continuous sum, but since the values acquired through the sensors are a function of the ticks of the acquisition device, i.e. voltage and current values are acquired for each tick, the function is discrete and therefore can be rewritten as

$$\bar{P}_e = \frac{1}{N} \sum_{tick=0}^N (V_a(tick) \cdot i_a(tick) + V_b(tick) \cdot i_b(tick) + V_c(tick) \cdot i_c(tick))$$

The relationship between tick and time is

$$tick = t[s] \cdot f \left[ \frac{tick}{s} = Hz \right]$$

where  $f$  is the acquisition frequency.

The first step to calculate the electrical power is to define the number of ticks  $N$  to acquire: considering that  $V$  and  $I$  are sinusoidal functions, their trend is repeated every period  $T$ . Therefore, the value  $N$  will be equal to a multiple of one electrical period.

The electrical period is related to the mechanical period by the following equation

$$\theta_e = \frac{P}{2} \cdot \theta_m$$

where

$\theta_e$  is the electric degree;

$P$  is the number of the poles of the motor;

$\theta_m$  is the mechanical degree.

Hence, the number of ticks of one period varies according to the working conditions. In fact higher the speed, shorter will the period be.

It needs to define a period  $T$ .

### 5.8.1 Period

The samples to consider for data acquisition are equal at least to that of a mechanical period that corresponds to a multiple of the electrical period, that is  $T_m = n \cdot T_e$  with  $n \in N, n \geq 1$ .

The acquisition of a single period, that is, a single rotation of the shaft is already sufficient to obtain the data necessary to evaluate the behavior of the motor in tested conditions. However, it should be noted that the acquisition of multiple periods allows for more reliable measurements as any inaccuracy in the acquisition can be spread over multiple values.

## 5.9 Efficiency and Post processing

Once the period has been defined, the average mechanical and electrical power for the given period are calculated and the efficiency is determined as the ratio between the two powers.

$$\bar{\eta} = \frac{\overline{P_m}}{\overline{P_e}}$$

The efficiency is therefore saved within an array and callback in the efficiency map plot.

At the end of the evaluation of each point of the motor, the acquired data are saved in two files in TDMS format. The first file contains the information of Torque, Speed, Position, Voltages and Currents for each point collected, useful for post processing phase; the second one collects mechanical, electrical power and efficiency to compute the efficiency map.

## 5.10 Algorithm

The algorithm to perform the actions mentioned above is schematized in the following diagram of *Figure 63*

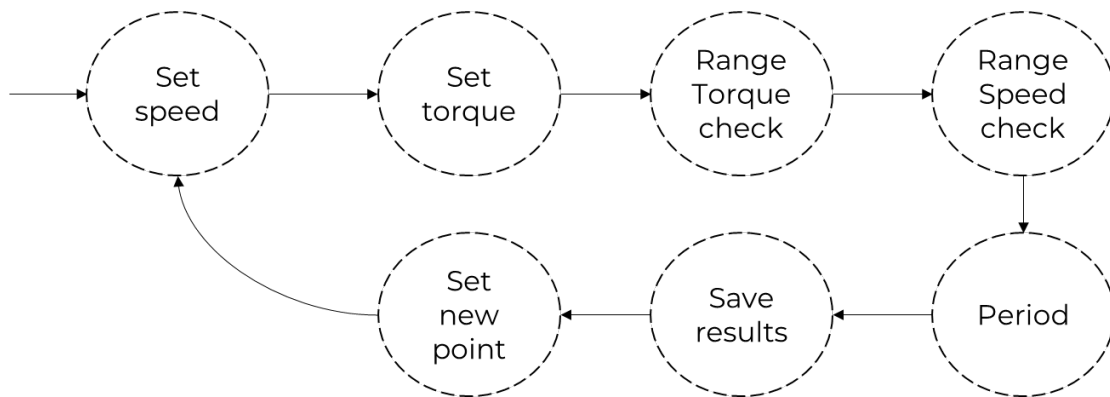


*Figure 63 – Program workflow*

The first stage of the workflow is the definition of the speed, in this phase the motor rotates at the initial speed defined in the settings.

The value contained in the *Imposed Speed* numeric field is converted into PWM value thanks to the function block called *RPM to PWM* which contains the equations that relate the parameters, then the output of the function is sent to Arduino board.

The *Imposed torque* value is sent to the load motor control loop, in the same action the *Torque Limit* is modified as this value determines the speed with which the torque tends to vary. The *Torque Limit* is equal to 5 Nm more than the *Imposed torque*. The relatively small difference between the two torques has been chosen since a slower variation helps to reach faster stationary speed conditions.



Figure 66 shows the action of the *Range torque check*. In the first part, it is verified that the torque is constant by comparing two moving average functions of the acquisition array.

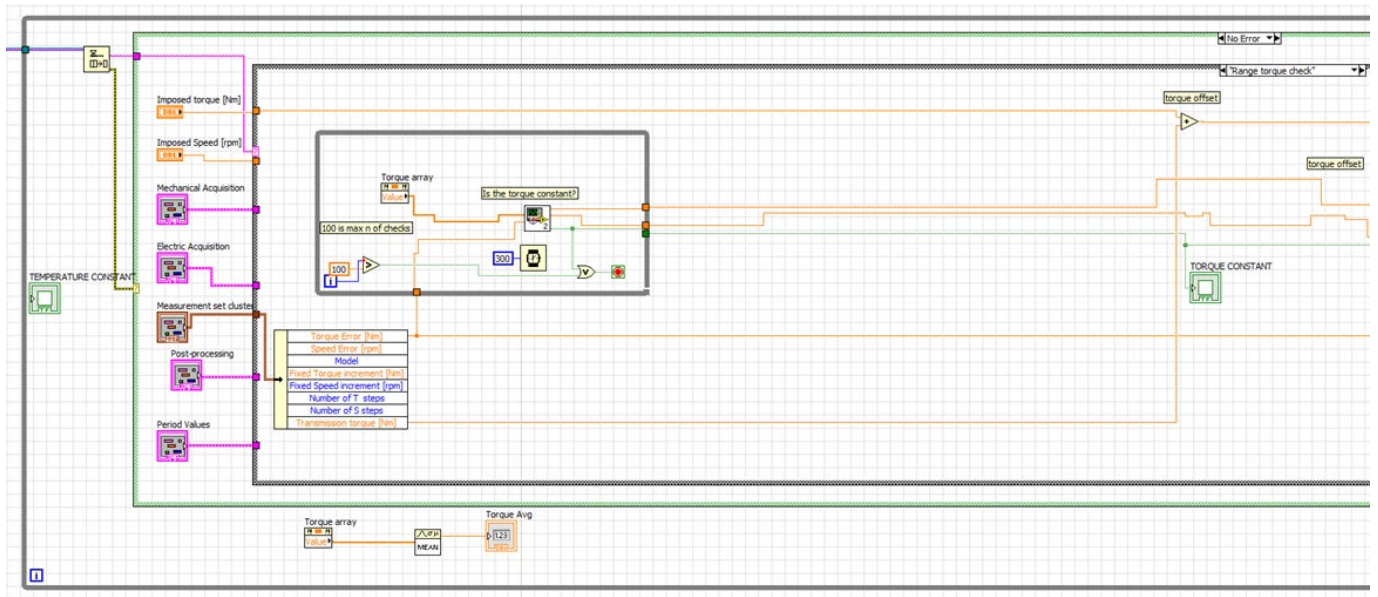


Figure 66 – LabVIEW programming code for “Range torque check” action: constant torque test

In the second phase, it is checked whether the torque is within the error range required by the user. If the torque is in range the function checks the speed range. If not, the user will receive a warning message.

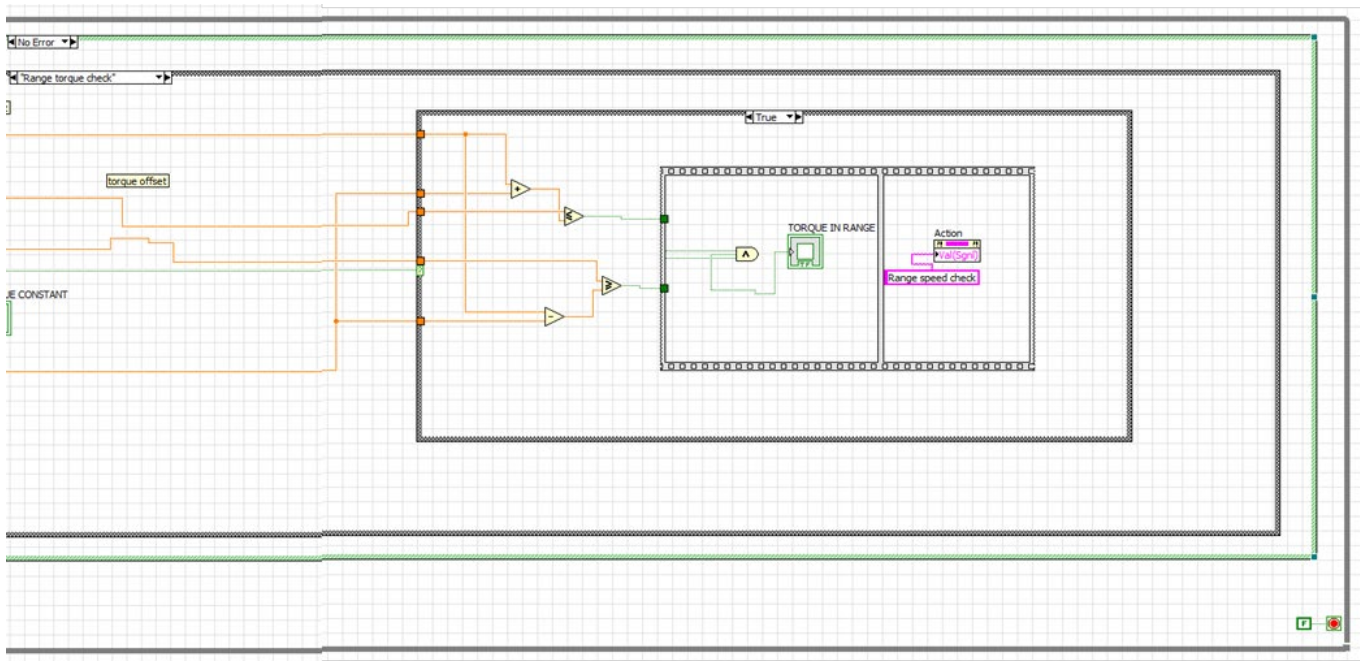


Figure 67 – LabVIEW programming code for “Range torque check” action: torque range test

Figure 68 shows the consumer loop relating to the *Range speed check* action.

Similar to the torque check, this action controls the stationarity of the speed by comparing two moving average values adequately distant in the acquisition array.

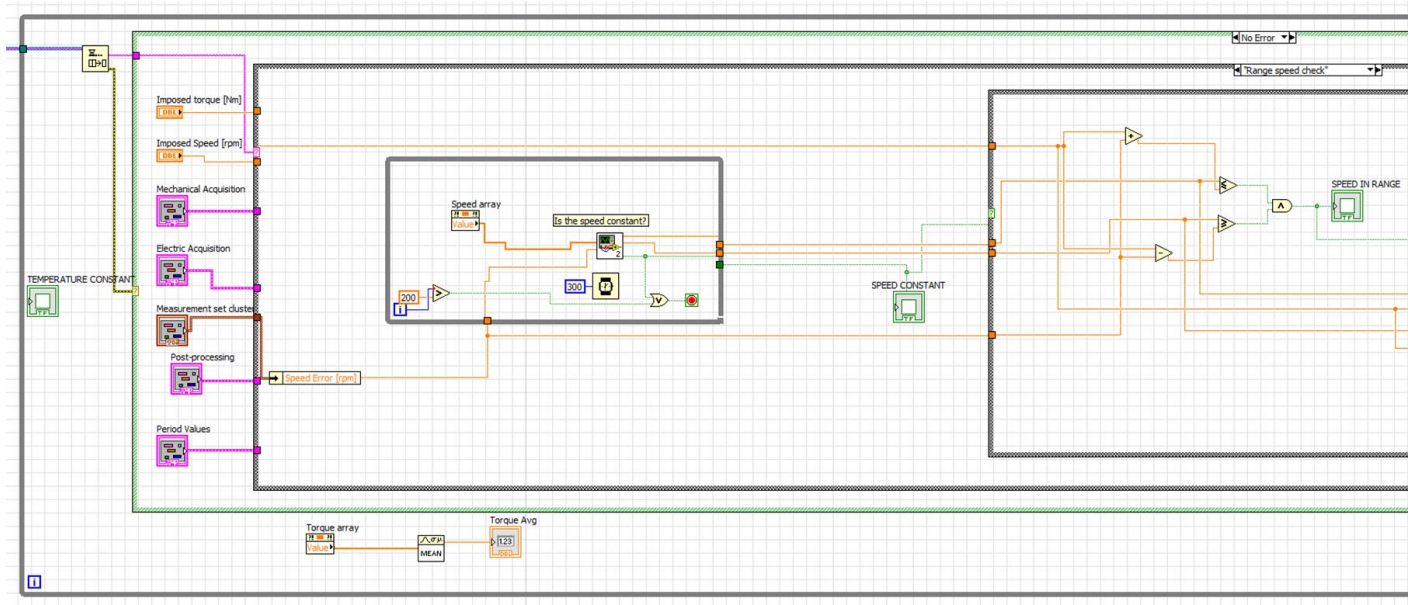


Figure 68 – LabVIEW programming code for “Range speed check” action: constant speed test

If the speed is constant, the range verification is performed.

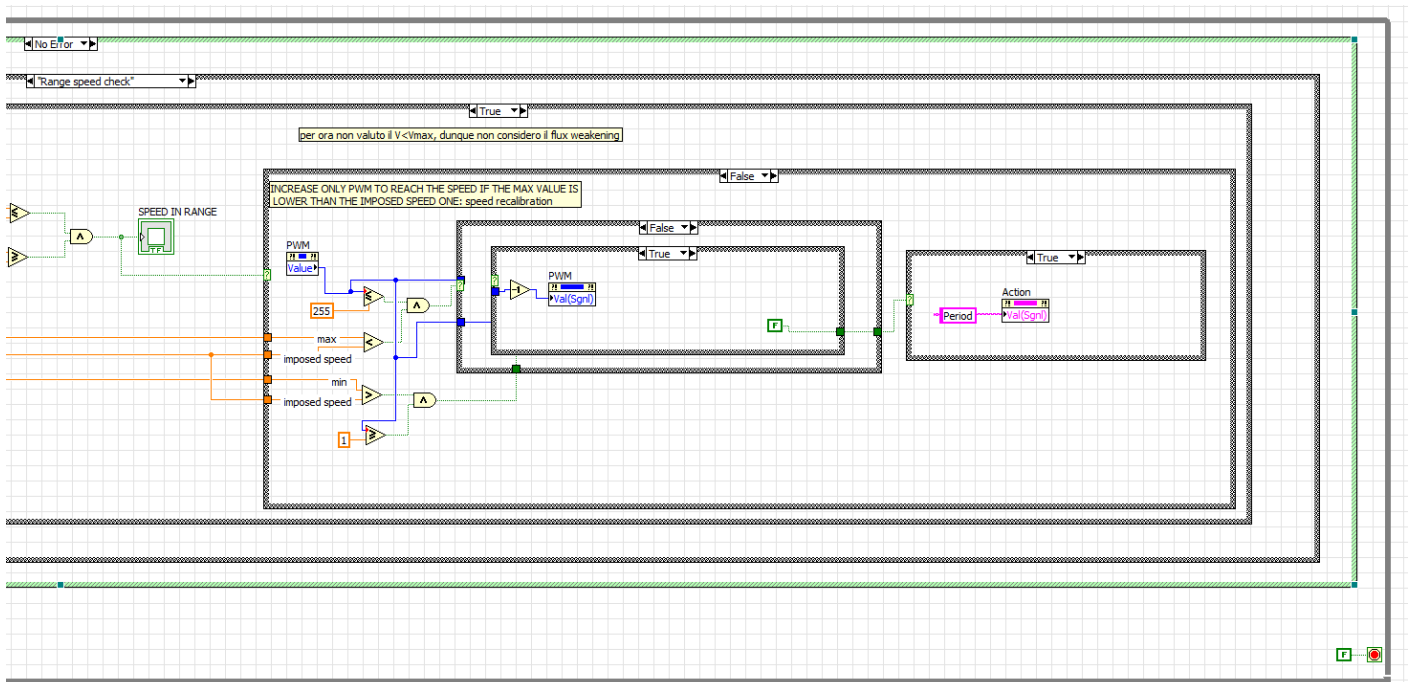


Figure 69 – LabVIEW programming code for “Range speed check” action: speed range test

If the speed is within the range indicated by the user, the Period action is performed. On the contrary, if the speed is not in range, the *auto-adjusting* function will vary the PWM value and repeat the range speed check function.

Figure 70 shows the consumer loop relating to the action *Period*.

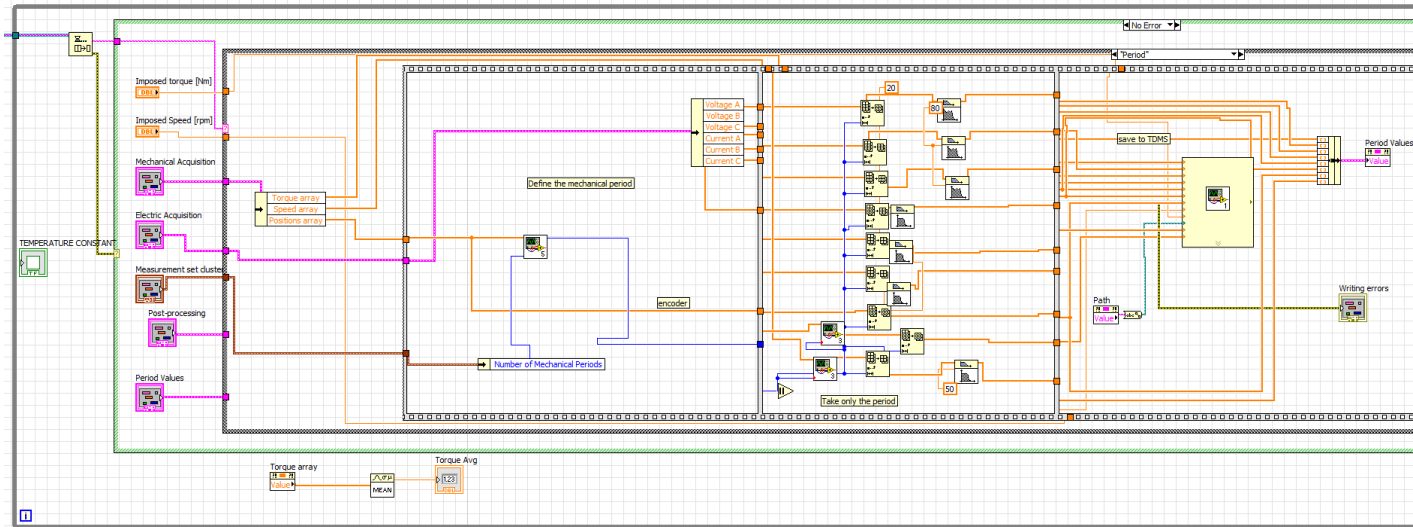


Figure 70 – LabVIEW programming code for “Period” action: determine the period

In this step, the period is defined through a sub-function that analyzes the encoder signal and as output provides the number of samples equivalent to the periods requested by the user. Sub-arrays with the length equal to the period are extracted from the voltage, current, position, speed and torque arrays. Finally, a filter is applied to the extracted period to clean the signal. Right after that, the values are saved in a TDMS file.

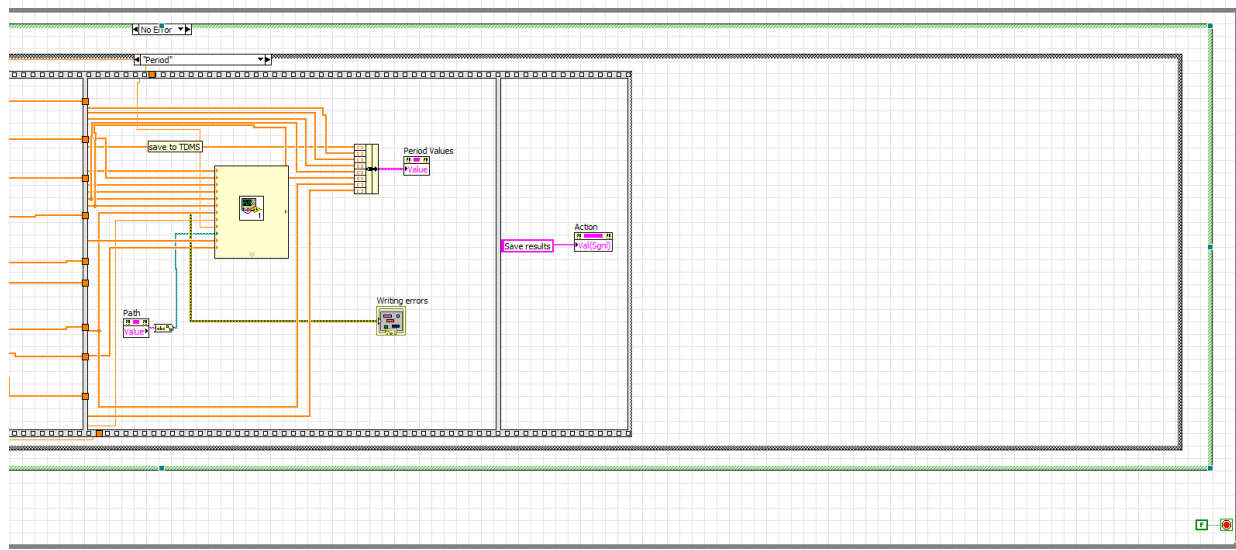


Figure 71 – LabVIEW programming code for “Period” action: save the period



At the end of this step, it proceeds with the "Save results" action.

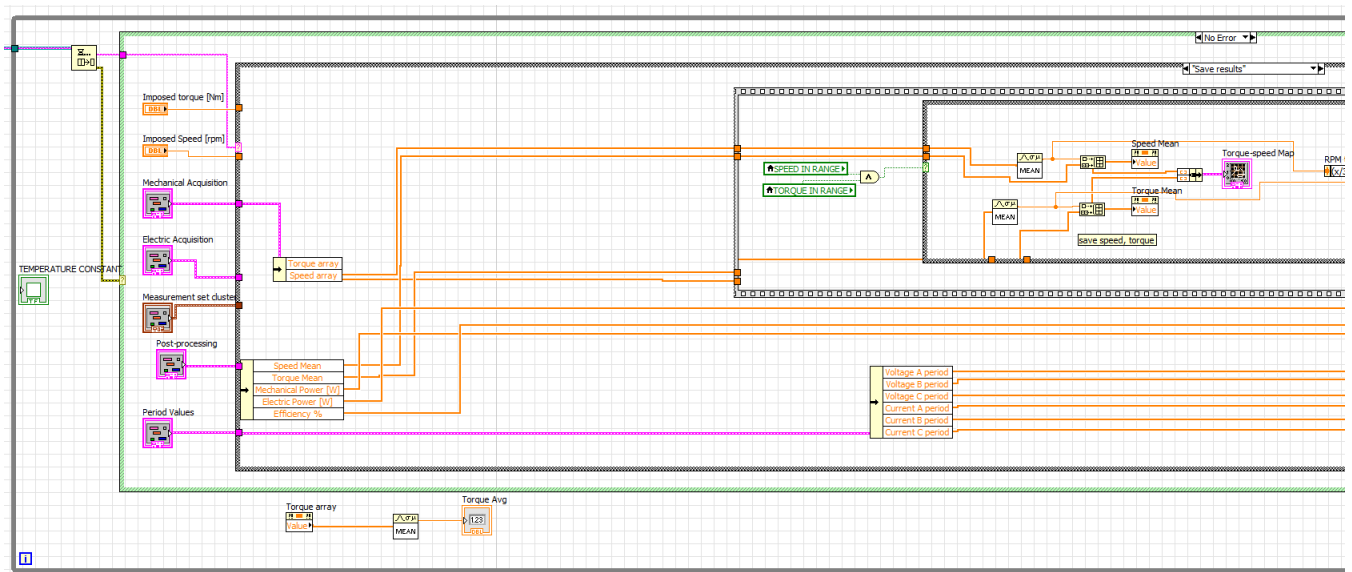


Figure 72 – LabVIEW programming code for "Save results" action

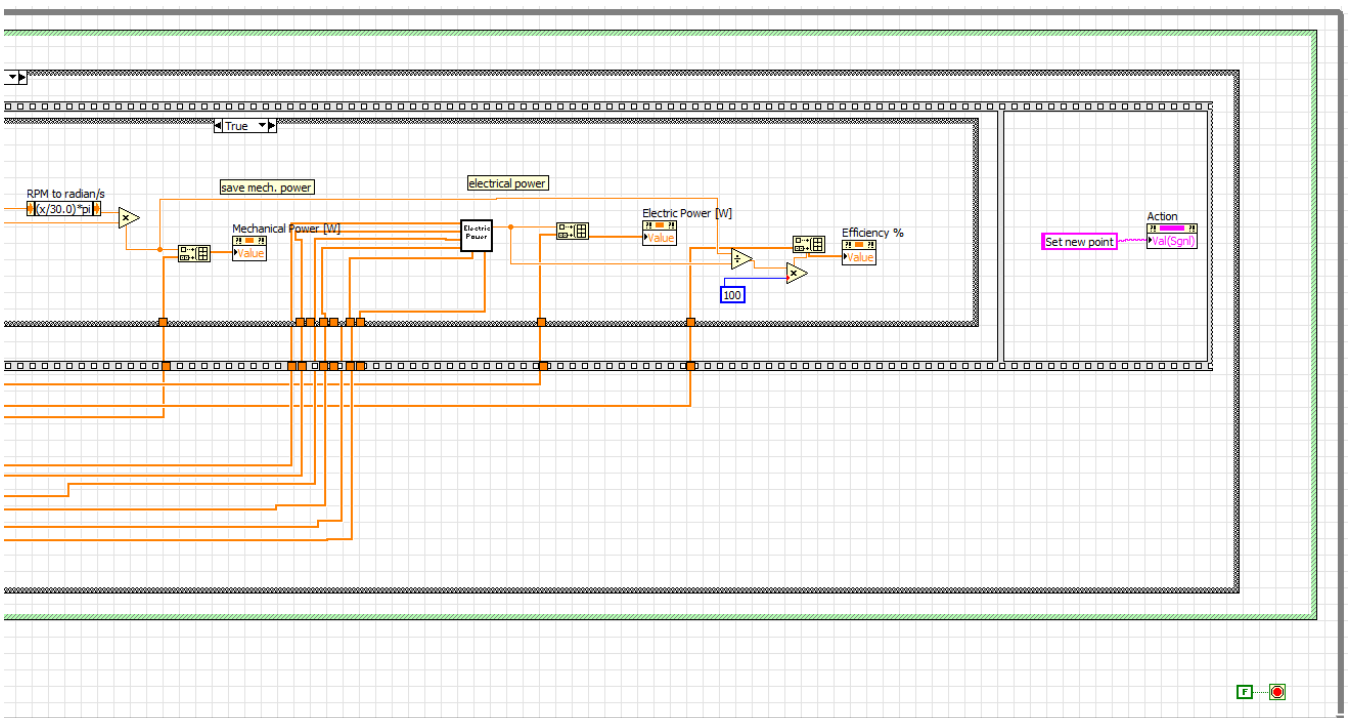


Figure 73 – LabVIEW programming code for "Save results" action

This function computes the electrical power and the average mechanical power from the mean value of speed and torque. At the end of the action the point is shown in the speed torque map in the user interface. Therefore, the percentage efficiency is calculated as a ratio between the powers.

The next step, in *Figure 74*, shows the consumer loop relating to the action *Set new point*.

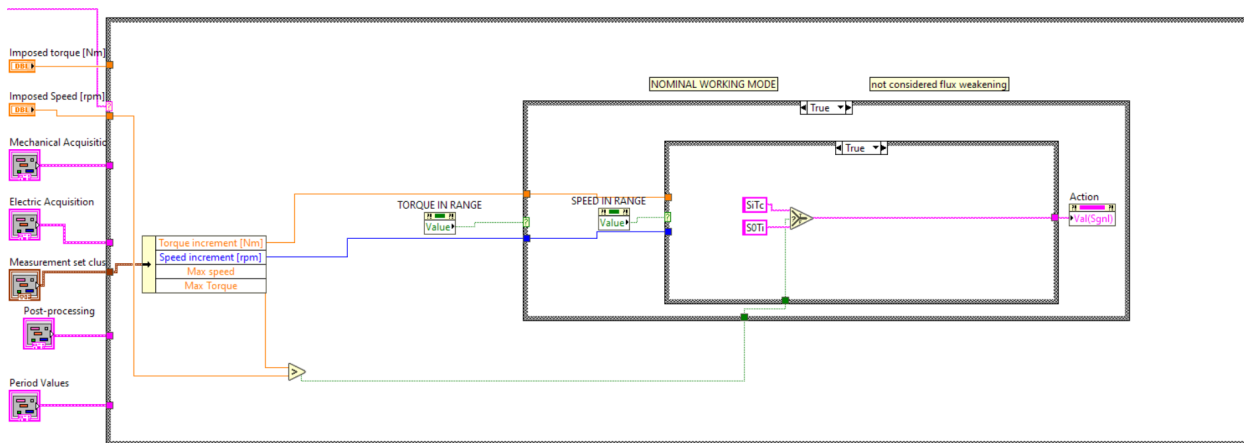


Figure 74 – LabVIEW programming code for “Set new point” action

This function decides the next point to evaluate. The point is determined starting from the outputs of the logical events that occurred during the measurements. In the event that both the speed and the torque are in range and the speed is lower than the maximum one set by the user, the speed is increased leaving the torque constant. In this case the action Speed Increase Torque constant (SiTc) is performed.

In the event that the speed has reached its maximum value, the torque is increased and the speed returned to the initial value, the event is *Speed zero Torque increase* (SOTi) where zero means a minimum speed equal to the increase speed value.

Once the new speed and torque have been defined, the loop restarts from the beginning to study the new point.

## 5.11 User Interface

The user interface of the program developed is implemented in the acquisition program and consists of four subsections. From the *Control* section it is possible to manage the simulation, establish the connection with Arduino and view the progress of the analysis in the map below; in the *Measurement Settings* section, are defined the study region, the engine characteristics, the increment model, the error range, the temperature settings and the number of periods to consider in the acquisitions. *Acquisitions* tab is the section in which the data from sensors are saved in vectors waiting to be processed. *Results* is the tab in which it is specified the save path and the results of mechanical power, electrical power and efficiency are displayed.

- Control

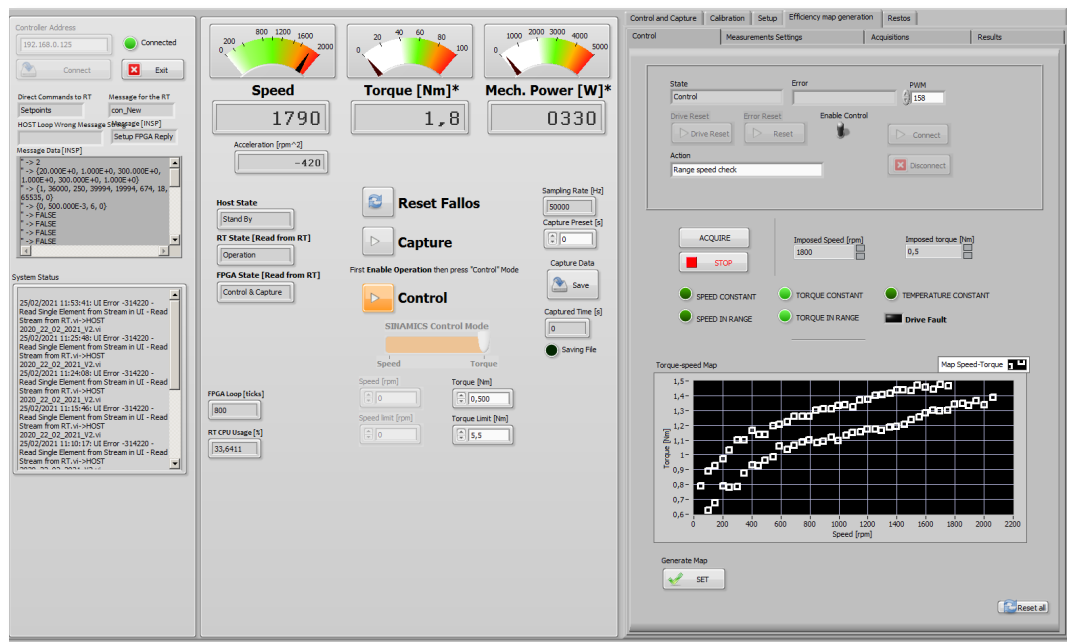


Figure 75 – LabVIEW interface for “Control” sub-tab

The first box contains the commands for connecting the Arduino and enabling the control; below there is the start acquisition button called “Acquire” and the point under consideration is indicated in the Imposed Speed and Imposed Torque textboxes. The leds indicate the status of the functions of speed, torque and temperature verification. At the bottom, the map with the already acquired points is shown.

- Measurements Settings

The motor max speed and max torque define the measurement region, in this case the speed is set to 2000rpm because it is limited by the bench and max torque is set to 100Nm as the actual max speed of the MUT is not known.

The increment speed model chosen is the Fixed one as illustrated in *Figure 76* and the final increment conditions are reported below.

The accepted error range is the zone in which the user can define the measurement error.

Figure 76 – LabVIEW interface for “Measurement settings” sub-tab

Acquisitions is the tab in which all the data are collected while the results tab displays just the result that came from the post processing of the acquisitions.

Control and Capture | Calibration | Setup | Efficiency map generation | Restos

Control | Measurements Settings | Acquisitions | Results

### Mechanical Acquisition

Positions array	Speed array	Torque array	Array Size
0	0	-0,0101501	1475
0	0	-0,0366623	
0	0	-0,0401909	
0	0	-0,0463898	
0	0	-0,00576324	
0	0	-0,0324661	

### Electric Acquisition

Voltage A	Voltage B	Voltage C
-3,30763	-3,19238	-3,57465
0,816455	0,692505	-0,10256
1,13701	1,16553	0,236108
-3,37236	-3,19238	-3,57465
1,10619	1,04041	0,112421

Current C	Current A	Current B
-0,00721542	-0,00665851	-0,0228519
-0,00554468	-0,00665851	-0,0219767
-0,00554468	-0,00753366	-0,0219767
-0,00976132	-0,00753366	-0,0228519
-0,00554468	-0,00586292	-0,0228519

### Period Values

Voltage A period	Voltage B period	Voltage C period	Current A period	Current B period
0,00434723	-13,1436	-0,683719	0,00207492	-0,00208447
0,00668841	-13,1734	-0,713496	0,0103149	-0,0103239
0,0192601	-13,1909	-0,736139	0,0265606	-0,0265534
0,0597093	-13,1713	-0,72782	0,0502578	-0,0502895
0,118141	-13,1274	-0,700701	0,0806794	-0,0807965

Current C period	Torque period	Encoder period
-1,14495E-5	1,77436	8305
-9,11966E-5	1,77365	8315
-0,000267113	1,77303	8324
-0,000476059	1,77248	8334
-0,000716862	1,77202	8343


Figure 77 – LabVIEW interface for “Acquisitions” sub-tab

Control and Capture | Calibration | Setup | Efficiency map generation | Restos

Control | Measurements Settings | Acquisitions | Results

### Post-processing

Speed Mean	Torque Mean	Mechanical Power [W]	Electric Power [W]	Efficiency %
298,686	1,69267	52,944	139,286	38,0111
199,53	1,66375	34,7636	94,1325	36,9305
98,3521	1,53417	15,801	52,7173	29,9731
0	0	0	0	0
0	0	0	0	0
0	0	0	0	0

Folder  
 

Project name

Test name

Path


Set path  
 SET

Figure 78 – LabVIEW interface for “Results” sub-tab

## 5.12 Specifications and limits

The program works automatically but relies on a user to perform most security test.

It is limited to work with digital IO and analog IO of the CompactRIO and its modules and it is tested only against a designated motor and motor drive. Moreover the program works over the existent LabVIEW software and uses the existent command queue system of the MAPRO Test Bench project.

The Arduino electronic board with which the drive is controlled is adequate for the purpose of the project both for the large availability of libraries and for the low cost. However, the limit of this equipment allows to control the speed only in the anticlockwise direction as the analog signal in output can assume only positive values.

The motor applied for the tests is low power which ensures a high safety condition for test phases in case of control fault, but it is not very suitable for the complete study of the efficiency map as the test rig is sized for motors of lower speed and greater torque.

## 6. Test

In this phase the program is tested and validated by making it work in actual operating conditions.

### 6.1 Preparation for the test

Preparation for the test is the phase in which it is verified that all the control and acquisition equipment is correctly connected and functioning.

The calibration of the sensors is a fundamental phase of preparation for the test as it is necessary to obtain measurements consistent with the real ones. The calibration of the mechanical sensors takes place in conditions of zero speed and torque. In these conditions, both sensors must indicate the value zero unless a small error occurs due to signal noise.

The electrical sensors are calibrated by studying the sinusoidal curves and verifying that the sinusoid of the current and voltage are well determined and that the amplitude is symmetrical with respect to the x axis.

Calibration takes place by acting on three parameters: Calibration factor, conversion factor and offset. The calibration factor relates the electrical value output in voltage to the actual value, the conversion factor is a multiplier of the measured value, while the offset adds a constant value to the signal.

Signal	Calibration Factor	Conversion Factor	Offset
Torque	20	100	-2.9
Current A	7.9	0.33	-0.01
Current B	7.9	0.33	-0.025
Current C	7.9	0.33	-0.01
Voltage A	1.01	100	0.2
Voltage B	1	100	0.25
Voltage C	1.031	100	0.4

Table 14 – Calibration settings

The torque has an offset equal to  $-2.9 \text{ Nm}$  since in static conditions of zero torque and zero speed the torque signal fluctuates around a value of  $+2.9 \text{ Nm}$ .

For current sensors the conversion factor is due to their connection to the motor, in fact the cable in which the current passes has been wrapped three times around a single current sensor, therefore the real current is equal to  $1 / 3$  of that measured. This choice allows to reduce the error on the current measurement as the same current is measured three times and then the average of the three is taken.

For safety reasons, a device is installed to protect the inverter in the event of faults. A resistor has been connected to the inverter to dissipate energy in the case the motor operates as a generator i.e. the torque of the load motor exceeds that of the MUT.

The installed resistor can dissipate up to 250W which, added to the internal resistance of 35W of the drive, is enough to work in safe conditions considering that the motor can act as a generator only for short transients. Anyway, a function called *Drive Fault monitor* is implemented which continuously checks the direction of the motor speed, if it is negative, zero torque is imposed to the load motor. This function allows to manage faults but however it relies on a user to perform most security test.



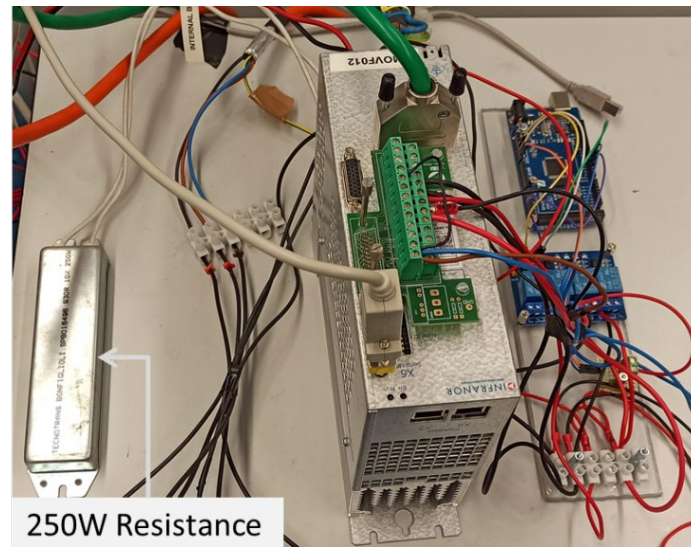


Figure 79 – Heatsink connection

Last stage of preparation is the position sensor adjustment in the inverter settings, it defines the mechanical shift between the motor and the position sensor reference and is set with Auto-phasing procedure in Gem Drive Studio software.

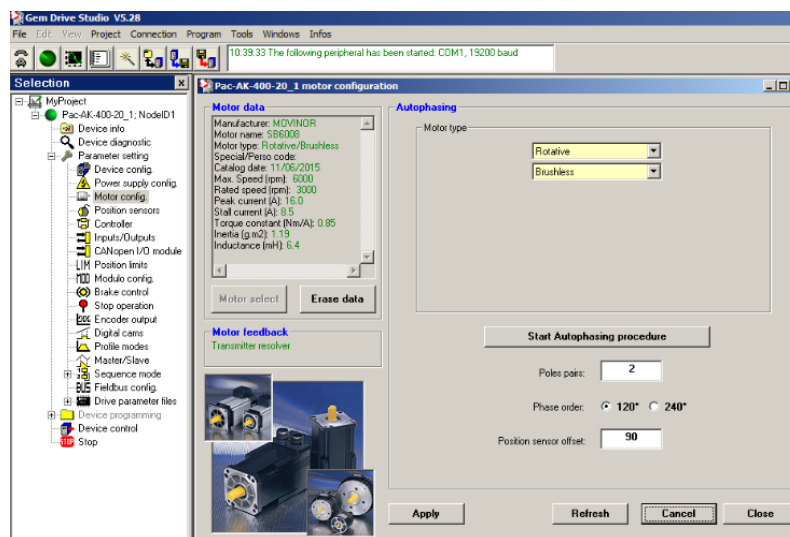


Figure 80 – Auto-phasing procedure

The position sensor offset is 90 deg.

## 6.2 Test settings

The test settings define the region to be studied, the allowable measurement error and the density of the measurements.

The maximum speed of the motor is limited by the test bench and is set equal to 2000 *rpm*, the maximum torque of the MUT is not known a priori, therefore by default the maximum torque value is set to that of the bench.

The speed increment model is set as *Fixed* and it define a speed increase of 50 *rpm* and a torque increase of 0.5 *Nm*. The minimum speed is equal to the increase one while the minimum torque is null.

The accepted error range is  $\pm 15 \text{ rpm}$  for speed and  $\pm 0.4 \text{ Nm}$  for torque. While the speed error range is constant for all the measurements made, the torque range cannot be constant as the resistance of the bench varies with the speed and therefore the difference between the requested value and the imposed one increases accordingly. Therefore it defines a transmission torque value which varies according to the resistance of the bench.

The working limit temperature of the motor is defined as  $100^\circ\text{C}$ ; the error of measurement is  $\pm 1^\circ\text{C}$ .

The mechanical periods for the acquisition is equal to ten periods and being the 4-pole motor, consequently twenty electrical periods are saved.

The frequency chosen for the test is 50kHz. The choice is a trade-off between capture accuracy and final file size. By carrying out some comparative acquisition tests, as the frequency varies it notes that for frequencies greater than the one chosen, the result variation is negligible even reaching the maximum allowed by the instruments equal to 82kHz.

Studied point	$\omega = 100 \text{ rpm}; T = 0.5 \text{ Nm}$
Frequency	Efficiency
50 kHz	31.5 %
75 kHz	31.8 %
82 kHz	31.9 %

Table 15 – Experimental correlation between acquisition frequency and detected efficiency

### 6.3 Post-processing

The results, saved in TDMS format, can be viewed with National Instrument's DIAdem software.

By accessing the results, they are divided into groups and channels: each group represents a point on the map, within a group there are nine channels which are the acquired signals relating to that point.

The groups of acquired data are named as “S\_SpeedValue\_T\_TorqueValue” where “SpeedValue” and “Torque Value” are respectively the Speed and Torque values set for each point. For each point the values of Position, Speed, Torque, Voltages and Currents are saved.

Figure 81 shows the results acquired for the point  $P = (1000 \text{ rpm}, 2 \text{ Nm})$ .

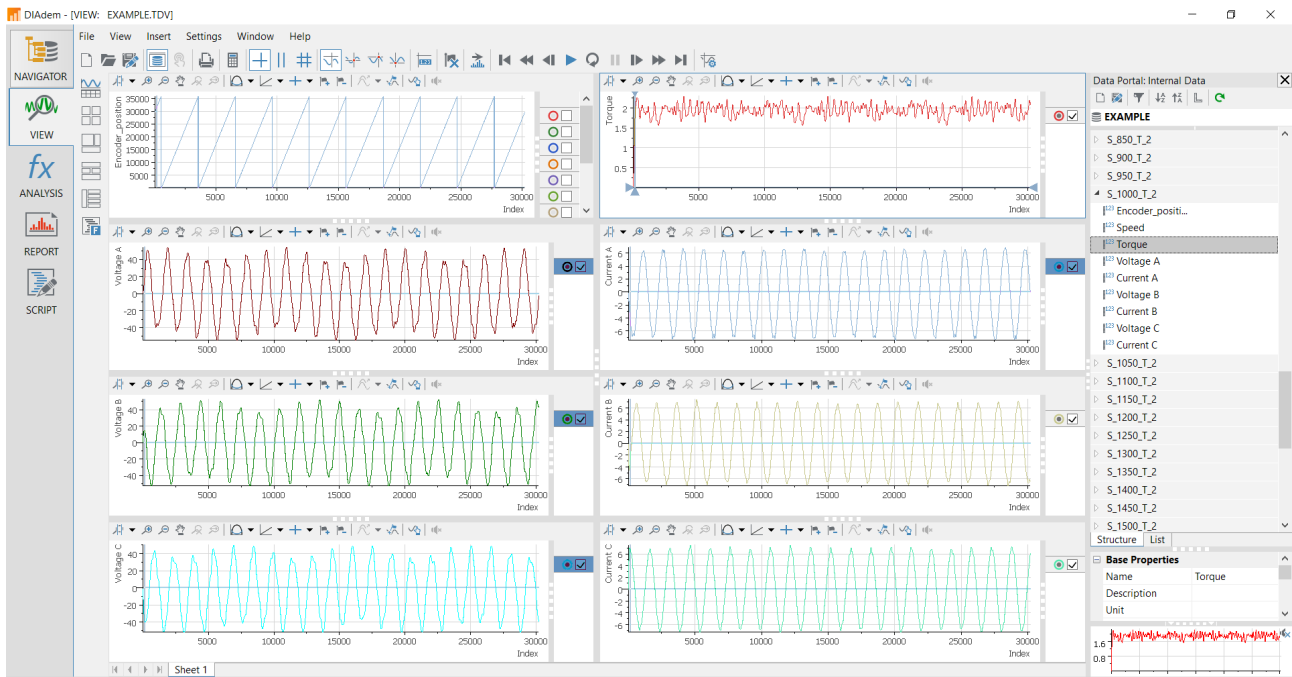


Figure 81 – Visualization of TDMS results with DIAdem software

In addition to the previous, a second file is generated containing the automatically post processed data to build the efficiency map such as mean speed, mean torque, mechanical power, electric power and efficiency.

## 6.4 Validation of measurements

Voltech PM6000 is a powerful and precise power analyzer. The accuracy and bandwidth of the PM6000 allow definitive measurements of all power quantities to be made on all electrical and electronic products. PM6000 provides stable, reliable and accurate measurement. This power analyzer has a very high accuracy of reading, up to 0.02% and bandwidth of 10MHz.

PM6000 has been installed between the motor and the inverter to provide high-precision information on the detected electric current with its wattmeter. The connection is realized as shown in the following connection diagram.

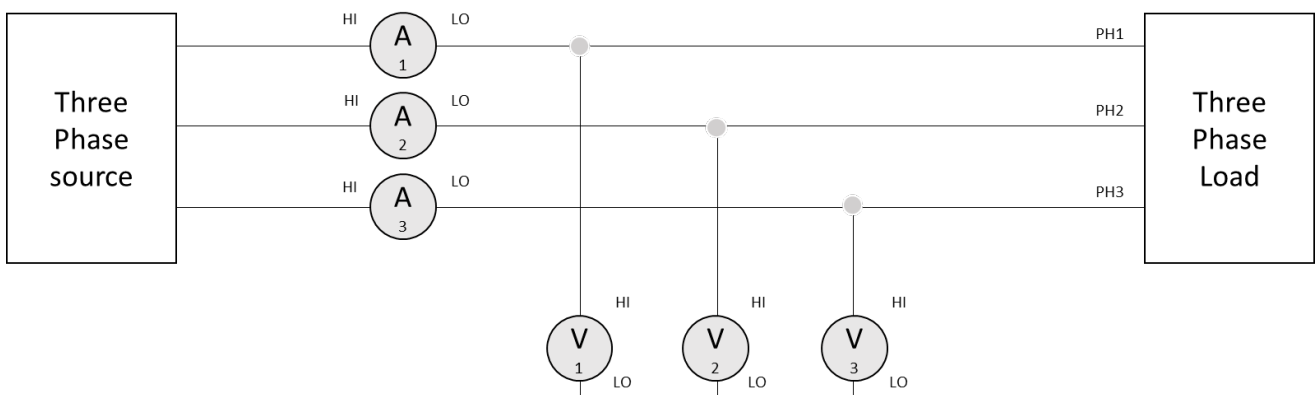


Figure 82 – Power analyzer connection diagram

Once configured, the Power Analyzer detects the electrical input power to the motor which will be rotated at some significant points of speed and torque. In this way the measurements made with the Power Analyzer are compared with those automatically acquired by the program.

Since the Power Analyzer is very precise, the Electric Power determined with the latter is considered exact. This is the reference for the evaluation of the measurement error of the developed program.



Figure 83 – Power Analyzer in operation mode

The application of the Power Analyzer is necessary to validate the measurements acquired by the program and indirectly the results that come from it.

Table 16 shows a comparison for seven significative points between the results obtained by the program and those determined by the Power Analyzer.

Imposed	Point	Acquired	Point	Electric Power (LabVIEW)	Electric Power (P6000)	Measurement error
<b>Speed</b>	<b>Torque</b>	<b>Speed</b>	<b>Torque</b>			
600 rpm	1 Nm	591 rpm	1.17 Nm	181 W	180 W	0.5 %
800 rpm	1 Nm	793 rpm	1.26 Nm	252 W	240 W	5.0 %
1500 rpm	1.5 Nm	1498 rpm	1.54 Nm	520 W	530 W	1.9 %
100 rpm	2.3 Nm	96 rpm	2.36 Nm	96 W	102 W	5.8 %
800 rpm	2.5 Nm	790 rpm	2.72 Nm	547 W	550 W	0.5 %
1800 rpm	3.3 Nm	1799 rpm	3.24 Nm	1406 W	1440 W	2.3 %
500 rpm	4.0 Nm	489 rpm	3.20 Nm	461 W	495 W	6.8 %

Table 16 – Electric power comparison and error statement

Therefore, with reference to the electric power computed by PM6000, the efficiency error made by the program is determined.

Imposed	Point	Acquired	Point	Efficiency (LabVIEW)	Reference efficiency	Efficiency error
Speed	Torque	Speed	Torque			
600 rpm	1 Nm	591 rpm	1.17 Nm	40.11 %	40.40 %	0.29 %
800 rpm	1 Nm	793 rpm	1.26 Nm	41.34 %	43.41 %	2.07 %
1500 rpm	1.5 Nm	1498 rpm	1.54 Nm	46.89 %	46.00 %	0.89 %
100 rpm	2.3 Nm	96 rpm	2.36 Nm	25.27 %	23.92 %	1.35 %
800 rpm	2.5 Nm	790 rpm	2.72 Nm	41.18 %	40.96 %	0.22 %
1800 rpm	3.3 Nm	1799 rpm	3.24 Nm	43.42 %	42.41 %	1.01 %
500 rpm	4.0 Nm	489 rpm	3.20 Nm	35.61 %	33.38 %	2.23 %

Table 17 – Efficiency comparison and error statement

From the results of the comparison, an overestimated return of 2.23% and underestimated of 2.07% was calculated. The error is not particularly relevant, it is hypothesized that this divergence is due to the number of periods considered in acquisitions, to the frequency achieved and to the error of the instruments.

The period is determined according to the ticks of the instrument, considering a greater number of mechanical periods and consequently of electrical periods, the average electrical power can be calculated on a greater number of samples, therefore spreading the error over a greater number of acquisitions. This change could make the result converge to the exact one.

The acquisition frequency, as demonstrated in the pre-test phase, affects the results. Consequently, the values will be more accurate if the acquisition frequency is higher. For the project,  $f = 50kHz$  was chosen for the excellent compromise between reliability of results and system load.

Therefore, errors in the measurements of electrical power could lead to an error up to 2% in term of efficiency. The error could be defined as acceptable.

The mechanical power is validated by comparing the speed and torque signals separately. The speed value acquired by the program is consistent with the speed value detected by the proprietary software of the Gem Drive Studio inverter which acquires the values of a second encoder present in the motor itself. The torque data, on the other hand, are compared with those supplied by the load motor and are consistent. For these tests the acquired mechanical power can be assumed to be correct.

Since the efficiency is defined as the ratio between the two acquired powers, whose values are both validated, the efficiency map generated by the program by transitive property is validated.

## 7. Results

### 7.1 Expected results

To assess the reliability of the results from the starting conditions the expected outputs are hypothesized and compared with the actual one obtained to prove their consistency.

As regards the speed and torque signals, an approximately constant trend is expected for both with a variation between the minimum and maximum included in the defined range.

The graph in *Figure 84* shows the acquisition of the speed for the point 2000 *rpm*, from this it is evident that the values are perfectly in the range  $2000 \pm 15 \text{ rpm}$  defined by the user. The trend, unless limited instantaneous variations, is stationary.

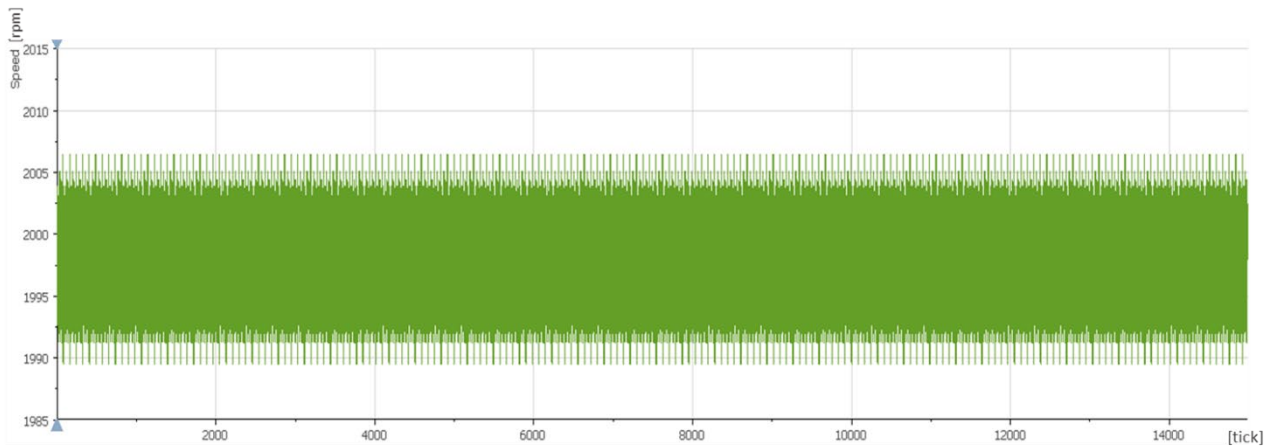


Figure 84 - Speed Acquisition for  $\omega=2000 \text{ rpm}$

Similarly, the torque has a stationary average value and is in the range of the imposed value

$$I_T = 2.0 \pm 0.4 + \text{transmission resistant torque Nm}$$

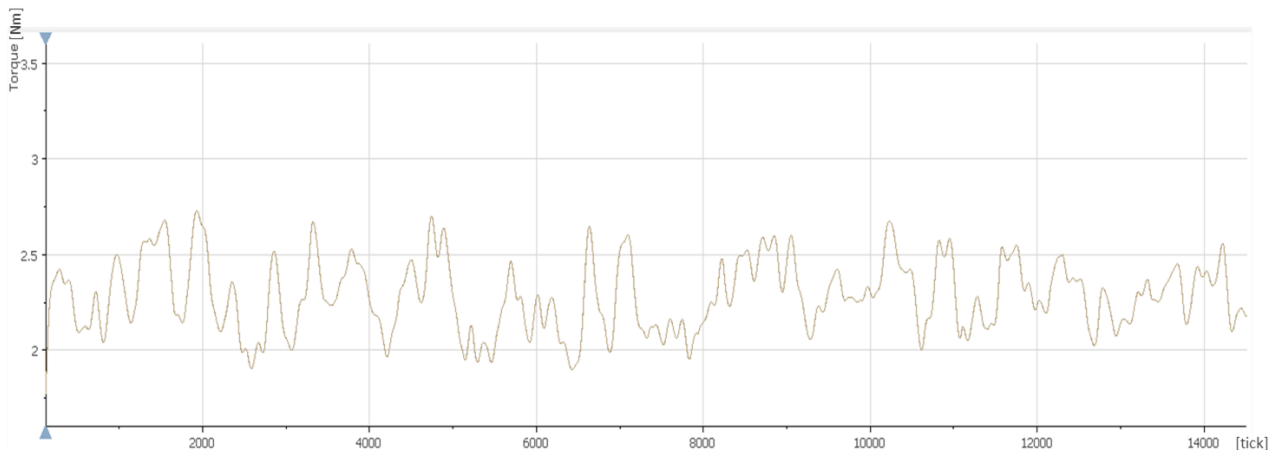


Figure 85 - Torque Acquisition for  $T = 2.0 \text{ Nm}$

Torque oscillations in the chart are due to torque ripple of the motor.



The period chosen is ten mechanical periods, hence, from the position signal, ten peaks should be found where the distance between one peak and another represents a rotation. For the same reason, recalling the relationship between the electrical period and the mechanical period  $\theta_e = \theta_m \cdot \frac{P}{2}$  for a four poles motor, twenty electrical periods are expected.

From the graph in *Figure 86* the mechanical periods are consistent with those expected and the graphs in *Figure 87* and *Figure 88* show the electrical periods equal to twice the mechanical ones.

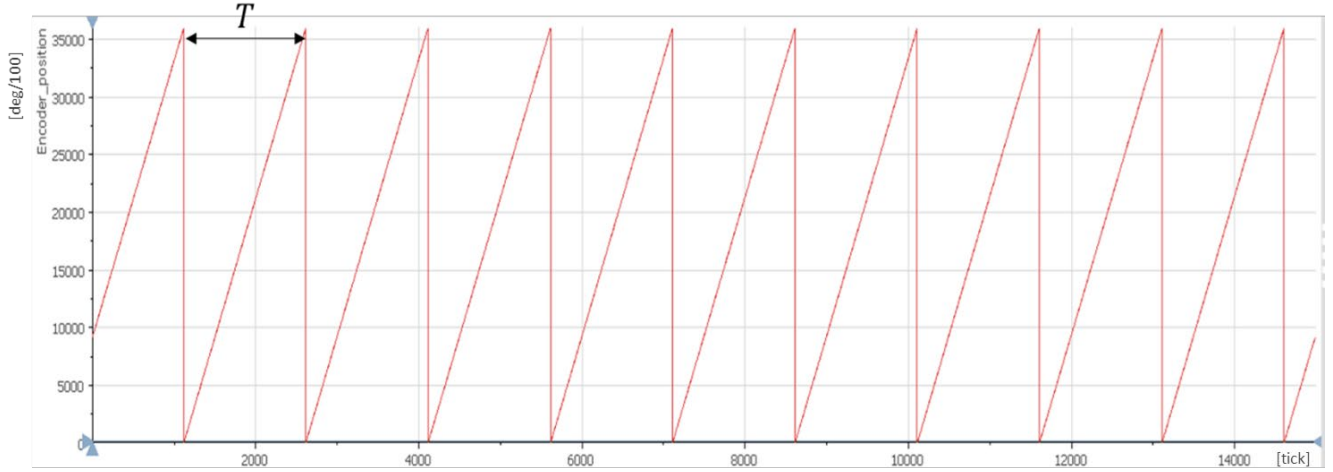


Figure 86 – Encoder Acquisition

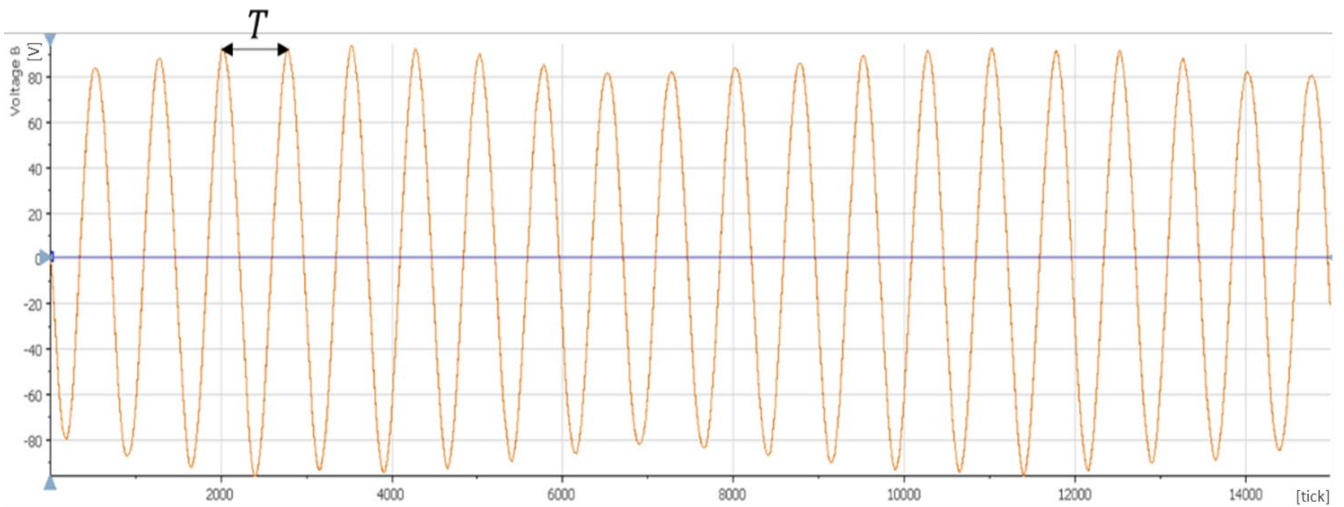


Figure 87 – Phase B voltage acquisition



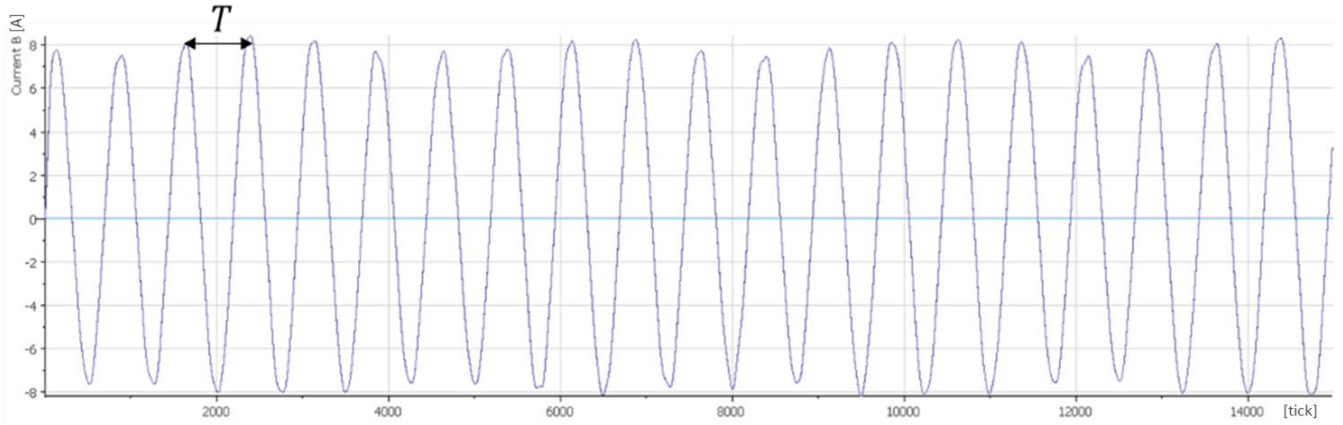


Figure 88 – Phase B current acquisition

Furthermore, both voltage and current functions have a sinusoidal trend and are out of phase by  $120^\circ$  in the order  $V_A, V_B, V_C$  and consistently  $I_A, I_B, I_C$  as expected.

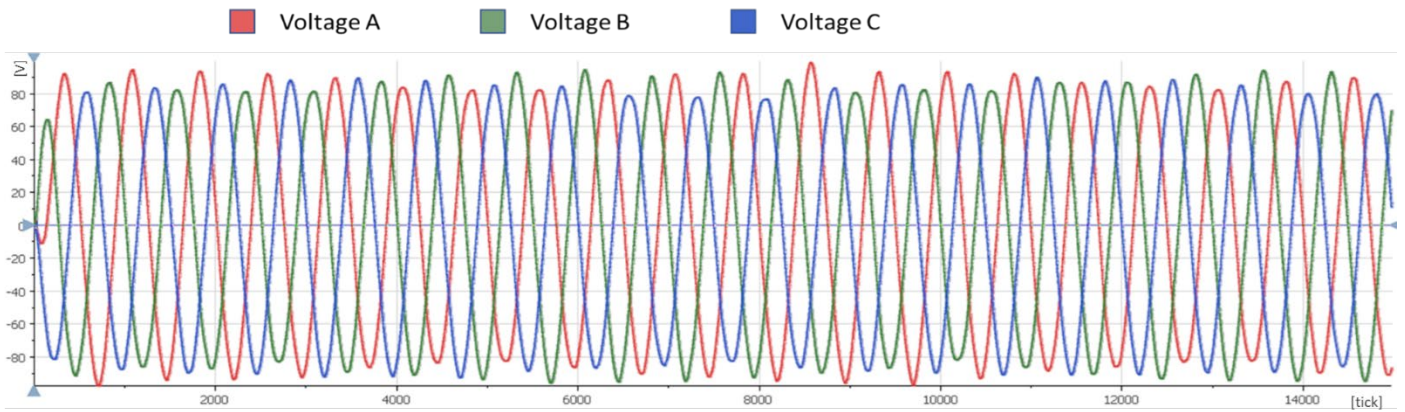


Figure 89 – Three phase voltage acquisition

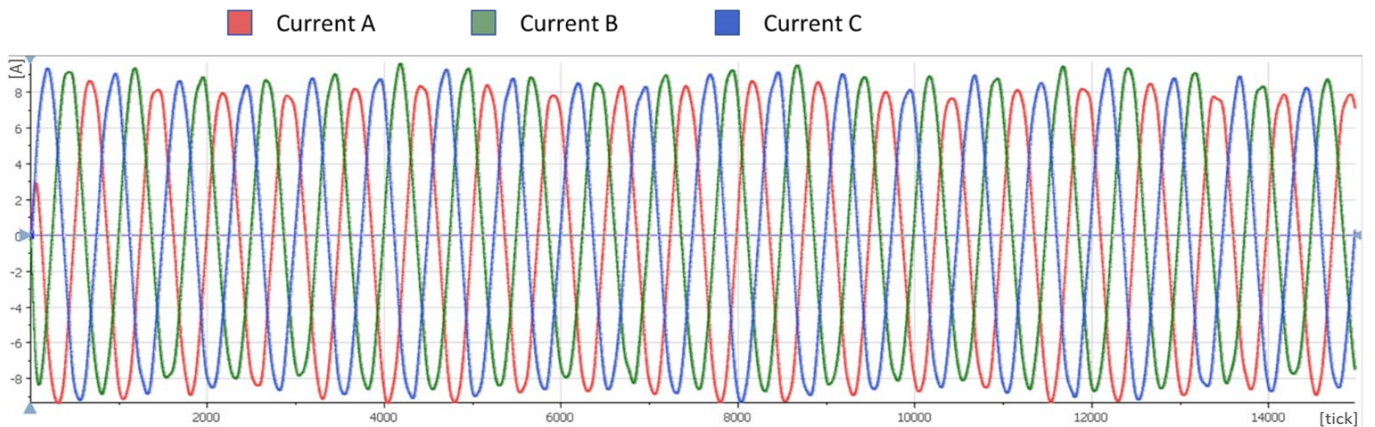


Figure 90 – Three phase current acquisition

Finally, for electric machines of this type is expected an efficiency map with maximum yield towards the center and minimum in the regions of high torque and low speed (Mahmoudi et al. 2015); furthermore, it is expected to recognize at the edge of the map the constant torque region in low-mid speed and the constant power zone for higher speeds.

Figure 91 shows a typical efficiency map of a SMPM motor.

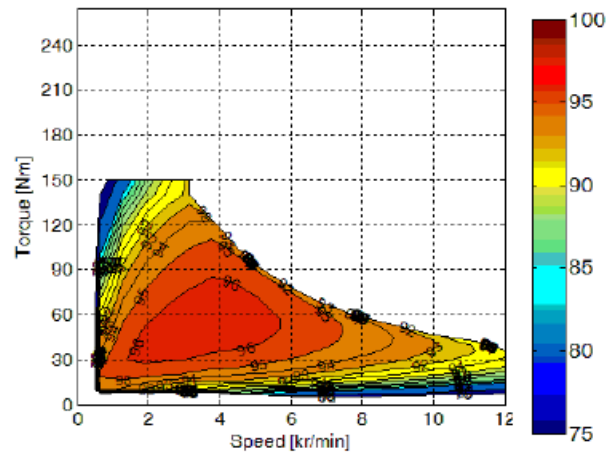


Figure 91 – Efficiency map for a SMPM motor - (*Efficiency maps of electrical machines* 2015)

## 7.2 Achieved results

The results obtained reveal only a partial efficiency map due to the limitations of the test bench, in fact, while the maximum speed of the engine under test is 6000 rpm, the maximum speed supported by the test bench is 2000 rpm. Only one third of the map can be evaluated.

Conversely, due to the low efficiency of the test rig transmission, it was not possible to test the motor for zero torque, in fact, even if the load motor imposes zero torque, the rotation of the transmission will determine a resistive torque, which will be proportional to the increase in speed. For such reason, the lower part of the efficiency map also cannot be evaluated.

The experimental relation between the resistive torque of the bench and the speed is reported below.

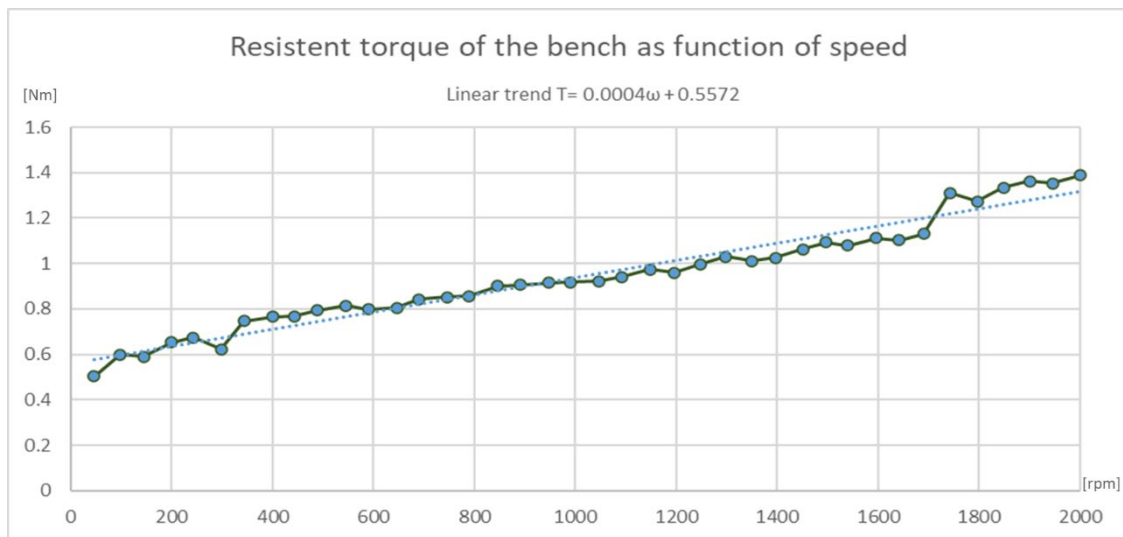


Figure 92 – Resistant torque of the bench as function of speed

The area under this curve cannot be evaluated as the bench is not suitable for low torque motors.

The function can be approximated by a linear trend function: note that even for minimum speeds of 50 rpm the torque delivered by the MUT is of 0.50 Nm.

The resistive torque of the bench is high, which makes it impossible to test a part of the efficiency map of the motor considered. This happens because the bench is designed to test high torque motors up to 100Nm which makes the loss information of a measurement area equal to 0.5 Nm negligible, i.e. about 1% of the total, while for motors with lower power there is a measurement gap which is a substantial percentage of the motor map.

In the case under consideration, the motor has a maximum torque of 3.5 Nm. Therefore about 27% of the working region of the motor is neglected. Hence, a significant part of the map cannot be evaluated because the bench is inappropriate for testing low torque motors because the transmission is not very effective.

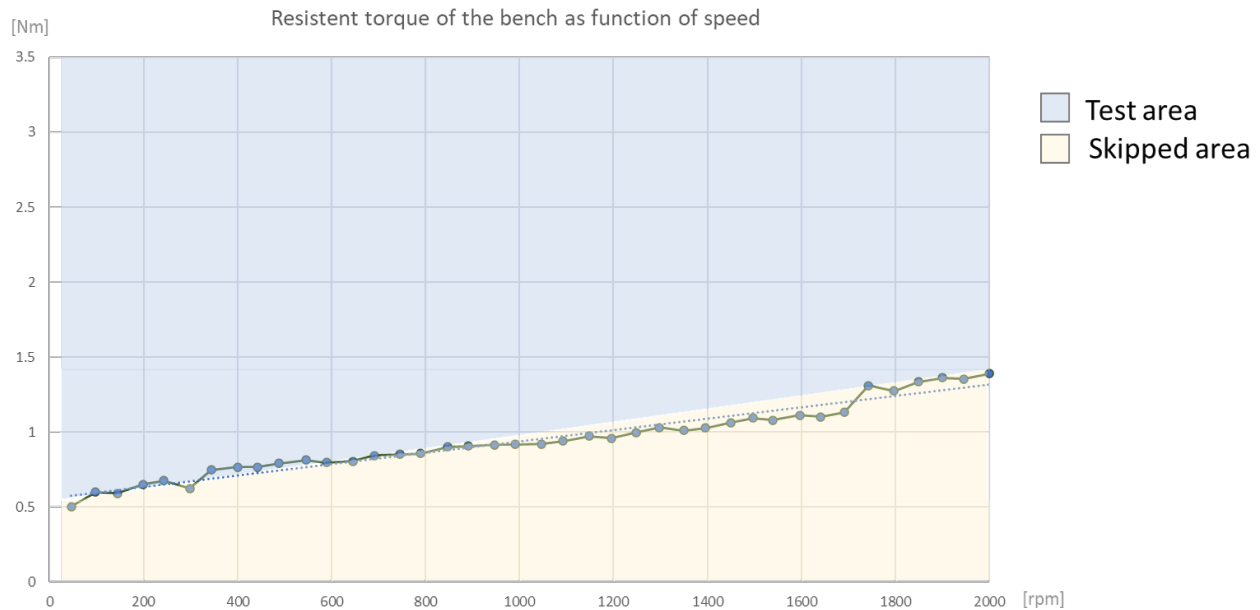


Figure 93 – Resistant torque of the bench as function of speed: division among areas

To test the skipped area, the resistive torque of the bench can be canceled by operating the load motor in the same direction of rotation of the speed so that it supplies propulsive torque by taking charge of the resisting torques of the bench. This solution is not applied as negative torques cannot be applied to the load motor control algorithm.

To build the map, 341 points are evaluated and it is achieved a maximum constant torque of 3.44 Nm and a peak efficiency of 52.5%. The efficiencies obtained are better represented in the efficiency map in Figure 94.

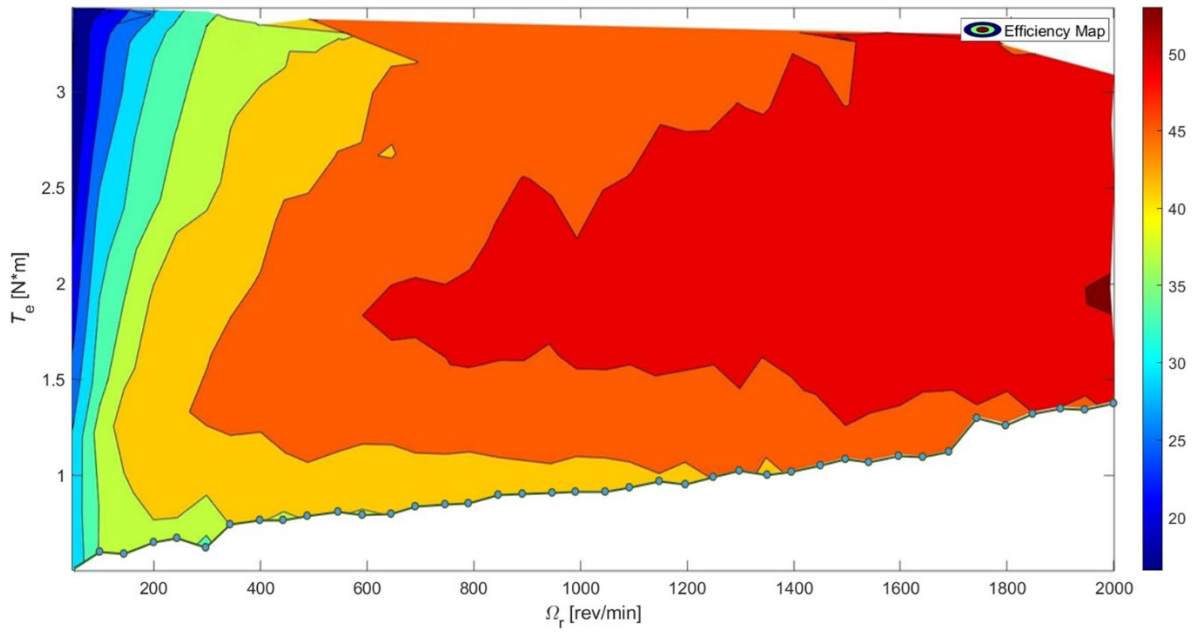


Figure 94 – Efficiency map results of the MUT

Therefore, due to the speed limitations of the bench, it is possible to test a third of the working area of the motor. In Figure 95 the whole expected efficiency map is shown.

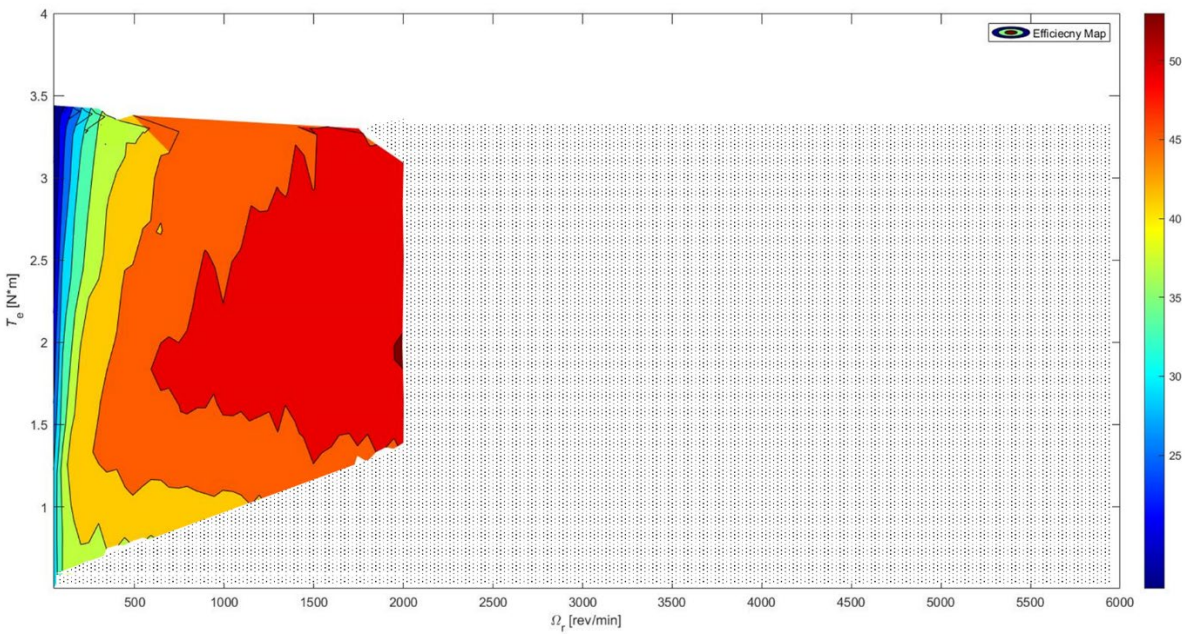


Figure 95 – Efficiency map of assessed and non-assessed region

However, comparing the results obtained with efficiency maps of similar motors, it has been shown that, while the trend is the same, the yields of these machines are much higher than those detected in the MUT.



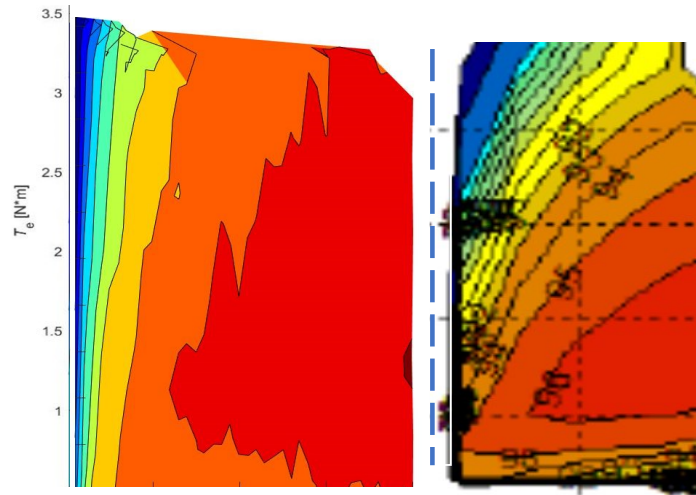


Figure 96 – Efficiency maps comparison

Comparing the trend of the reference map with the one obtained, it can be seen, in proportion to the torque scale, how the efficiency trend is consistent, in fact for high torque and low speed the efficiency reaches the minimum of its value. Lower efficiencies are present even at high speeds and minimum torques.

From the comparison, it notes that the efficiency values found are lower than those expected. Since the data acquired by the program are validated, it is assumed that the cause of the divergence is the control strategy of the MUT which could be improper.

The first factor to be evaluated to verify the correct operation of the drive and therefore a correct control strategy is the power factor. A load with a low power factor draws more current than a load with a high power factor for the same amount of useful power transferred.

Imposed	Point	Power factor
Speed	Torque	$\cos(\varphi)$
600 rpm	1 Nm	0.16
800 rpm	1 Nm	0.2
1500 rpm	1.5 Nm	0.3
100 rpm	2.3 Nm	0.05
800 rpm	2.5 Nm	0.2
500 rpm	4.0 Nm	0.15
1800 rpm	3.3 Nm	0.35

Table 18 – Power factor results

It immediately notes that the power factor has values much lower than the unit, and this certainly implies an ineffective operation of the drive.

Moreover, it is assumed that the controller is not placing the current vector towards the quadrature axis but rather an important component is directed towards the direct axis, which implies that a part of the absorbed current does not produce torque.

Under optimal conditions, the control translates all the current into torque and only in flux-weakening conditions the current vector takes non-zero component on the d-axis.

The performances detected are lower than those expected even because the motor is not tested in its entire working area but only in a part of it. The greatest efficiency would be reached in the area that has not been tested yet. In favor of this hypothesis, it can be noted that the greatest efficiencies occurred in areas at the right edge of the efficiency map Figure 94, which most likely indicates the beginning of a region with higher efficiency.

In addition to the efficiency map, the map of the total losses of the motor can be indirectly obtained from the power acquisitions.

In the losses map it expects higher loss values as the speed increases because of bearings friction and windage, and as the torque increases due to the increase of current that it involves and therefore the consequent Joule effect.

As demonstrated in Figure 97, the losses rise when speed and torque increase.

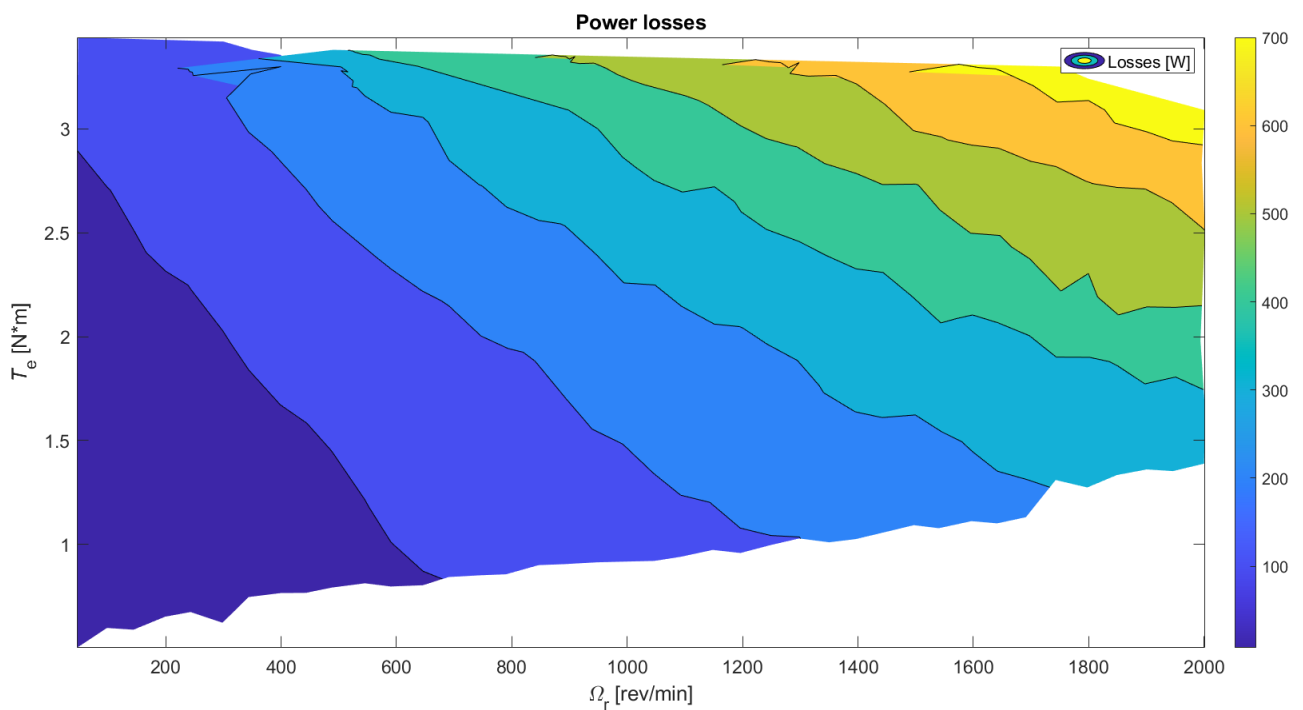


Figure 97 – Losses map

## 8. Conclusions

The purpose of the paper is to study a generic electric motor under several working conditions in order to build its efficiency map automatically. Considering the results achieved by the developed tool, the purpose of the thesis is realized.

The developed tool, which is implemented as an extension of the test bench capture program, allows the operator to acquire data and determine efficiency maps of the motor under test.

Once the sensors have been calibrated, the tool's settings are customized to match the objective of the simulation. A model for increasing speed and torque can be set; the limits of the test region can be established and the maximum acceptable measurement range can be introduced. After that, the simulation can be started.

The program operates in stationary conditions and therefore autonomously checks that both speed and torque are constant and in the appropriate range.

The program acquires voltage, current, speed and torque signals of a single point. Then the signals are processed to get mechanical and electric power. Mechanical and electrical period are extracted from the measurements in order to process and save only the data necessary for post-processing and not all the acquisition performed. Hence, it saves the data of the sensors in a TDMS file and process them to determine the efficiency. Afterwards it proceeds to the next point.

The speed of the motor is controlled by the Arduino board. The inverter of the MUT is connected to the Arduino which in turn communicates with the program via a finite state machine. This connection makes it possible to control the speed of the motor under test via analog signals and to reset errors or shut down the drive itself, via digital signals.

Moreover, the program is enriched with safety sub-functions, which shut down the drive in case of a drive fault.

The validation of the program has been realized on the "MAPRO" test bench of the Research Center "Motion Control and Industrial Application" (MCIA) of Universitat Politècnica de Catalunya.

In order to carry out the program validation in a safety zone of operation, the considered motor under test corresponds to a low torque motor for general purpose.

Have been recorded 341 points and the efficiency map of the MUT was extracted from the acquired data. The highest torque measured in stationary conditions is  $3.44 \text{ Nm}$  while the peak efficiency is detected for  $\omega = 1988 \text{ rpm}$ ,  $T = 1.86 \text{ Nm}$ . Due to the losses of the transmission system, the minimum torque detected is  $0.503 \text{ Nm}$  for a speed of  $50 \text{ rpm}$ .

From the results obtained, the waveforms of electric and mechanical parameters are coherent with the expectations. Even the trend of efficiencies is in accordance with expectations while, the efficiency values are lower than those predicted, the maximum achieved efficiency results to be 52.51%. Such divergence is justified by the non-optimal configuration of the inverter, which made the current vector assume a non-negligible component on the d-axis.

In conjunction with the efficiency map, motor losses have been computed. These latter increase, according to the expectations, when torque and speed increase. The maximum value is  $774.13 \text{ W}$  for max speed and max torque.



The program performances in terms of time resources are around 40 seconds for the valuation of each point without considering the possible action of the auto-adjusting function which correct the speed. To run the program, the LabVIEW platform is needed and combined with sufficient memory for saving data. The results file dimension depends on the frequency of acquisition and the number of acquired points, for this project the amount of data is equal to 2Gb. Furthermore, the DIAdem software is recommended for viewing and postprocessing the results.

This project allowed to apply the theoretical knowledge to a practical field by adapting the ideal conditions of the literature to the real ones of the laboratories. The development of this document occurred transversely, including mechanical, electronic, and computer science fields.

The development of the paper provided an overview of test bench work procedures and on adoption strategies for data acquisition and motor testing. In addition, the LabVIEW programming has been deepened and the ability to post process and read output data improved.

The automation of the processes greatly simplifies the work of users who are only interested in the final measurements. The developed tool is suitable for testing any type of electric motor both DC and AC and can be installed on any test bench with a LabVIEW platform.

## 8.1 Future works

Future development focuses on the control of the electrical machine. The implementation of a more effective inverter's control for the MUT is fundamental to let the electric machine work at its best performances and obtain more reliable results.

Moreover, the work can be extended by including the functionality of testing the motor even in transient conditions by performing dynamic and non-stationary tests. Furthermore, a strategy can be implemented to analyze the motor behavior in a cycle to simulate dynamic conditions.

## Bibliography

- ANFIA, A. S. e S. (2020). "L' industria automotive mondiale nel 2019 e trend 2020."
- Christopher Jaszczolt. (2017). "Understanding permanent magnet motors." *Yaskawa America Inc.*, <<https://www.controleng.com/articles/understanding-permanent-magnet-motors/>> (Mar. 2, 2021).
- Dilshad, M. R., Ashok, S., Vijayan, V., and Pathiyil, P. (2016). "An energy loss model based temperature estimation for Permanent Magnet Synchronous Motor (PMSM)." *Proceeding of IEEE - 2nd International Conference on Advances in Electrical, Electronics, Information, Communication and Bio-Informatics, IEEE - AEEICB 2016*, 172–176.
- EuropeanParliament. (2019). "Emissioni di CO2 delle auto: i numeri e i dati." <<https://www.europarl.europa.eu/news/it/headlines/society/20190313STO31218/emissioni-di-co2-delle-auto-i-numeri-e-i-dati-infografica>> (Mar. 17, 2021).
- HBM. (n.d.). "Case Study: Highly Efficient Test Bench For e-Motors | HBM." <<https://www.hbm.com/en/7037/schabmueller-highly-efficient-test-bench-for-electric-motor/>> (Dec. 13, 2020).
- John E. Hopcroft, Rajeev Motwani, and Ullman, J. D. (1981). *Introduction to automata theory, languages, and computation*. Pearson Education, (Pearson Education, ed.).
- Mahmoudi, A., Soong, W. L., Pellegrino, G., and Armando, E. (2015). "Efficiency maps of electrical machines." *2015 IEEE Energy Conversion Congress and Exposition, ECCE 2015*, (2015), 2791–2799.
- Meier, S. (2002). "Theoretical design of surface-mounted permanent magnet motors with fieldweakening capability." *Master Thesis. Royal Institute of Technology Department of Electrical Engineering Electrical Machines and Power Electronics Stockholm*, 79.
- Oghomwen Igbinovia. (n.d.). "Constituent parts of a plug-in hybrid electric vehicle [20] | Download Scientific Diagram." <[https://www.researchgate.net/figure/Constituent-parts-of-a-plug-in-hybrid-electric-vehicle-20\\_fig3\\_309049006](https://www.researchgate.net/figure/Constituent-parts-of-a-plug-in-hybrid-electric-vehicle-20_fig3_309049006)> (Mar. 15, 2021).